NOTICE

The quality of this microform is heavily dependent upon the quality of the original thesis submitted for microfilming. Every effort has been made to ensure the highest quality of reproduction possible.

If pages are missing, contact the university which granted the degree.

Some pages may have indistinct print especially if the original pages were typed with a poor typewriter ribbon or if the university sent us an inferior photocopy.

Reproduction in full or in part of this microform is governed by the Canadian Copyright Act, R.S.C. 1970, c. C-30, and subsequent amendments.

AVIS

La qualité de cette microforme dépend grandement de la qualité de la thèse soumise au microfilmage. Nous avons tout fait pour assurer une qualité supérieure de reproduction.

S'il manque des pages, veuillez communiquer avec l'université qui a conféré le grade.

La qualité d'impression de certaines pages peut laisser à désirer, surtout si les pages originales ont été dactylographiées à l'aide d'un ruban usé ou si l'université nous a fait parvenir une photocopie de qualité inférieure.

La reproduction, même partielle, de cette microforme est soumise à la Loi canadienne sur le droit d'auteur, SRC 1970, c. C-30, et ses amendements subséquents.

SITE-SPECIFIC ^{57}Fe MOSSBAUER RECOILLESS FRACTIONS IN TRUE TRIOCTAHEDRAL MICAS

by

MICHEL ROYER

Thesis submitted to the School of Graduate
Studies of the University of Ottawa
in partial fulfillment of the requirements
for the degree of Master of Science
in Physics

DEPARTMENT OF PHYSICS
FACULTY OF SCIENCE
UNIVERSITY OF OTTAWA
Ottawa, Ontario, Canada

ISBN 0-315-75021-9

Canada

UNIVERSITÉ D'OTTAWA
UNIVERSITY OF OTTAWA

ABSTRACT

The accurate determination of site populations from ^{57}Fe Mössbauer spectroscopy requires that spectra be corrected for absorber thickness effects and that site-specific Mössbauer recoilless fractions (f-factors) be known. This thesis uses a novel method to perform thickness-effect corrections, then uses the temperature dependence of the thickness-corrected spectral areas of selected peaks to obtain site-specific f-factors at 80 K and 300 K for the iron sites in true trioctahedral micas. A preliminary study of a biotite single crystal showed the site-specific nature of the f-factors. Five samples – three biotites rich in octahedral Fe^{3+}, a phlogopite rich in tetrahedral Fe^{3+}, and a synthetic annite – were then studied to quantify the site-specific f-factors. Our final values, taken to be representative of all true trioctahedral micas, are:

octahedral Fe^{2+} sites	$f^{[2+]}(300\ K) = 0.56 \pm 0.06$
	$f^{[2+]}(80\ K) = 0.82 \pm 0.02$
octahedral Fe^{3+} sites	$f^{[3+]}(300\ K) = 0.69 \pm 0.07$
	$f^{[3+]}(80\ K) = 0.87 \pm 0.07$
tetrahedral Fe^{3+} sites	$f^{<3+>}(300\ K) = 0.75 \pm 0.10$
	$f^{<3+>}(80\ K) = 0.90 \pm 0.03$

These f-factors are used in conjunction with thickness-corrected sub-spectral areas to obtain the first accurate iron site populations for annite:

$$[Fe^{2+}]/Fe = (90.5 \pm 1.0)\ \%$$
$$[Fe^{3+}]/Fe = (5.3 \pm 1.0)\ \%$$
$$\langle Fe^{3+}\rangle/Fe = (4.2 \pm 0.3)\ \%$$

Experimental uncertainties related to each part of the work are considered in detail, and evaluated where possible.

Acknowledgements

First and foremost, my most grateful thanks go to my supervisor, Denis Rancourt, whose guidance and help were invaluable in every facet of this project. Warm thanks are also extended to Roger Thiele, who taught me squash and how to fix "my" cryostat. Other contributors to this project whose help is gratefully recognized are Iain Christie, for collecting the annite spectra, Peter Hargraves, for collecting and obtaining first fits of the MOC2661 spectra, Gilles Lamarche, for the loan of his temperature controller, and André Lalonde, for sharing his invaluable knowledge of mica and for asking the simple question, "What's the ratio of Fe^{2+} to Fe^{3+} in this mica sample?" that helped launch a Master's project.

Thanks are also extended to the grad. students with whom I shared lab space, computers, volleyball games, interesting discussions, and friendship. A special thank-you to Ricc for his friendship and moral support.

Finally, the financial assistance of NSERC during this project is gratefully acknowledged.

Table of Contents

List of Tables

List of Figures

1. Introduction

1.1 Mössbauer Spectroscopy

In 1957, Rudolf Mössbauer discovered that nuclei could resonantly absorb gamma rays. This phenomenon, thereafter known as the Mössbauer effect, earned him a share in the 1961 Nobel prize in Physics and became the basis of a new spectroscopic technique, Mössbauer spectroscopy. For the reader unfamiliar with this tool, there exist many reviews and books which provide excellent introductions: from the very complete work of Greenwood and Gibb [1] to the elementary but informative book edited by Leopold May [2] for the non-physicist. The reader is referred to these works for a description and understanding of Mössbauer spectroscopy, chapters treating recoilless fractions and spectral intensities being most relevant to this work.

Mössbauer spectroscopy studies transitions between nuclear energy levels in an isotope. About forty elements totalling 72 isotopes and 88 transitions lend themselves to this technique. Only one transition of one isotope is studied in a given experiment; the 14.4 keV transition between the ground and first excited state of ^{57}Fe is by far

the most commonly utilized and is the one used in the experiments of this thesis. The advantage of Mössbauer spectroscopy is that the probe isotope will reveal a spectrum specific to its electronic environment. A spectrum for a sample is thus composed of the various sub-spectra specific to the environments experienced by the (^{57}Fe) isotope nuclei.

Since each site (i.e. collection of ions in nearly identical environments) leads to a sub-spectrum[1], it should be possible to obtain populations which are site-specific and/or ion-type-specific from sub-spectral areas. This can prove, however, a difficult task. Spectra can suffer from many inherent problems due to their features (the overlapping of peaks being a common difficulty). They may also be subject to several experimental artifacts – line broadening due to external vibrations, effects due to the finite sizes of channels, and other problems. Most artifacts can be averted if the experiment is done carefully but some effects cannot be avoided. For instance, in ^{57}Fe Mössbauer absorption spectroscopy, the thickness of the

---

[1]Ions of different valence but in otherwise identical environments will also produce different sub-spectra as the *nuclei* will experience different environments.

absorber always has a significant effect on the lineshape and on the spectral areas [3]. A spectrum that is not corrected for the effects of absorber thickness will not provide correct measurements of site populations.

Spectral areas are also affected by Mössbauer recoilless fractions. Consider a free excited nucleus at rest. Upon emission of a gamma ray the nucleus recoils, and its recoil energy, unavailable to the photon, is sufficient to prevent the gamma ray from exciting a like nucleus at rest. By fixing the nucleus in a crystal, the recoil becomes negligible (unless a phonon is created). The emitted photon could then excite a like transition in a nucleus identical to the first in an environment like the first – provided no phonon is created upon absorption. So the Mössbauer recoilless fraction for a material, also called its f-factor, is the probability that an emission (or absorption) of a gamma ray by a nucleus is recoilless (i.e. no phonon is produced). This probability will depend on bond strength, sample temperature, isotope mass, and gamma ray energy. Since bond strengths may vary from site to site, so should the f-factors. Mössbauer recoilless fractions should thus be site- (and ion-) specific and are necessary in obtaining site populations from a spectrum.

A common error is to assume that the bond strengths are

similar enough at each site that the same recoilless fraction could be used for all sites. The ratio of sub-spectral areas would thus reveal the ratio of site populations in a spectrum corrected for absorber thickness effects. This is done in practice because of the difficulties involved in measuring site-specific f-factors. In his Ph.D. thesis [4], Whipple offers an illustration of these difficulties. In what is perhaps the only previous attempt at measuring site-specific, recoilless fractions of ^{57}Fe in micas, Whipple examined f-factors of Fe^{2+} and Fe^{3+} and found contradictory results (the Fe^{2+} site was found to have a greater f-factor than the Fe^{3+} site in one sample, but the reverse was true in a second sample).

The experiments in this work are designed to most accurately determine the site-specific recoilless fractions of the various ^{57}Fe sites in mica. Experiments were done with care, spectra were corrected for absorber thickness effects, and problems arising from the overlap of peaks from different sub-spectra were addressed. This thesis will thus demonstrate a general method for the measurement of f-factors, illustrate their importance, and obtain useful site-specific f-factors for mica.

1.2 Thesis road map

The presentation of this thesis corresponds to the following format. The remainder of this introductory chapter will present mica, giving the relevant details of structure and nomenclature, and discuss how f-factors can be determined – especially from the temperature dependence of spectral areas.

The next chapter describes how the Mössbauer spectra were accumulated. The experimental setup is described, as are the samples and techniques of data analysis. An important section in this chapter describes how spectra can be corrected for effects due to absorber thickness.

Results can then begin. Chapter 3 will present the data obtained from preliminary experiments and discuss what was hence deduced. Chapter 4 is the key section as it describes the main set of experiments from which this work draws its conclusions. A discussion of these results is also given.

Chapter 5 goes a step further and, using the f-factors obtained in chapter 4, calculates the site-specific populations for the mica end-member, annite.

The final chapter presents a summary of the conclusions obtained from this research.

1.3 Mica: structure, nomenclature, and site occupancies

Accurate site populations are often desirable, for various reasons. The illustration of a technique able to measure site-specific recoilless fractions is thus worthwhile even had mica not been chosen as the test sample. But by selecting mica, this work obtains recoilless fractions which are of use and of interest to a broad scientific community including mineralogists and geologists. The ratio of Fe^{2+}/Fe^{3+} in a mica is a measure of the oxygen fugacity of its environment at the time of its formation [5]. Mica, therefore, has great potential use as an oxygen geobarometer – this avenue of research is being pursued in our laboratory.

To understand the Mössbauer spectrum of mica, and to understand differences between samples, the structure of mica should be known. A brief discussion will be presented here; further details may be sought in other references [6, 7].

Mica is a layered silicate. It consists of layers of

tetrahedral (T) and octahedral (O) cages arranged in a TOT stacking (fig. 1.1) with cations separating each TOT triple-layer. The tetrahedral cages are made of oxygen ions, the octahedral cages consist of oxygen and hydroxyl groups, normally with 4 oxygen ions and 2 hydroxyl groups forming each octahedron. Various cations are found within both the tetrahedral and the octahedral cages. A structural formula for mica is thus:

$$\{\}_1 \quad []_{2 \text{ or } 3} \quad <>_4 \quad O_{10} \quad (OH)_2 \qquad (1.1)$$

where {} represent interlayer cations, [] are octahedral cations (two of them in dioctahedral micas, three in trioctahedral micas; see below), and <> represent the cations in the tetrahedral cages.

If the interlayer cations are monovalent (e.g. K^+), the sample is a "true" mica. Micas with divalent interlayer cations (e.g. Ca^{2+}) are "brittle" micas. Only true micas were studied in this work, though the methods used could be applied to brittle micas as well.

The tetrahedral cages, being small, will hold nothing larger than Fe^{3+} ions. They usually contain Si^{4+} and Al^{3+} (and occasionally small amounts of Ti^{4+} and/or Fe^{3+}), every cage containing a cation. Such is not necessarily the case

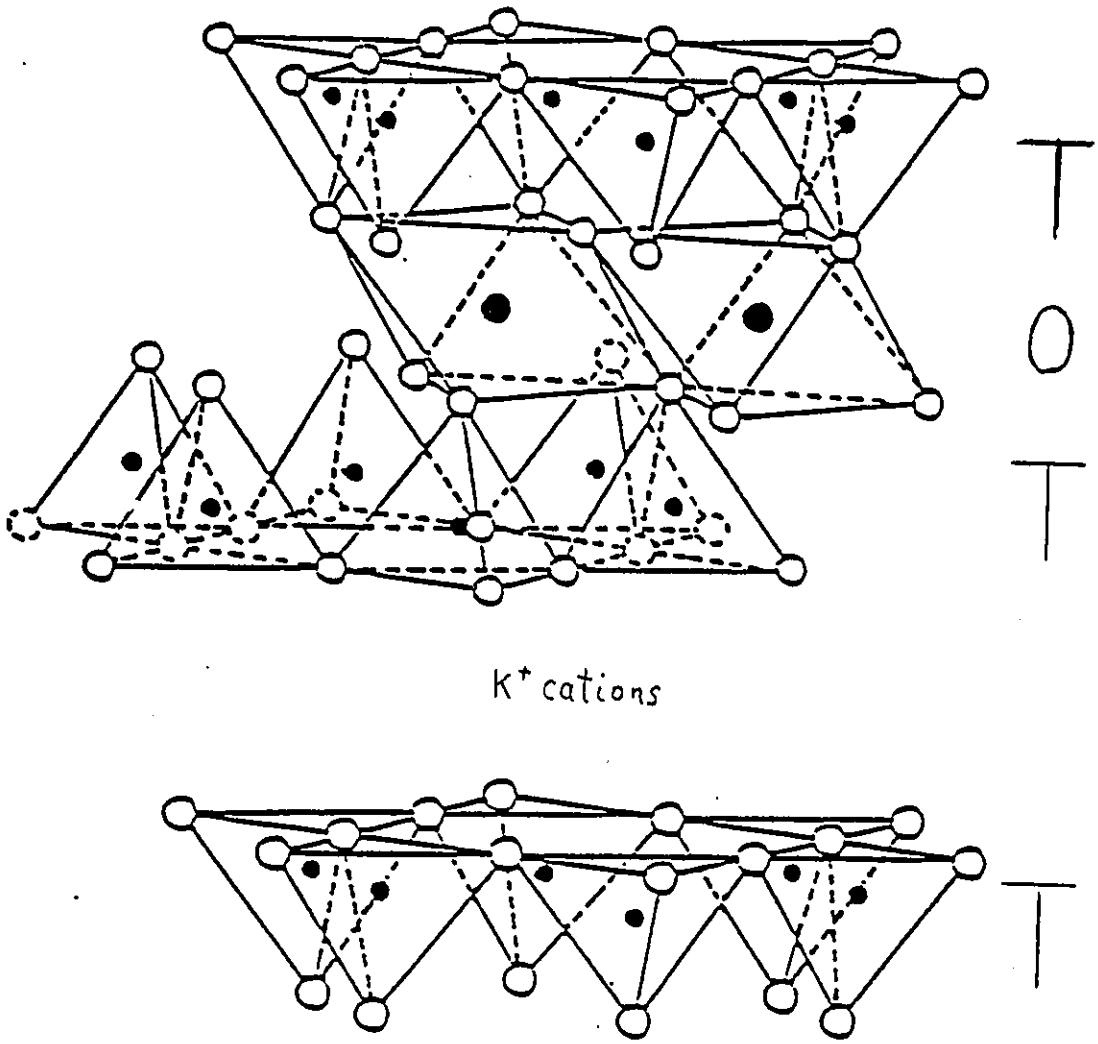

Figure 1.1 Mica TOT layers. The large full circles are the octahedral cations (including $[Fe^{2+}]$ and $[Fe^{3+}]$), the small full circles are the tetrahedral cations (including $<Fe^{3+}>$).

with the octahedral cages. Dioctahedral micas have cations in two thirds of the octahedral cages, trioctahedral micas have a cation in every octahedral cage. Typical octahedral cations are Fe^{2+} and Mg^{2+}, some Fe^{3+} is usually found there as well.

Considering only the true trioctahedral micas, there are still further distinctions based on iron content in the octahedral cages. Iron-deficient micas (Fe/(Fe+Mg) < 0.33) are called phlogopites. Phlogopite may also refer to the end-member of this Fe-Mg field with no Fe^{2+} in the octahedral cages. Iron-rich micas (Fe/(Fe+Mg) > 0.33) are known as biotites. The end-member, annite, should only contain Fe^{2+} in the octahedral cages, and Si and Al in the tetrahedral cages. For structural reasons this mineral cannot exist – to obtain a stable structure some of the iron must be Fe^{3+} in either the tetrahedral or octahedral cages (or both) and a corresponding number of hydrogen atoms must be lost. Such micas, which differ in composition from ideal annite by these few hydrogen atoms, are called annites nonetheless.

As stated, Fe^{3+} can be found in either the tetrahedral cages, $<Fe^{3+}>$ or in the octahedral cages, $[Fe^{3+}]$. Fe^{2+} can only be found in the octahedral cages, $[Fe^{2+}]$. These are the three iron "sites" of true trioctahedral micas that can

be distinguished by Mössbauer spectroscopy. Thus, by "site", we mean here a particular valence state of the ion (Fe^{2+} or Fe^{3+}) and a particular anion coordination (tetrahedral or octahedral coordination). Each such "site" is therefore an entire family of "crystallographic sites" that differ by such characteristics as precise anion positions, next near neighbour positions, next near neighbour ion-types, etc.

The octahedral "sites" can be split into two categories, CIS and TRANS, depending on and referring to the positions of the OH groups in the surrounding cage. (Note that the octahedral cations of dioctahedral micas only occupy the CIS sites.) However, at least above the magnetic ordering temperature of mica, the CIS and TRANS sites cannot be distinguished by Mössbauer spectroscopy [8].

A Mössbauer spectrum illustrating the three "sites" that are resolved by Mössbauer spectroscopy can be seen in fig. 1.2. Each site contributes two peaks to the spectrum. The corresponding site-specific sub-spectrum is therefore termed a "doublet". The lower energy portions of each doublet combine to form peak A.

Were the spectrum not affected by absorber thickness effects (or if the data was corrected for these effects) and

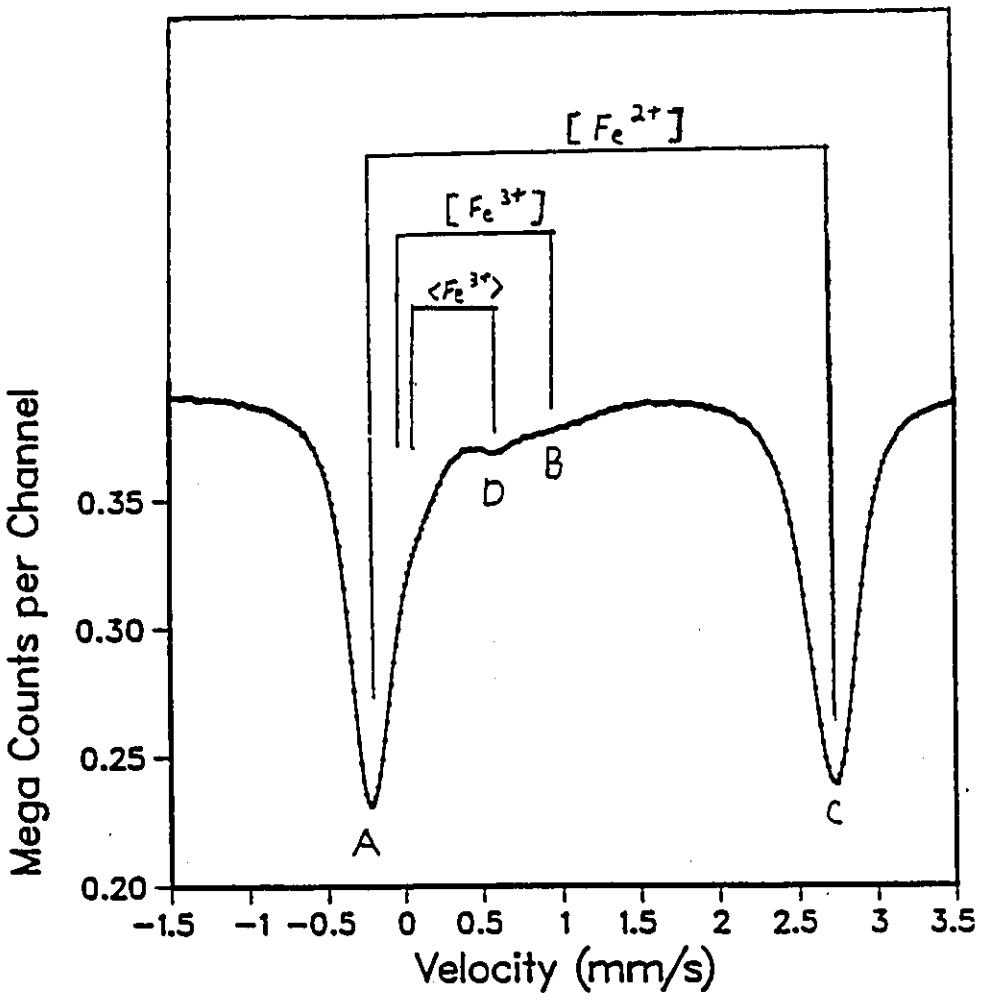

Figure 1.2 A Mössbauer absorption spectrum of annite at 83 K showing the approximate positions of the $[Fe^{2+}]$, $[Fe^{3+}]$, and $<Fe^{3+}>$ doublets. The visible peaks are labelled A, D, B, and C in this thesis (in order of increasing energy).

if the nuclei for a given site were in exactly the same environment, each peak of these doublets would have a Lorentzian profile. The splitting of the doublet peaks would correspond to the splitting in the I = 3/2 energy level of the ^{57}Fe nuclei (as determined by the interaction of the nuclear electric quadrupole moment with the electric field gradient felt by the nuclei).

All the nuclei of a given mica site are not, however, in identical environments. This causes a distribution in the splittings of the I = 3/2 energy level among a site's nuclei which can be approximated by a sum of Gaussian distributions [3]. As a result, each peak is better described by a sum of Voigt lines (a convolution of Gaussian and Lorentzian lineshapes – see Appendix 5) than by a Lorentzian line.

The spectrum is also affected by thickness-effects. If the intensities are corrected for these effects, they become proportional to the product of the number of absorbing nuclei for each site by that site's f-factor. Obtaining accurate site populations from sub-spectral intensities thus requires the knowledge of the site-specific f-factors. Determining these f-factors for the three mica iron sites is the main purpose of this thesis.

1.4 *Determination of f-factors*

How does one obtain site-specific f-factors for a sample? The first step is to collect a spectrum – avoiding all experimental artifacts that can be avoided – and to correct it for absorber thickness effects. A method to achieve this correction is described in section 2.4. The next step will depend on the spectrum.

Consider first the simplest possible case, where every spectral peak is distinct, all sub-spectral areas can be accurately measured, the site populations are known a priori, and only f-factor ratios between sites are desired. Then this ratio can be obtained by comparing ratios of sub-spectral areas to the ratios of their site populations.

A common complication is the overlap of spectral peaks. The areas of these peaks become difficult (or impossible) to ascertain with accuracy, but sub-spectral areas can still be determined provided certain conditions are met: at least one peak in each sub-spectrum must be distinct and the ratio of its area to the total sub-spectral area must be known. The latter occurs most readily with perfectly powdered samples as their spectra do not depend on sample orientation and the ratio of a peak's area to the area of its sub-spectrum is known. In single crystals and samples which

exhibit texture effects (the sample looks like a powder but is actually made of oriented crystals so its spectrum is orientation-dependent), calculation of sub-spectral area from a single peak is not possible unless enough is known about the particular sample. And without accurate sub-spectral areas the determination of f-factors from a single spectrum becomes impossible.

Of course, Nature is rarely so helpful as to make the determination of f-factors easy in materials of interest. Consider the micas studied in this thesis (recall fig. 1.2). They consist of 2 or 3 doublets due to $[Fe^{2+}]$, $[Fe^{3+}]$, and $<Fe^{3+}>$ (when present), the high energy peaks of each corresponding to peaks C, B, and D, respectively, the lower energy portions of each overlapping to form peak A. By its layered nature, truly powdered samples of mica are difficult to obtain (it is difficult to powder a mica sample to a point where is it is fine enough to not exhibit texture effects). The resulting difficulties in obtaining sub-spectral areas and the limits in accuracy of the chemical means used to obtain Fe^{2+}/Fe^{3+} ratios lead to inconclusive Fe^{2+}/Fe^{3+} f-factor measurements in previous studies on mica [4].

To counter these difficulties, we have developed a method to determine f-factors that involves measuring the

temperature dependence of a sample's (thickness-corrected) spectrum and that does not depend on chemical measurements. This method does require that the material not change composition or structure over the temperature range studied and that at least one peak in each sub-spectrum have an area that can be accurately measured. The ratio of the area of the distinct peak to that of the sub-spectrum is then a constant, and the area of this peak is proportional to the f-factor for its sub-spectrum; hence the temperature dependence of the peak's area (and of the sub-spectral area) will correspond to the temperature dependence of the f-factor. This is sufficient to allow the determination of the f-factor at temperatures of interest.

A few words need now be said concerning this temperature dependence. Given the phonon spectrum of a crystal, f-factors can be calculated. Should this phonon distribution correspond to that postulated by the Debye model of lattice vibrations, the resulting expression for the f-factor becomes

$$f = \exp\left[\frac{-6\ E_R}{k\ \theta_D}\left\{\frac{1}{4} + \left(\frac{T}{\theta_D}\right)^2 \int_0^{\theta_D/T} \frac{x\ dx}{e^x - 1}\right\}\right] \qquad (1.2)$$

where k is the Boltzmann constant, E_R is the recoil energy of the Mössbauer transition (the kinetic energy of a free

nucleus upon absorption/emission of the transition's photon) and θ_D is the Debye temperature for the material. The material's f-factor is thus known at all temperatures provided the Debye temperature, θ_D, is known. A similar expression arises if the Einstein model is more appropriate:

$$f = \exp\left[- \frac{E_R}{k\,\theta_E} \left(\frac{2}{\exp\,(\theta_E / T) - 1} + 1 \right) \right] \qquad (1.3)$$

where θ_E is the Einstein temperature. Note that since f-factors should be site-specific, each site must be characterized by a θ_D (or θ_E). Such a site-specific Debye (or Einstein) temperature should be considered merely a parameter which best describes the f-factors for a site given a certain model, rather than attributing a particular physical meaning to it.

This digression has explained the motivation for obtaining site-specific Debye temperatures and has suggested a method of obtaining them from the temperature dependence of sub-spectral areas. In this work, curves of area of a peak were plotted against temperature for the various mica sites studied, the shapes of these curves being sufficient to obtain site-specific Debye temperatures. This in turn revealed the f-factors for each site at temperatures of interest and, as explained in the following paragraphs,

showed them to indeed be site-specific and significantly different at room temperature.

A preliminary test on a biotite single crystal, in which five spectra were accumulated between liquid nitrogen and room temperatures, indicated the [Fe^{2+}] Debye temperature, $\theta_D^{[2+]}$, to be smaller than the effective Debye temperature, $\overline{\theta_D}$, and hence smaller than the [Fe^{3+}] Debye temperature, $\theta_D^{[3+]}$, the temperature dependence of peak C being less than that of the total spectral area (note that the same can then be said of the f-factors, $f^{[2+]} < f^{[3+]}$, at all temperatures).

To obtain the f-factors more accurately, improvements were made to the experimental setup (the cryostat was improved and a better temperature controller was used, see section 2.1) and five samples were studied at room and liquid nitrogen temperatures. Ratios of room temperature to liquid nitrogen temperature spectral areas for peaks B, C, and D revealed the site-specific Debye temperatures, hence the f-factors for any given temperature. They showed that $f^{[2+]} < f^{[3+]} \leq f^{<3+>}$. The actual values of these f-factors at 80 K and 300 K are given in chapter 4 of this text.

2. Experimental methods, equipment, and samples

2.1 Equipment and spectral acquisition

For each experiment, a ^{57}Co source in a rhodium matrix was used. The source was mounted on a constant acceleration transducer which covered a -4 mm/s to +4 mm/s energy scale. The absorber itself was normally mounted inside a cryostat (with mylar windows allowing the passage of the gamma rays through the cryostat and through the absorber). A proportional counter was used to detect the gamma rays; pulses it transmitted to a spectroscopy amplifier were reshaped and amplified, then sent to a single channel analyzer (SCA). The SCA acted as a filter, removing pulses outside of a certain energy range. Thus only pulses corresponding to approximately 14.4 keV (the energy of the Mössbauer gamma rays) were passed on to a multichannel scalar.

This scalar counted the pulses and provided the counts to computer software which placed these counts in 1024 channels of data. The time base for the channel advance was set to cover a full period of the transducer with the 1024 channels: two spectra of about 512 channels each were thus

simultaneously collected, one roughly the mirror image of the other (one corresponding to increasing energies along the x-axis, the second corresponding to decreasing energies).

Spectra were typically collected over one to three days, until excellent statistics were obtained. Between experiments on mica samples, spectra of an ^{57}Fe enriched foil at room temperature (22 °C) were accumulated. These were used to "fold" the two mirror image mica spectra onto each other to obtain a single spectrum with a flat background, and to calibrate the energy scale (Appendix 1). Finally, MINUIT, a CERN-produced minimization package [9], was used in conjunction with a user-supplied subroutine (Appendix 2) to minimize χ^2 to obtain fits for each spectrum.

To model the spectra, Voigt lineshapes (Appendix 5) were used for each peak. Typically two to three Voigts were required to fit peak A (recall fig. 1.2), another two to three for peak C, one for peak B, and one for peak D (when present). Thus a "3-1-1-2" fit would use three lines for peak A, one for D, one for B, and two for C (so ordered according to the spectral positions of peaks A, B, C, and D).

The number of Voigts used is arbitrary: perfect fits to each spectrum were first required in order to correct the spectra for sample thickness effects, for which case the number and positions of the Voigt lines were not constrained to be physical. And even in the spectra corrected for thickness-effects, only accurate peak areas were of concern, so the number of Voigt lines used in a peak does not have physical significance.

The zero energy position (on the x-axis) corresponds to the center of the six line hyperfine pattern produced by pure metallic iron at 22°C... except in the case of one absorber, the annite, whose spectrum was accumulated with the use of an exchange-gas cryostat instead of the cold-finger type used for the other samples (the cold-finger cryostat is described below). The zero for the annite spectra is offset by the shift in the center position of a pure metallic iron pattern from 295 K to 83 K, the temperature at which the source was when the spectrum of the calibration foil (which was at room temperature) was collected. In brief, the annite spectra appear displaced by about 0.14 mm/s relative to the usual room temperature α-Fe calibration.

The cryostat used for the preliminary experiments was a cold-finger model made of brass. A thermocouple could be

attached to the sample head which also was removable and had space allocated for a small heater (resistive wire wrapped around the sample head). Temperatures between liquid nitrogen and room temperature could be reached. But leaks were detected and the sample temperature had an associated error of 3 to 7 K, so various improvements were made to better the cryostat's vacuum and the measurements of temperature.

A finer, E-type thermocouple replaced the first. The original feed-through being most inconvenient, a feed-through head with three four-hole feed-through's was constructed and added. This head also had an attached valve by which pressure sensors could be connected, and a removable lid which also had a valve, this one leading to a vacuum pump.

A diode was added to the setup. It could be attached to various points on the sample head. This diode would serve for both temperature measurements and temperature control. New heater wire was inserted to fit the requirements of the controller which accompanied the diode. A cryogenic pump (which simply consisted of crushed charcoal in a fine mesh within a can with many large holes) was added. Finally, large-diameter copper plumbing was used to connect the cryostat to a pumping station. A cross-section

of the improved cryostat is given in figure 2.1.

A helium leak detector could not find any leaks in the cryostat which can keep a sample at 82 K for up to forty hours with a single filling of liquid nitrogen. By placing the diode at various points on the sample head, the static temperature gradient over the sample was determined to be 2 K at most (82 ± 1 K for the accumulated spectra). And the thermocouple provided an extra check of the temperature – it read 1 K higher than the diode at both room and liquid nitrogen temperatures. The temperature was very stable with respect to time as well: variations were less than 0.1 K for spectra at 305 K, those collected at 82 K showed less than 0.3 K variations while a vacuum pump continually evacuated the sample space, and 1 K in a day if the valve to the pump was closed.

Spectra were accumulated at various temperatures during a preliminary experiment (see chapter 3). All spectra collected with the cold-finger cryostat for the main set of absorbers were at 82 ± 1 K or 305.0 ± 0.1 K. Those collected using the exchange-gas cryostat were at 83 ± 1 K and 300 ± 2 K. With the cold-finger cryostat, the source remained at room temperature; the source was at sample temperature when the exchange-gas cryostat was used.

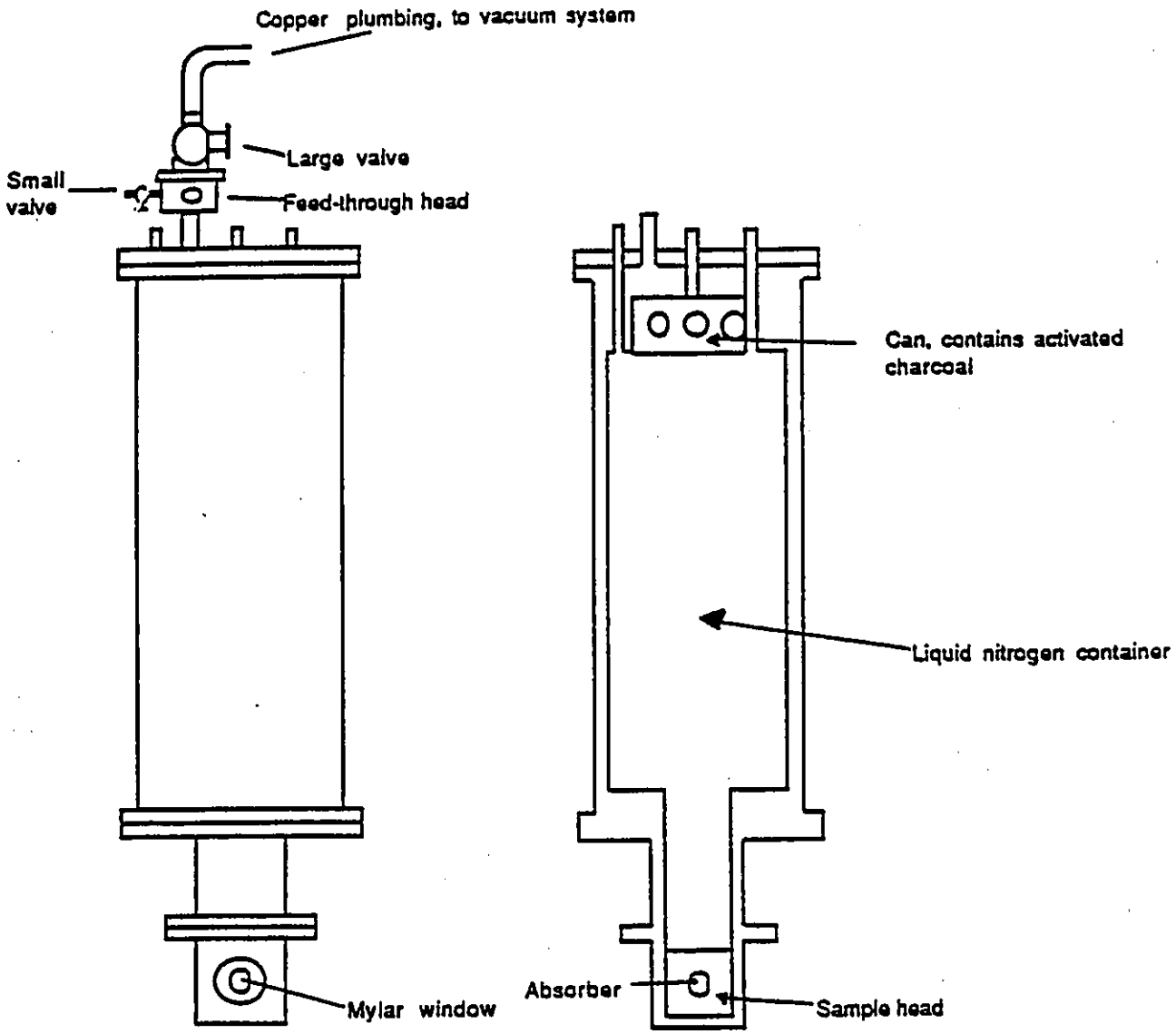

Figure 2.1 Cold finger cryostat. On the left is a frontal view, on the right is a cross-section. The space around the liquid nitrogen container is evacuated when the cryostat is in use.

Table 2.1 Descriptions of samples and absorbers

Sample	Description
MOC2661	Biotite from the Silver Crater Mine near Bancroft, Ontario. Sample MOC2661 from the Canadian Museum of Nature, Mineral Sciences Division. Large single crystal wafer: 4 cm x 5 cm x 150 μm from which absorber is cut. Microprobe and X-ray analyses show 4.567×10^{21} Fe atoms/($cm^2 \cdot \mu m$ thickness). [10, 11]
BL531	Biotite from the Bishop intrusive suite, Northwest Territories, Canada. Large flakes (≈ 2 mm diam.) manually separated from rock and used to make a mosaic absorber (129 ± 10 mg over a 15 mm diam.). Microprobe analysis indicates 1.210×10^{21} Fe atoms/g. [11, 12]
BL315	Biotite from the Bishop intrusive suite, N.W.T. Very small flakes; 175 ± 10 mg in a 0.75 inch (diam.) holder. Microprobe analysis indicates 1.637×10^{21} Fe atoms/g. [12]
BZ53	Biotite from the Bishop intrusive suite, N.W.T. Very small flakes. 168 ± 2 mg in a 0.75 inch (diam.) holder Microprobe reveals 1.590×10^{21} Fe atoms/g. [12]
MCC	Phlogopite from the McCloskey carbonatite area, Québec. Small flakes separated from rock. Also deposited in Royal Ontario Museum mineral collection (sample no. M44527). 156 ± 2 mg in a 0.75 inch (diam.) holder. From microprobe analysis, 5.43×10^{20} Fe atoms/g. [11, 13, 14]
IKO	Synthetic annite prepared by J.-L. Robert (at the Centre de Recherches sur la Synthèse et Chimie des Minéraux, CNRS, France). Very fine powder (no texture effects in spectra). 81.5 ± 2 mg in 0.75 inch (diam.) holder. From nominal formula, 3.530×10^{21} Fe atoms/g. [15]

2.2 Sample description

To obtain quantitative values of the f-factors of the various iron sites in true trioctahedral micas, six samples were selected. In a preliminary experiment, a natural single crystal of biotite (MOC2661) was used. A synthetic powdered annite (IKO), two natural biotites (BL315, BZ53), a mosaic of flakes from a natural biotite (BL531), and a natural phlogopite (MCC) were chosen for the subsequent experiments.

The three iron sites could then be observed: all samples contained [Fe^{2+}] and [Fe^{3+}], the phlogopite and the annite also contained <Fe^{3+}>. The particular phlogopite studied was very rare; unlike most micas (including other phlogopites) most of its Fe^{3+} is found within the tetrahedral cages. Further information on these samples is given in Table 2.1.

2.3 Absorber preparation

All experiments required the use of a cryostat for room and liquid nitrogen temperature spectra, thus dictating a certain preparation of the samples into absorbers. The single crystal absorber used in the preliminary experiment was sandwiched between two ultra-pure aluminum sheets, then

held to the sample head of the cryostat by a brass ring. Ample vacuum grease was used between all layers to insure good thermal contacts in the can vacuum.

Another absorber, BL531, was a mosaic of small crystals, all crystals being oriented with their cleavage plane in the absorber plane. The absorber preparation was identical to the above except that the crystals were first placed on adhesive tape to form the mosaic.

The other samples were powders or very tiny flakes. Uniform absorbers are required for thickness-effect corrections, so the following preparations were necessary. A sheet of ultra-pure aluminum was squeezed between two brass rings, forming a bowl of sorts. Vacuum grease was placed within the holder which was heated to the melting point of the grease (below 100 °C, not hot enough to cause oxidation within the mica). A measured amount of the sample was added and was mixed with the molten grease. As the holder was removed from the heat, the grease congealed and a uniform gelée formed. Another sheet of ultra-pure aluminum covered the top and tiny holes were punctured in top and bottom sheets so that any air in the holder might escape when the sample space in the cryostat was evacuated. The holder could then be attached to the sample head by four screws – again, with vacuum grease between all components to

insure good thermal contact between sample head and absorber. The validity of this method of absorber preparation was verified by comparing a spectrum of a so-prepared absorber with that of an absorber prepared by placing some of the same material between two mylar sheets. No oxidation could be detected in the spectrum of the flakes-in-melted-grease absorber.

One of the parameters needed to correct spectra for the effects of absorber thickness is the number of ^{57}Fe atoms per square centimeter normal to the gamma ray beam (n_a). Included in Table 2.1 are the physical sizes of the absorbers prepared for each sample, their masses, and the number of iron atoms per unit mass (or, for MOC2661, per unit thickness). The number of iron atoms per unit mass was obtained from elemental analyses, except for the annite. In that case, n_a was calculated using the nominal formula for annite

$$\{K\}\ [Fe_3]\ \langle Al\ Si_3\rangle\ O_{10}\ (OH)_2 \qquad (2.1)$$

From these amounts of iron per unit mass, absorber sizes and masses, and using the proportion of ^{57}Fe found in natural iron (2.19%), values of n_a were calculated for each absorber. The results are stated in Table 2.2.

Table 2.2 Values of n_a for each absorber

Absorber	n_a (^{57}Fe atoms / cm^2)
MOC2661	$(1.466 \pm 0.045) \times 10^{18}$
BL531	$(2.66 \pm 0.26) \times 10^{18}$
BL315	$(2.20 \pm 0.13) \times 10^{18}$
BZ53	$(2.046 \pm 0.025) \times 10^{18}$
MCC	$(6.51 \pm 0.04) \times 10^{17}$
IKO	$(4.102 \pm 0.041) \times 10^{18}$

The uncertainties in n_a can be explained as follows. Repeated measurements of the thickness of MOC2661 were consistent to within 3%, which determined the relative uncertainty in its value of n_a. Some of the material for BL315 was lost during the experiment; its mass and n_a uncertainties are subsequently large. The uncertainty in the mass of BL531 is also large as this mosaic was placed on adhesive tape before it was weighed. Furthermore, being a mosaic, its exact area was difficult to determine, so a total uncertainty of 10% in n_a was estimated for this absorber. The other values of Δn_a are obtained from mass uncertainties – which is a slight underestimate as other uncertainties (absorber inhomogeneity, uncertainty in the actual proportion of the iron in the samples being ^{57}Fe) are ignored.

2.4 *Treating effects due to absorber thickness*

When obtaining site populations or site-specific f-factors from a spectrum, the most complex step is the correction of the spectrum for effects due to absorber thickness. As gamma-rays pass through an absorber, some are scattered, some are absorbed. So nuclei deeper within the absorber see a smaller gamma-ray flux hence absorb proportionately fewer photons. Furthermore, this effect is not uniform across a spectrum: the reduction in gamma ray

flux is most important at energies corresponding to deep peaks in a spectrum, and the areas of the deep peaks will be more attenuated than those of the small peaks. A complete discussion of the effects of absorber thickness on a spectrum is provided by Rancourt [3].

Within his article is a method to obtain a normalized absorption cross-section for a spectrum. Since this cross-section is free of the effects of absorber thickness, the process of obtaining it for a spectrum will be called "thickness-correction" as these cross-sections essentially appear to be thickness-corrected emission spectra.

For consistency with fitting and plotting programs of our laboratory, it was useful to generate thickness-corrected spectra that actually resembled *absorption* spectra. "Thickness-corrected spectra" (including those displayed later in this thesis) will thus refer to "spectra" with $y_{tc}(\psi)$, the number of counts at energy ψ (or in channel ψ), corresponding to:

$$y_{tc} = 1000000 - 100000 \cdot \sigma_a'(\psi) \qquad (2.2)$$

instead of $\sigma_a'(\psi)$ (the actual normalized absorption cross-section).

Rancourt suggests a process by which a statistically perfect fit (i.e. where there are only small fluctuations of random sign between data and fit) of N Voigt lines to a spectrum can be used to generate the the normalized absorption cross-section, $\sigma_a'(\psi)$, for that sample.

The perfect fit spectrum would be represented by equation 2.3

$$y_{fit}(\psi) = BG - \sum_{k=1}^{N} V(h_k, \gamma_k, \sigma_k, \omega_k; \psi) \qquad (2.3)$$

where y_{fit} is the number of gamma-rays of energy ψ (or, alternatively, the number of gamma-rays counted in channel ψ), h_k is the height parameter for the k^{th} Voigt line, γ_k is the Lorentzian full width at half maximum (FWHM), σ_k is the Gaussian standard deviation, and ω_k is the energy corresponding to the center of the k^{th} Voigt line. No exact closed form analytic expression exists for $V(h_k, \gamma_k, \sigma_k, \omega_k; \psi)$, however analytic approximations [16] are sufficient.

Rancourt shows that, for a uniform absorber, the normalized absorber cross-section, $\sigma_a'(\psi)$, is given by

$$\sigma_a'(\psi) = -\ln\left[1 - \sum_k \eta_H f_S \, V\left(\frac{h_k}{\eta_H f_S}, \gamma_k - \Gamma_o, \sigma_k, \omega_k; \psi\right)\right] \qquad (2.4)$$

where f_s is the source's f-factor, Γ_o is the natural FWHM of the Mössbauer transition (0.09702 mm/s for the ^{57}Fe 14.4 keV transition), and η_H is the number of Mössbauer gamma rays (whether recoilless or not) that would have been counted in a channel during an experiment if an otherwise identical sample containing only non-Mössbauer isotopes had been used. The spectrum of an absorber with only ^{56}Fe would be the flat background, $BG = \eta_o + \eta_H$, η_o being those counts <u>not</u> due to Mössbauer gamma rays.

A plot of $\sigma_a'(\psi)$ versus ψ is essentially an emission spectrum corrected for the effects of sample thickness. So correcting a spectrum always involves determining $\eta_H f_s$ for that experiment. It is possible to obtain this value by several methods [17, 18], none of which are trivial.

The method presented and used here has two advantages over others. It is based on the temperature dependence of spectra which is also needed for the f-factor determination, thus killing two proverbial birds with one stone. Also, this method is not significantly more complex than other equally valid ones and, having been developed in this laboratory, it is the method with which we are most familiar and whose subtleties we best understand.

Several points form the basis of the utilized method:

Point #1: The normalization constraint on equation 2.4 is

$$\int_{-\infty}^{+\infty} \sigma_a'(\psi)\, d\psi = \frac{\pi}{2}\, n_a\, \overline{f_a}\, \sigma_o\, \Gamma_o \qquad (2.5)$$

where σ_o is the absorption cross-section at resonance, n_a is the total number of Mössbauer nuclei per unit area (normal to the gamma ray beam) in the sample and $\overline{f_a}$ is the effective f-factor for the absorber (a weighted mean of the site-specific f-factors: $n_a\overline{f_a} = \Sigma\, n_{a,i} f_{a,i}$, $n_{a,i}$ being the number of absorber nuclei per unit area in the i^{th} site).

Therefore, $\eta_M f_s$ can be determined knowing n_a and $\overline{f_a}$ by substituting equation 2.4 into equation 2.5. n_a can be obtained with accuracy by elemental analysis. $\overline{f_a}$, at a given temperature, can be obtained from the effective Debye temperature, $\overline{\theta_D}$.

Point #2: Recalling the arguments of section 1.4, the temperature dependence of a spectrum will be needed to obtain site-specific f-factors. These spectra can also be used to obtain $\overline{\theta_D}$. Spectra not yet corrected for thickness effects can be used to get a first guess of $\overline{\theta_D}$. This would most likely be an overestimate: as f-factors decrease with increasing temperatures, so do the thickness effects, and the result will overestimate $\overline{\theta_D}$.

Point #3: For pairs of spectra accumulated under identical conditions except for their temperatures, T_1 and T_2, the following constraint must hold on their values of $\eta_M f_S$

$$\frac{BG(T_1)}{BG(T_2)} \cdot \frac{f_S(T_1)}{f_S(T_2)} = \frac{\eta_M\, f_S(T_1)}{\eta_M\, f_S(T_2)} \qquad (2.6)$$

where $BG(T_i)$ is the background number of counts for the experiment at temperature T_i, $f_S(T_i)$ is the source's f-factor during the experiment in which the absorber was at temperature T_i (the source could be at some other temperature).

Using this information (points #1 to #3, above), an algorithm was constructed to obtain $\eta_M f_S$ self-consistently and correct spectra for absorber thickness effects. The following flow diagram describes the process...

$$\overline{\theta_D} \longrightarrow \bar{f}\ (T_1) \longrightarrow \eta_M f_S\ (T_1) \longrightarrow \eta_M f_S\ (T_2) \longrightarrow \bar{f}\ (T_2) \qquad (2.7)$$

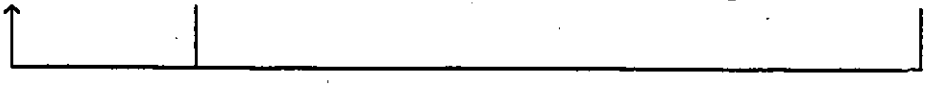

By iterating enough times, the $\overline{\theta_D}$ consistent with all above constraints is found. Equation 1.2 is used to obtain $\overline{f}(T_1)$ from the first guess of $\overline{\theta_D}$ (T_1 and T_2 are known), equations 2.4 and 2.5 are used to get $\eta_M f_S(T_1)$, then equation 2.6 gives $\eta_M f_S(T_2)$, and the normalization constraint (2.5) allows the calculation of $\overline{f}(T_2)$ from $\eta_M f_S(T_2)$. The $\overline{\theta_D}$ that best gives $\overline{f}(T_1)$ and $\overline{f}(T_2)$ (as derived from equation 1.2) is obtained and the loop is repeated until convergence is attained ($\Delta\overline{\theta_D} < 0.1$ K). Convergence is always rapid, unique, and unambiguous, typically requiring about five iterations.

The computer code for this algorithm is given in Appendix 3; the main point is that it allows the determination of values of $\eta_M f_S$ for pairs of spectra. And these values are then used to generate spectra corrected for thickness effects.

A final note concerns spectral areas of fits to be presented in the following chapters. The area of a Voigt peak, $\int_{-\infty}^{+\infty} V(h,\gamma,\sigma,\omega;\psi)d\psi$, is $\pi h\gamma/2$ (if γ is the FWHM). But the "areas" of peaks as presented in this thesis will correspond to $h\gamma/2$, where h has been arbitrarily increased by a factor of 10^5 (recall equation 2.2). So, should the reader wish to obtain an f-factor from the total area of a thickness-corrected spectrum presented herein, the following

formula must be used:

$$\bar{f} = \frac{2 \times 10^{-5}}{n_a \sigma_o \Gamma_o} \times \text{(Total area quoted)} \qquad (2.8)$$

since the total area quoted corresponds to $\Sigma (h_k \gamma_k / 2)$.

3. Preliminary study of f-factors from the temperature dependence of spectra

3.1 Overview of the chapter

A first attempt in this thesis to demonstrate the site-specific nature of the f-factors of true trioctahedral micas was the analysis of an experiment performed by Peter Hargraves in our laboratory. In this experiment, spectra of a biotite single crystal (MOC2661) were accumulated at five temperatures between liquid nitrogen and room temperatures but under otherwise identical conditions. An early analysis of this experiment was presented at the GAC-MAC conference in Vancouver, B.C., in May of 1990 [19].

From this preliminary study, we concluded that $f^{[3+]} > f^{[2+]}$. This conclusion is based on the comparison of $[Fe^{2+}]$ and effective Debye temperatures obtained from the MOC2661 spectra once corrected for thickness effects.

The method for determining the value of the effective Debye temperature, $\overline{\theta_D}$, necessary to thickness-correct the spectra is discussed in the following section (3.2). Included is additional information obtained from the MOC2661

spectra prior to thickness-corrections.

The thickness-corrected spectra are presented in section 3.3. It is from these spectra that the [Fe^{2+}] Debye temperature, $\theta_D^{[2+]}$, is calculated using the temperature dependence of peak C.

The final section of this chapter deals with the difficulties encountered during this preliminary experiment, and suggests methods to counter these problems in the next set of experiments. Particular attention is paid to the difficulties involved in determining the spectral area of a peak when it overlaps with adjacent peaks.

3.2 Uncorrected spectra and the determination of the effective Debye temperature

The spectra prior to thickness-effect corrections are shown in figures 3.1 (a-e). These figures also show the perfect fits drawn through the data and, above them, the difference spectra (differences between fit and data). The parameters which describe these fits (and, in fact the parameters for <u>all</u> fits used in this thesis) are given in Appendix 4 (A4.1 - A4.2 for these fits).

These spectra serve two main purposes. They are used

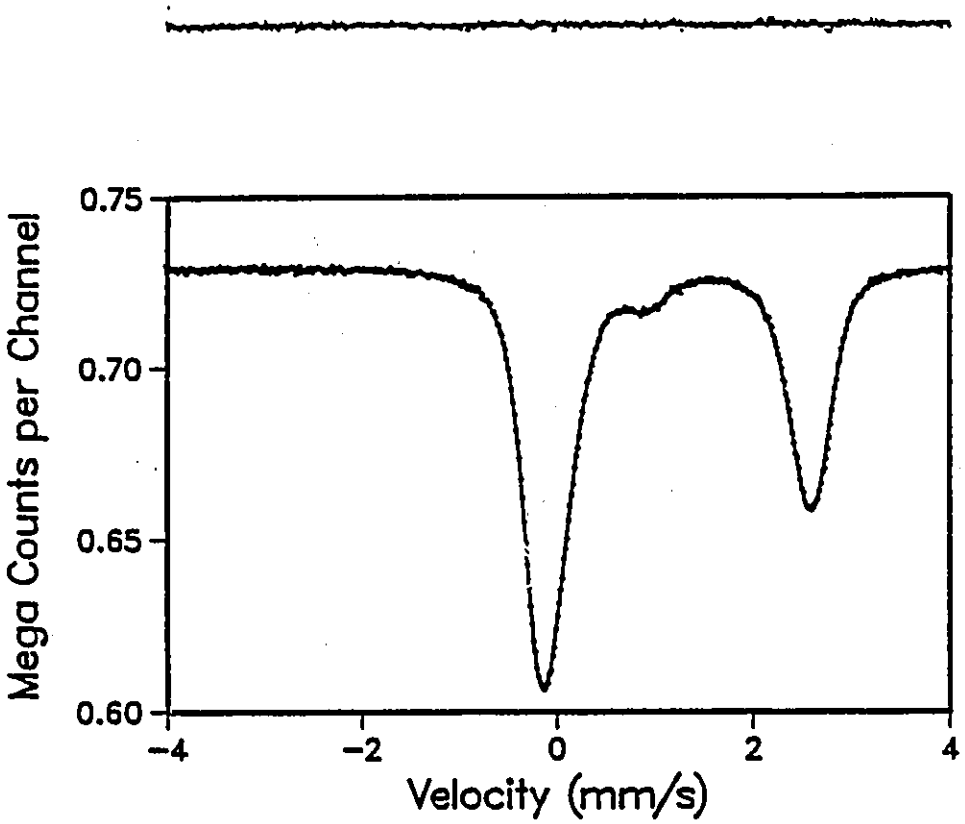

Figure 3.1 (a) Uncorrected 106 K spectrum of MOC2661. The vertical scale of the difference spectrum is the same as for the data above which it is shown.

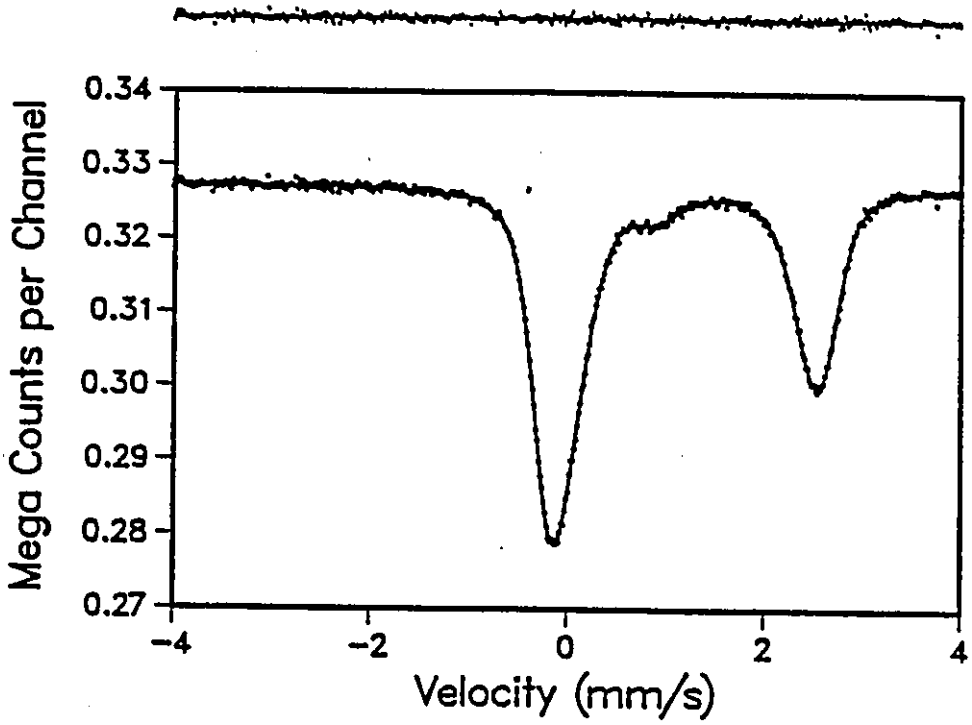

Figure 3.1 (b) Uncorrected 158 K spectrum of MOC2661.

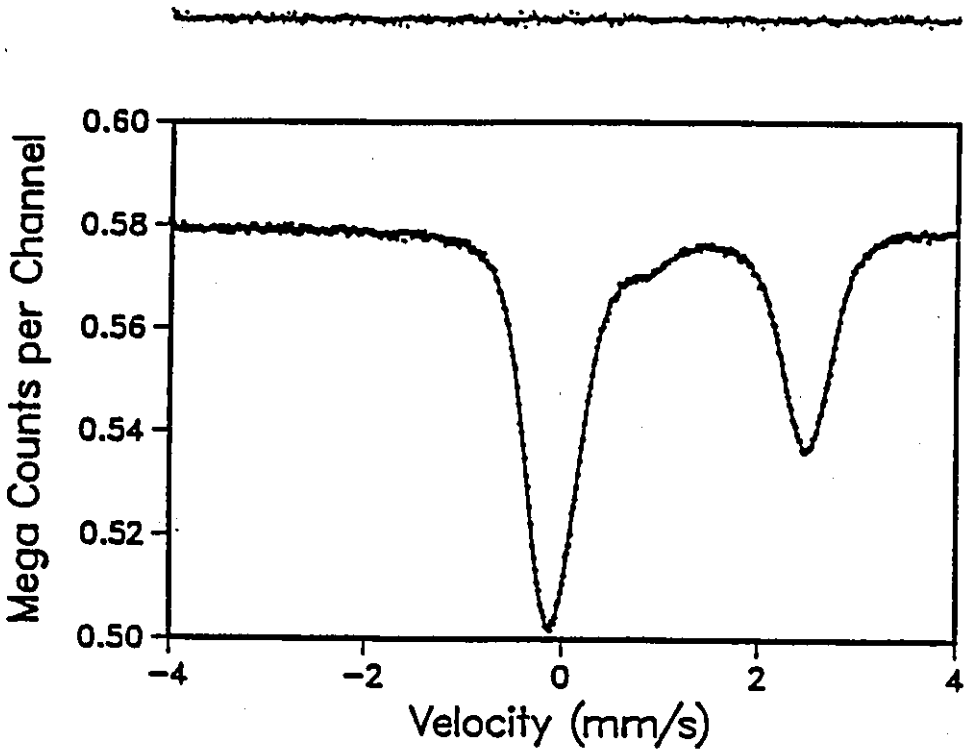

Figure 3.1 (c) Uncorrected 187 K spectrum of MOC2661.

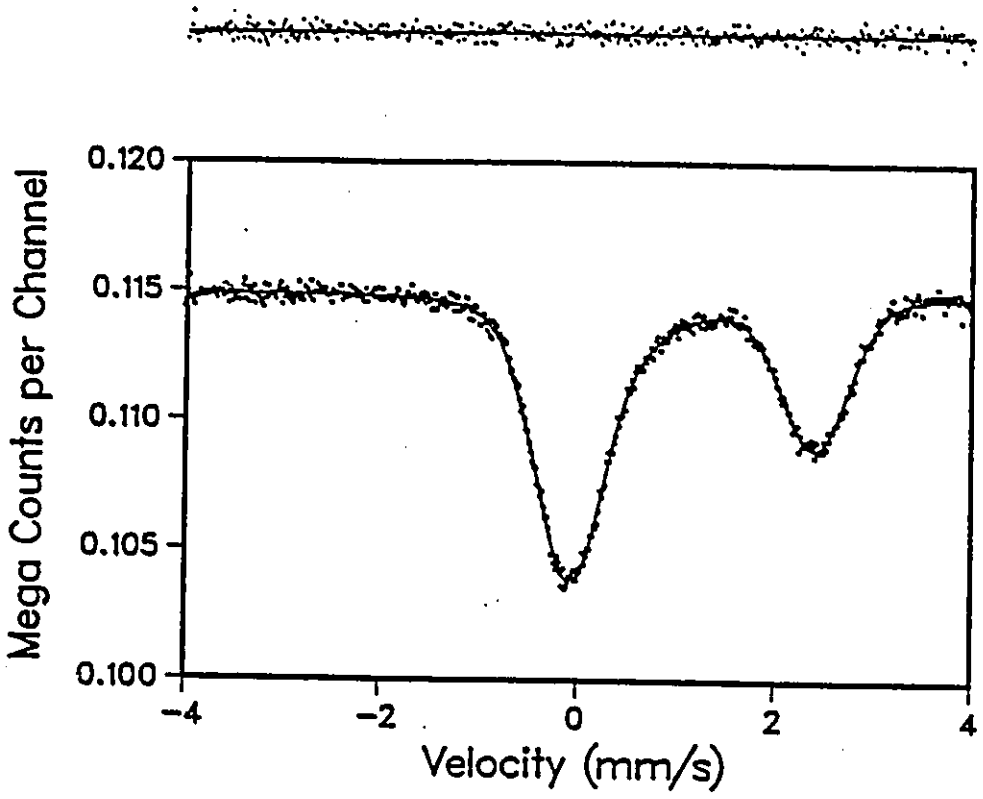

Figure 3.1 (d) Uncorrected 244 K spectrum of MOC2661.

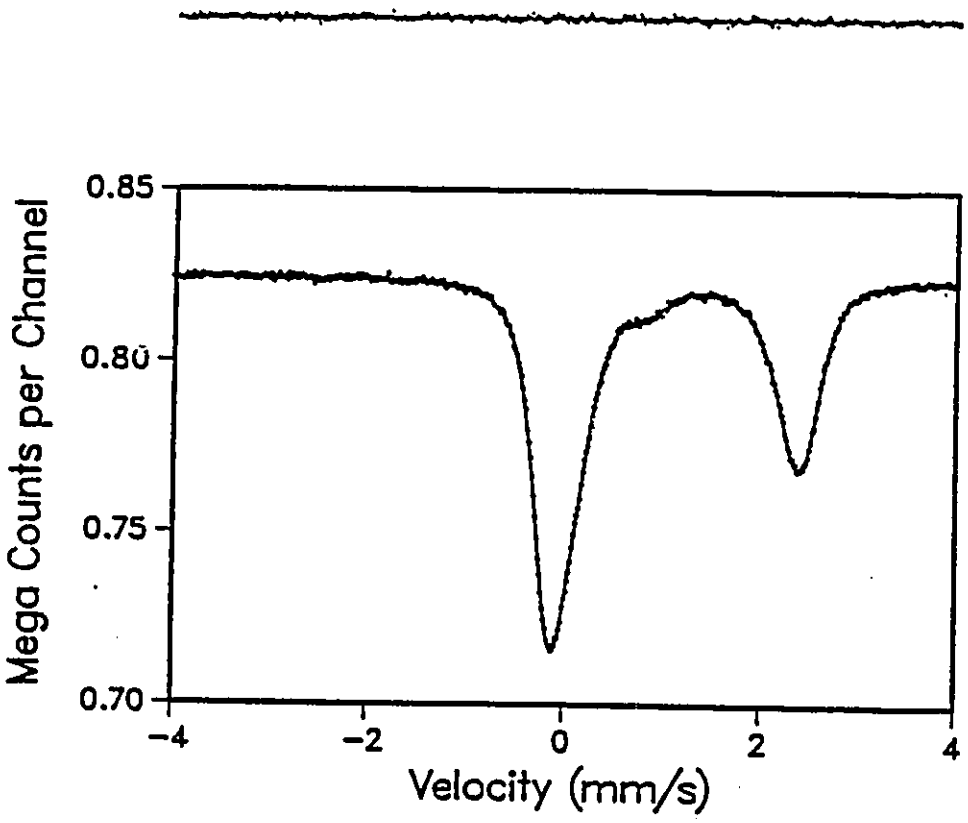

Figure 3.1 (e) Uncorrected 296.5 K spectrum of MOC2661.

to generate thickness-corrected spectra from which accurate Debye temperatures are determined. They are also used to obtain the effective Debye temperature which is necessary to generate the thickness-corrected spectra. This $\overline{\theta_D}$ is determined from the temperature dependence of the total spectral area; Table 3.1 thus lists the temperature and total spectral area of each MOC2661 spectrum (the areas of peak C are also included).

Note that Table 3.1 presents areas normalized by spectral background (BG). This arises because the time of spectral accumulation varied from spectrum to spectrum. It is, though, the background which must be used to normalize spectral areas to allow comparisons between spectra. It is a better parameter than time, for small changes in absorber alignment (due to thermal contraction of the cold finger, or actual nudging of the cryostat during the experiment) could change the fraction of the absorber irradiated. The background and spectral areas would remain proportional to each other, but spectral area and time would not remain so (nor would BG and time). Sample to sample fluctuations in BG/time were used as an estimate of the uncertainty in spectral areas normalized by the background.

Now before determining $\overline{\theta_D}$, consider first what information can be obtained from the five uncorrected

spectra of MOC2661. It can be seen from figures 3.1 (a-e) that spectra between those at room and liquid nitrogen temperatures suffer from line broadening. This is due to vibrations arising from nitrogen boil-off (which is more violent when the cold-finger is heated, as is necessary for these intermediate spectra). This broadening should not, however, affect the total area of the spectrum.

It also appears from these spectra that the relative area of peak C is decreasing with temperature. The relative areas of peak C as indicated by the perfect fits (Table 3.1) generally concur with this observation. If this decrease is real, it implies the [Fe^{2+}] Debye temperature is less than the effective Debye temperature... and thus less than that of [Fe^{3+}] as there are no other contributions to the spectrum [11].

The uncorrected data has suggested $\theta_D^{[2+]} < \theta_D^{[3+]}$ ($f^{[2+]} < f^{[3+]}$). Now, to best measure these site-specific Debye temperatures, the spectra must be corrected for absorber thickness effects. To generate the thickness-corrected spectra, $\overline{\theta_D}$ was required; it was hence determined from the temperature dependence of the total spectral area (normalized by the background number of counts in the spectrum).

These normalized areas are proportional to the effective f-factor of the sample. By multiplying both sides of equation 1.2 by this constant and fitting this equation to the normalized total areas of Table 3.1, both the proportionality constant and the effective Debye temperature can be determined. Figure 3.2 illustrates the value of $\overline{\theta_D}$ obtained from the best fit of the (normalized) spectral area versus temperature curve for MOC2661. It corresponds to an effective Debye temperature of 310 K ± 10 K, maximum error boxes considered.

Using this effective Debye temperature of 310 K ± 10 K, the values of $\eta_M f_S$ needed to perform the thickness-corrections for each spectrum were calculated. This value of $\overline{\theta_D}$ has one major drawback: because of how thickness effects decrease with decreasing effective f-factor (and increasing temperature), the temperature dependence of uncorrected spectra provides an overestimate of $\overline{\theta_D}$ that will generate spectra whose areas are overestimated, and all the more so at higher temperatures. The implication of this statement is that site-specific and effective Debye temperatures obtained from these "corrected" spectra will also be overestimated.

Table 3.1 Absorber temperatures and spectral areas, MOC2661

Temperature (K)	Area / Background (mm/s)		Relative Areas (Area / Total)
	Peak C	Total	Peak C
106 ± 3	0.0200	0.0591	0.338
158 ± 3	0.0181	0.0542	0.333
187 ± 7	0.0175	0.0524	0.334
244 ± 4	0.0151	0.0488	0.309
296.5 ± 1.5	0.0148	0.0461	0.321

Table 3.2 Spectral areas of MOC2661 after thickness-corrections

Temperature (K)	χ^2	Areas (cts•mm/s)			Area / Total	
		Peak B	Peak C	Total	Peak B	Peak C
106	21	1047	7866	25654	0.0408	0.307
158	13	900	7064	23914	0.0376	0.295
187	7	943	7075	22898	0.0412	0.308
244	3	1033	6577	21541	0.0480	0.305
296.5	2	799	5827	19855	0.0402	0.293

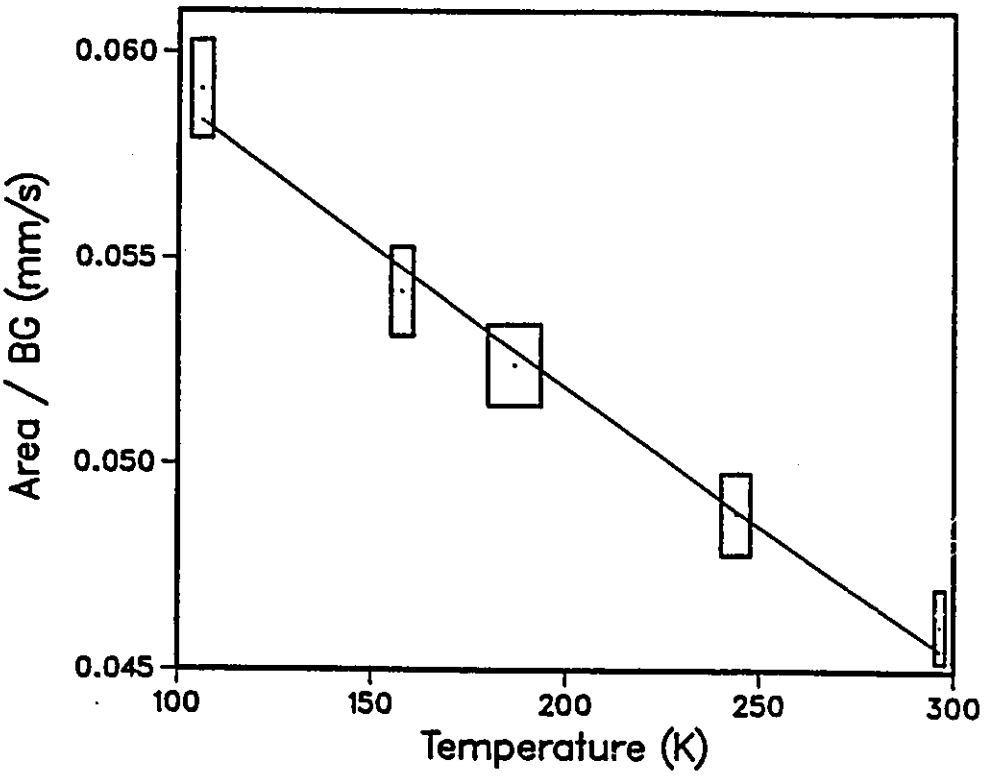

Figure 3.2 Effective Debye temperature obtained from the temperature dependence of the uncorrected total area normalized by background.

3.3 Results from thickness-corrected MOC2661 spectra

The thickness-corrected spectra (i.e., plots of 1000000 - 100000·$\sigma_a'(\psi)$ versus ψ) for MOC2661 are shown in figures 3.3 (a-e), along with the curves of best fit and difference spectra. The parameters for these fits are again given in Appendix 4 (A4.3) with peak areas (for B, C, and total area) being summarized in Table 3.2. From the temperature dependence of peak C, $\theta_D^{[2+]}$ was determined (overestimated, rather). Figure 3.4 illustrates this temperature dependence. The errors in temperature are the same as in Table 3.1; a 2% uncertainty in area was estimated (corresponding to the uncertainty in normalized total area of the uncorrected spectra and the uncertainty in BG/time). As a result, a $\theta_D^{[2+]}$ of 296 ± 10 K was obtained; its curve is also shown in figure 3.4.

From the temperature dependence of the total thickness-corrected spectral area, $\overline{\theta_D}$ was recalculated. Figure 3.5 illustrates the best fit to the total corrected area versus temperature curve, with $\overline{\theta_D}$ = 309 ± 20 K. It was expected that this value be very close to the effective Debye temperature used to thickness-correct these spectra ($\overline{\theta_D}$ = 310 K) as these spectra were generated and normalized using this effective Debye temperature. Verifying the $\overline{\theta_D}$ versus temperature curve provides a self-consistency check which

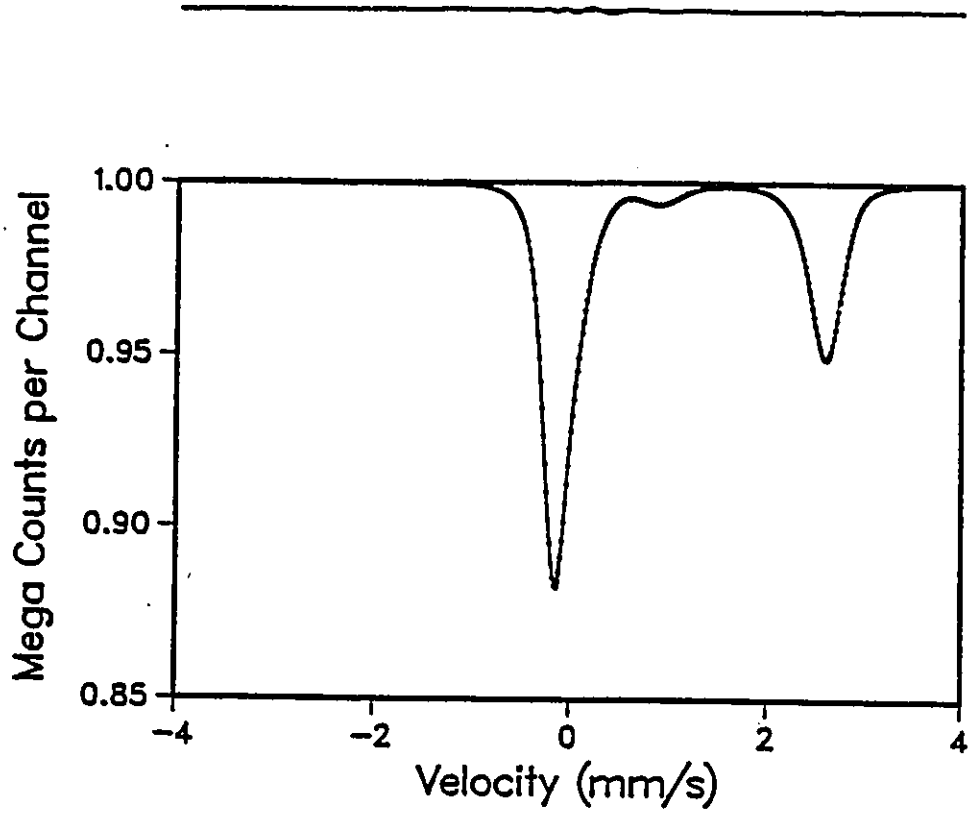

Figure 3.3 (a) Thickness-corrected 106 K MOC spectrum.

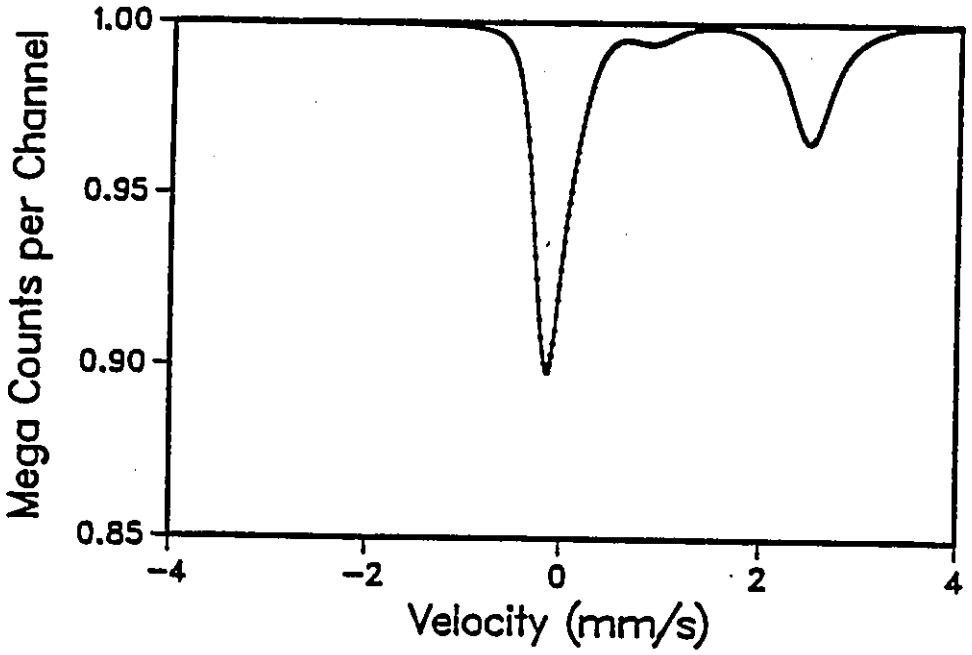

Figure 3.3 (b) Thickness-corrected 154 K MOC spectrum.

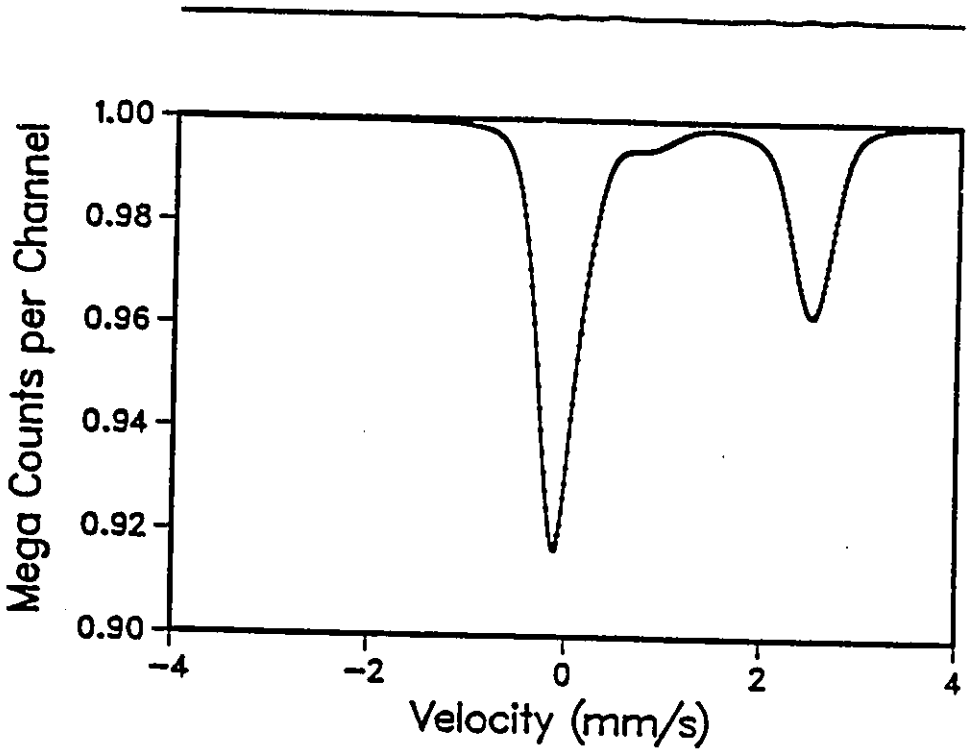

Figure 3.3 (c) Thickness-corrected 187 K MOC spectrum.

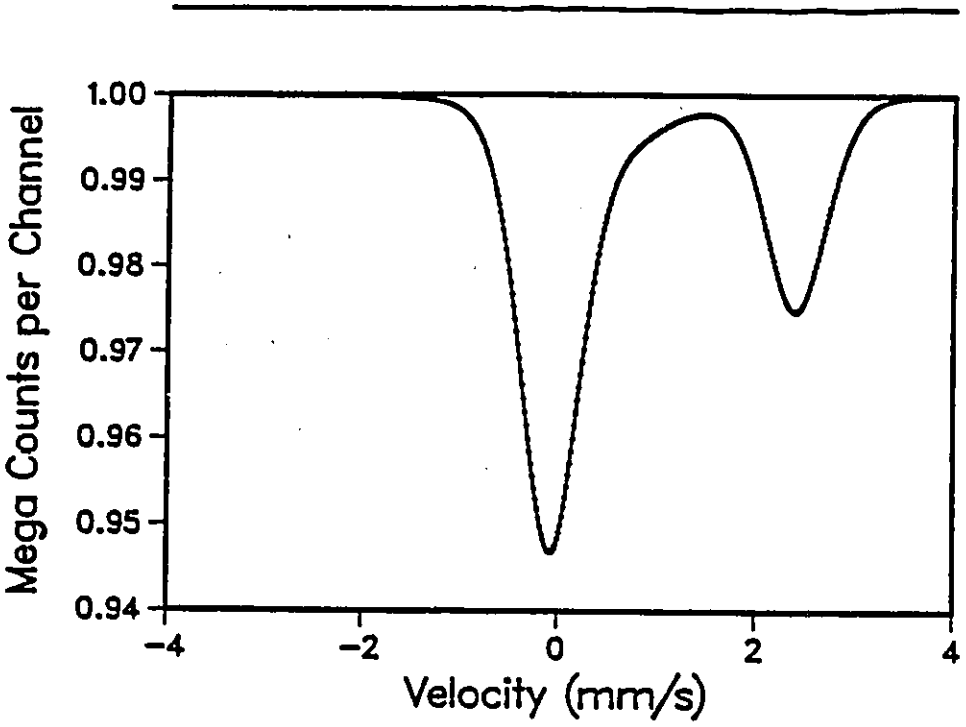

Figure 3.3 (d) Thickness-corrected 244 K MOC spectrum.

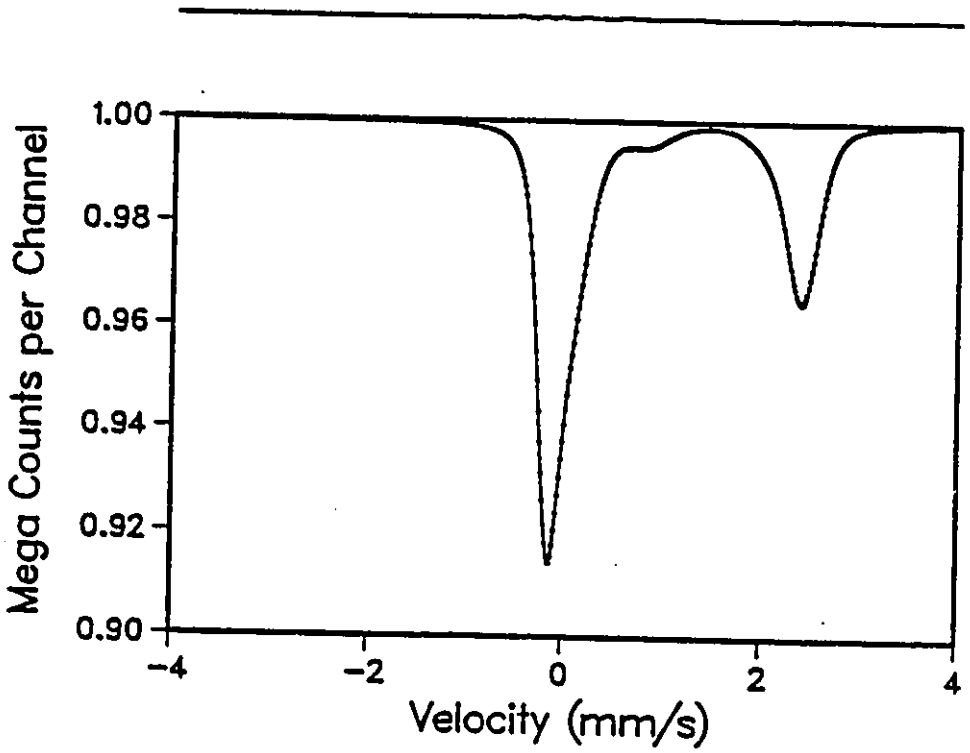

Figure 3.3 (e) Thickness-corrected 296.5 K MOC spectrum.

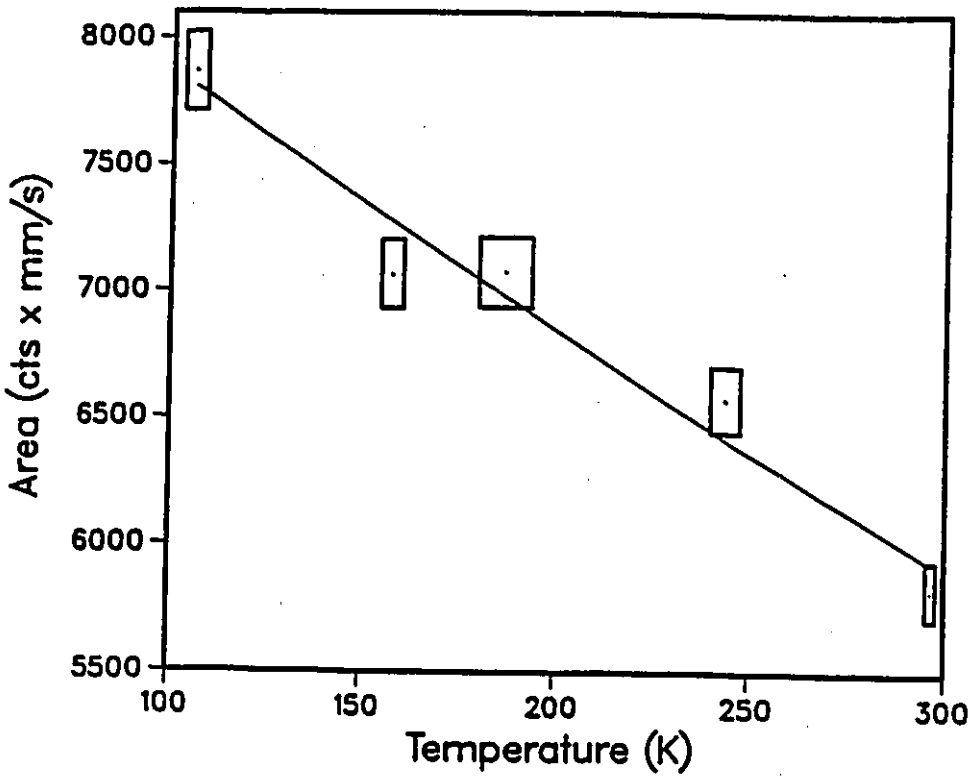

Figure 3.4 [Fe^{2+}] Debye temperature obtained from the temperature dependence of the thickness-corrected spectral area of peak C.

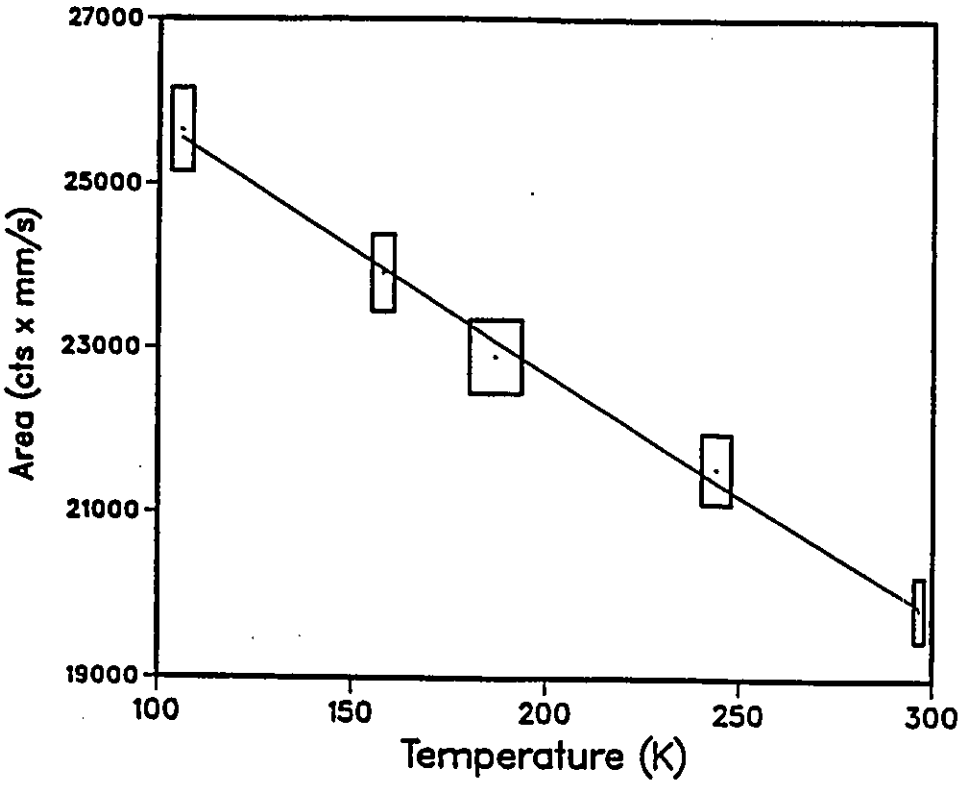

Figure 3.5 Effective Debye temperature obtained from the temperature dependence of the thickness-corrected total spectral area.

points out any improperly generated thickness-corrected spectra.

The object of this section is to determine site-specific Debye temperatures and f-factors. $\theta_D^{[2+]}$ and $\overline{\theta_D}$ have been calculated, the [Fe^{3+}] Debye temperature should also be determined. It should be possible to measure $\theta_D^{[3+]}$ the same way $\theta_D^{[2+]}$ was measured, except using the temperature dependence of peak B instead of peak C. But Table 3.2 shows the area of peak B to fluctuate significantly. This fluctuation arises from peak B being small and near peak A. The area in the overlap between these peaks is split differently in different fits, thus causing the fluctuations. And, peak B being small, these fluctuations are significant enough to prevent a meaningful calculation of $\theta_D^{[3+]}$.

So $\theta_D^{[3+]}$ was not calculated for this experiment. And $\theta_D^{[2+]}$, as explained in the previous section, is an overestimate. This experiment has thus failed to produce accurate site-specific f-factors and Debye temperatures. But it may still demonstrate their site-specific nature if it can be shown that $\theta_D^{[2+]} < \overline{\theta_D}$ (which must then be less than $\theta_D^{[3+]}$ as there are no other contributions to the spectrum).

Compare then $\theta_D^{[2+]} = 296 \pm 10$ K to $\overline{\theta_D} = 310 \pm 10$ K (or to $\overline{\theta_D} = 309 \pm 20$ K). Although the difference between $\theta_D^{[2+]}$ and $\overline{\theta_D}$ does not appear to be significant, one must consider that their uncertainties due to fluctuations in temperature and BG/time ratios are related. That is, the errors in temperature and BG/time must have the same sign for both $\overline{\theta_D}$ and $\theta_D^{[2+]}$ calculations. The uncertainties in both these Debye temperatures due to absorber temperature and BG/time are thus of the same sign, so in the difference, $\overline{\theta_D} - \theta_D^{[2+]}$, these uncertainties nearly cancel. Hence the uncertainty in $\overline{\theta_D} - \theta_D^{[2+]}$ is smaller than the uncertainty of either Debye temperature. And, given the values at the start of this paragraph for $\overline{\theta_D}$ and $\theta_D^{[2+]}$, it can be concluded that the difference between $[Fe^{2+}]$ and effective Debye temperatures in this sample is indeed real.

3.4 *Experimental difficulties to be considered for improving subsequent experiments*

Beyond determining that $\theta_D^{[2+]} < \theta_D^{[3+]}$ (and that $f^{[2+]} < f^{[3+]}$), these experiments have also illustrated which factors required consideration in an improved set of experiments. These factors and sources of error are addressed in the following paragraphs.

To obtain the best $\overline{\theta_D}$, pairs of spectra can be used

with algorithm 2.7 to avoid the overestimate of the effective Debye temperature which occurs when $\overline{\theta_D}$ is obtained from the temperature dependence of uncorrected spectra. To rely on only two spectra, excellent temperature control is crucial since small fluctuations can have a significant impact on $\overline{\theta_D}$. To this end, the cryostat was improved and the temperature fluctuations and gradients were reduced to 1 K at 82 K and 0.1 K at 305.0 K.

Also, choosing the room and liquid nitrogen temperature spectra as the pair to be used eliminates the boil-off problem which characterized the spectra accumulated between these temperatures. It is unclear how much faith can really be placed in the spectra affected by nitrogen boil-off. The total spectral area should remain unaffected... but this is difficult to prove. Eliminating these questionable spectra improves the confidence one can have in the spectral areas.

Another crucial factor which must be considered and properly handled is the overlap of peaks. In MOC2661, the area of peak B was significantly affected by overlap with peak A. In future samples, the presence of peak D will present a further source of overlap. Several steps can be followed to minimize the uncertainties in peak areas due to overlap. The first is to obtain samples rich in Fe^{3+} to insure large areas for peak B (and/or D). This also

accentuates the difference between $\overline{\theta_D}$ and $\theta_D^{[2+]}$. The biotites selected for the next series of experiments were chosen expressly for their relatively large $[Fe^{3+}]$ content.

The second step to combat overlap difficulties is to allot enough time for data acquisition to insure excellent signal-to-noise ratios for the spectra, as improvements in signal-to-noise ratios also improve the resolution of the spectral peaks.

And, most importantly, great care must be taken when obtaining spectral fits. The fits to the peaks which overlap should be examined visually: if the fit to the visible part of the peak doesn't look "good" (e.g., the fit appears too wide or too narrow for the peak), the portion overlapping with the neighbouring peak is probably not well fit either.

The parameters describing the fit must also be examined to insure no line was placed in (or too near) the area of overlap. The reasoning behind this suggestion is that if narrow lines near the center of a peak fit the visible part of the peak well, then the portion of the peak that overlaps with its neighbour should also be well fit. That is, one can have confidence that the areas within the overlap have been correctly shared between the adjacent peaks if these

peaks appear well fit by narrow, well separated lines.

There are no absolute criteria which determine how separate or narrow lines must be to insure the overlap of peaks is properly handled (consider, for instance, that a physical peak may actually exist in the area of overlap). The guideline used in this thesis is to consider $\omega \pm (\sigma + \gamma/2)$ for each Voigt line in a spectrum. Recall that ω is the center position of a Voigt line, $V(h, \gamma, \sigma, \omega; \psi)$, modelling a peak, σ is its Gaussian standard deviation, and γ is the FWHM of the underlying Lorentzian line; $\sigma + \gamma/2$ is a measure of the width of the Voigt. If $\omega \pm (\sigma + \gamma/2)$ of one line overlaps with $\omega \pm (\sigma + \gamma/2)$ of a line in an adjacent peak, then the areas of these Voigts (and peaks) are not considered to be resolved, and only their sum is trusted.

To accurately determine the uncertainty in peak area due to overlap, one should produce several fits, systematically varying the number of lines used, their positions, widths, and heights, as well as underlying Lorentzian width and background, to determine the maximum and minimum area for each overlapping peak that could be obtained from the various physical fits.

However, a thorough and accurate determination of the

maximum and minimum possible areas for each overlapping peak is a very tedious process. A more practical method of estimating uncertainties due to peak overlap is to select a test sample and obtain several fits to it – varying the number of Voigt lines, the width and positions of peaks, "first guesses" of the parameters in the minimization program, etc. – then eliminate visually unacceptable fits and those with $\omega \pm (\sigma + \gamma/2)$ overlap, and see how much variation exists in the areas of the overlapping peaks in the remaining fits. These variations provide estimates of the uncertainty in the peak areas; furthermore, these uncertainties can be used as an estimate of the uncertainties in the areas of the corresponding peaks in other spectra – provided the fits to these other spectra meet the same restrictions concerning $\omega \pm (\sigma + \gamma/2)$ overlap and visual correctness of fit. This method of determining uncertainties in spectral areas will be applied in the following chapter.

4. Main study of temperature dependence

4.1 An overview of the chapter

The ultimate objective of this chapter is to accurately determine the 80 K and 300 K f-factors for the [Fe^{2+}], [Fe^{3+}], and <Fe^{3+}> sites of true trioctahedral mica. As such, it is the principal chapter of this thesis.

To achieve its objective, this chapter will study five samples, obtain site-specific and effective Debye temperatures from their uncorrected spectra, then generate thickness-corrected spectra which will also be used to obtain site-specific and effective Debye temperatures. From these last values the desired f-factors will be calculated.

Problems encountered with MOC2661 (i.e., peak overlap) will be addressed. Other difficulties will also be discussed, such as the effect on Debye temperatures of the uncertainty in parameters used during the generation of thickness-corrected spectra (parameters such as absorber temperature, n_a, and source f-factor). The sample-to-sample differences in Debye temperature are examined (can they be explained by the experimental uncertainties?) and, finally,

the best values to date of the site-specific 80 K and 300 K f-factors are presented.

4.2 *Spectra prior to thickness-corrections*

4.2.1 *Presentation of uncorrected spectra*

Of the five samples studied in this section, three are biotites selected because of their large [Fe^{3+}] contribution and the total absence of <Fe^{3+}> in their spectra. They should exhibit areas for peak B which are easier to measure than was the case with MOC2661. The MCC phlogopite was chosen because of a large <Fe^{3+}> content. It was not believed to contain any [Fe^{3+}], but the analyses of thi chapter indicated an [Fe^{3+}] contribution to the spectrum. The annite was not selected because of relatively large areas of peaks B and/or D (they are in fact relatively small and not well resolved), but because knowledge of its [Fe^{3+}] and <Fe^{3+}> site populations was desired.

Spectra were accumulated for each of these materials at liquid nitrogen and room temperatures; these are illustrated in figures 4.1 (a-e) along with the perfect fits through the data and the difference spectra. As with MOC2661, peak areas from these fits are normalized by spectral background (BG) to allow comparisons between spectra (of the same

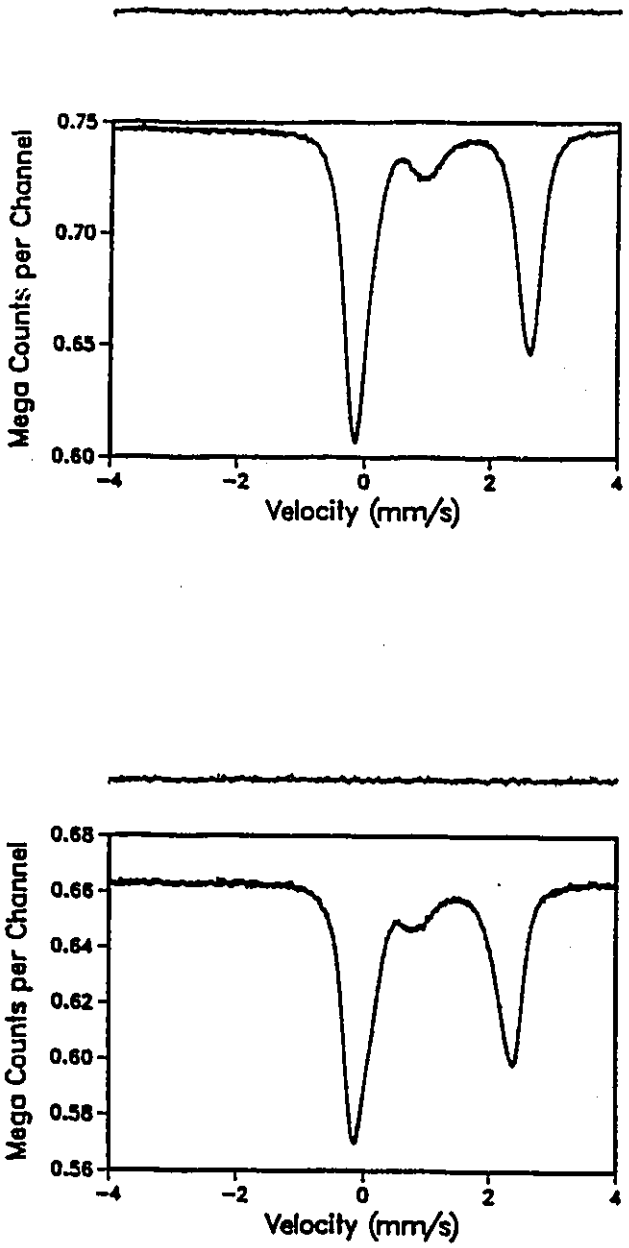

Figure 4.1 (a) Uncorrected 82 K (top) and 305 K (bottom) spectra for BZ53.

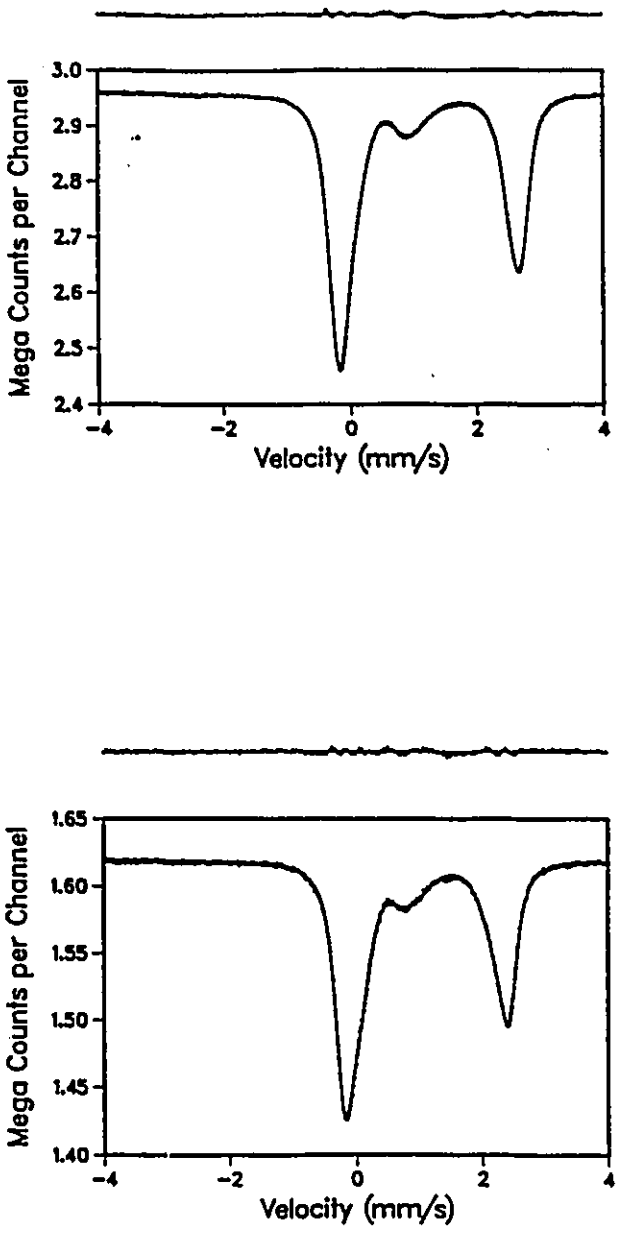

Figure 4.1 (b) Uncorrected 82 K (top) and 305 K (bottom) spectra for BL315.

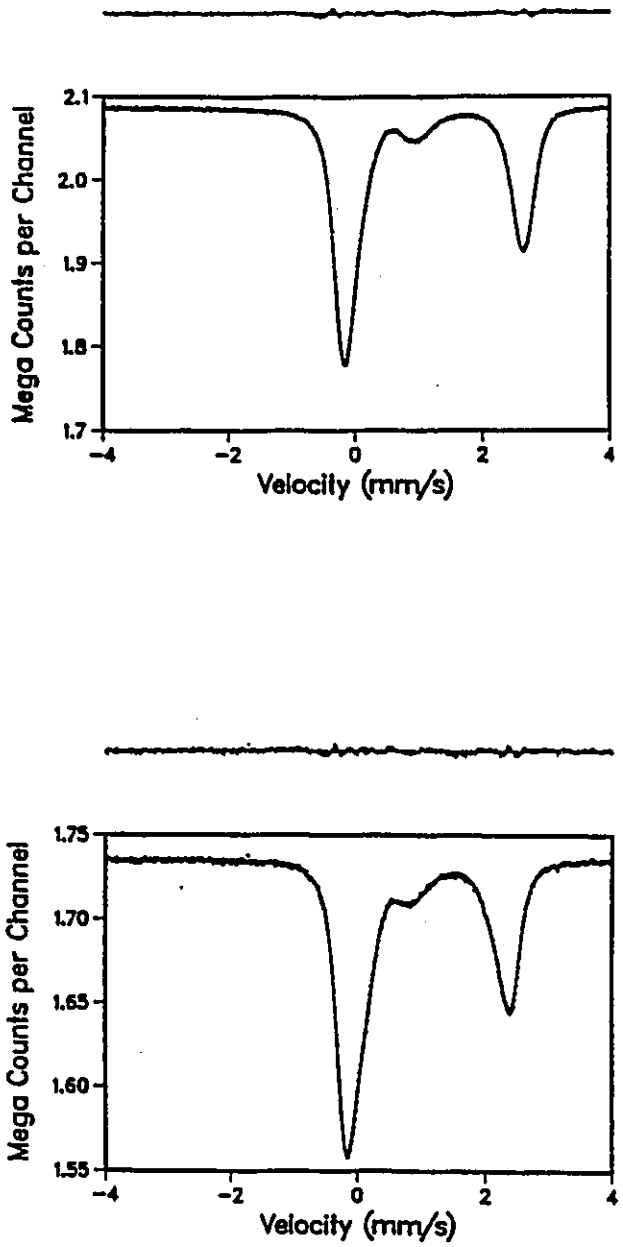

Figure 4.1 (c) Uncorrected 82 K (top) and 305 K (bottom) spectra for BL531.

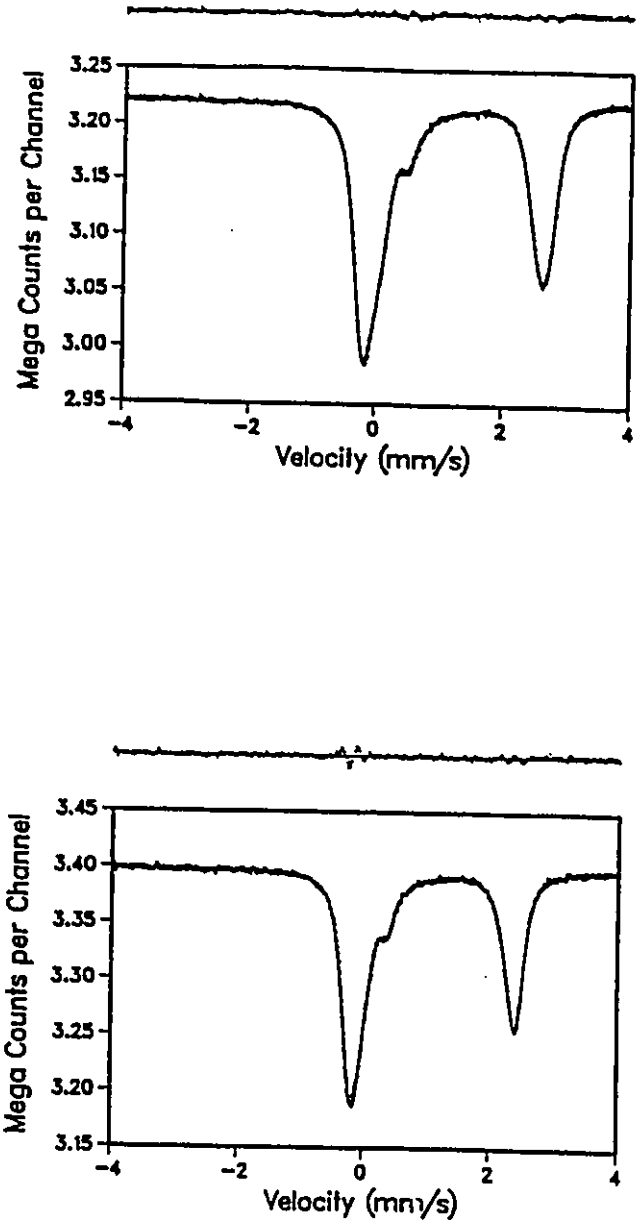

Figure 4.1 (d) Uncorrected 82 K (top) and 305 K (bottom) spectra for MCC.

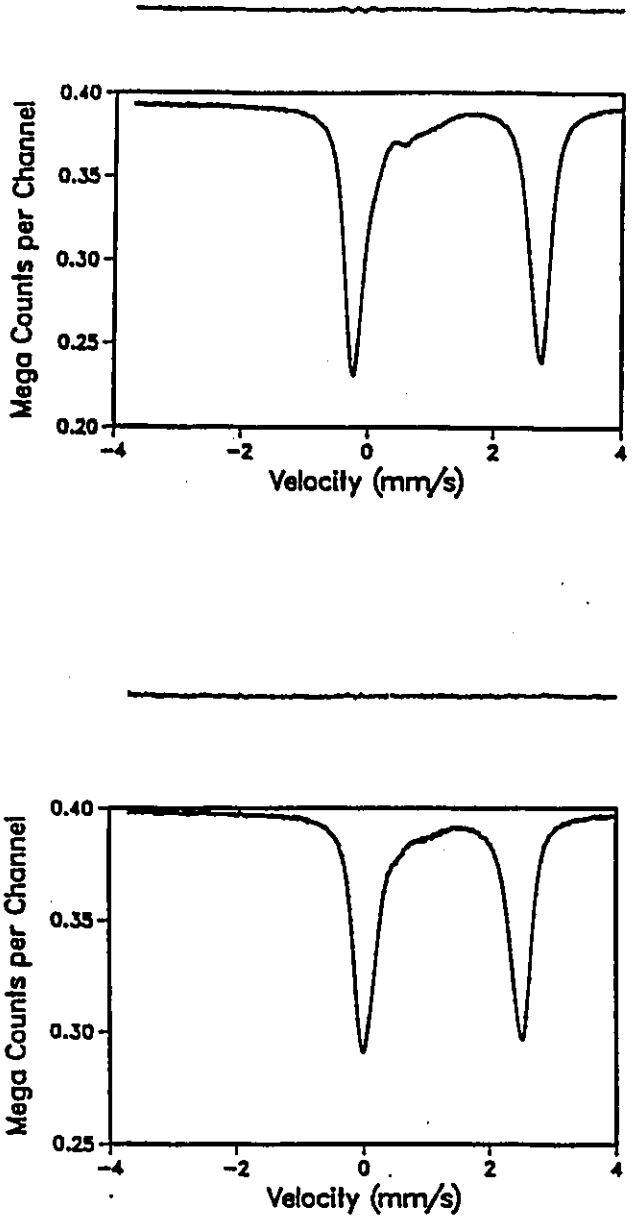

Figure 4.1 (e) Uncorrected 83 K (top) and 300 K (bottom) spectra for IKO.

sample); these peak areas being given in Table 4.1 (with the parameters of the best fits in Appendix 4: A4.4 - A4.6).

4.2.2 *Estimation of uncertainties in peak areas*

Although one could, at this point, simply generate the thickness-corrected spectra for each sample and make no further use of the uncorrected spectra, it was deemed worthwhile to obtain additional information from these raw spectra.

In particular, BZ53 was chosen as a test sample with which the uncertainties in peak areas (including the uncertainty due to peak overlap) could be measured, as suggested at the end of chapter 3 of this text. The uncertainties obtained for its peak areas can be used as an estimate for the uncertainties of the corresponding peaks in other spectra, including spectra corrected for thickness effects.

The normalized and relative areas resulting from eight fits to BZ53 (four fits at 305 K, four at 83 K) are shown in Table 4.2 (with the complete list of fitting parameters being in App. 4: A4.7 - A4.9). The number of lines used to fit the peaks varies from fit to fit, producing a variety of line positions and widths.

Table 4.1 Normalized and relative peak areas of perfect fits

Sample	χ^2	Temp. (K)	Area / Background (mm/s) Peak B*	Peak C	Total	Area / Total Peak B*	Peak C
BL531	591	82	0.00380	0.0149	0.0463	0.0821	0.322
BL531	410	305	0.00297	0.0103	0.0341	0.0871	0.300
BL315	1067	82	0.00578	0.0203	0.0588	0.0982	0.345
BL315	545	305	0.00463	0.0149	0.0440	0.105	0.339
MCC	397	82	0.00330	0.00956	0.0276	0.120	0.346
MCC	500	305	0.00209	0.00664	0.0198	0.106	0.335
IKO	435	83	0.0123	0.0650	0.1480	0.0831	0.439
IKO	306	300	0.00886	0.0449	0.1008	0.0879	0.445
BZ53	366	82	0.00634	0.0248	0.0669	0.0948	0.371
BZ53	287	305	0.00498	0.0193	0.0526	0.0947	0.367

* Includes area of peak D when present (IKO, MCC).

Table 4.2 Normalized and relative areas from fits to BZ53

# lines A-D-B-C	Background (counts)	γ_h (mm/s)	χ^2	Temp. (K)	Area / Total Peak B	Area / Total Peak C	Area / Background (mm/s) Peak B	Area / Background (mm/s) Peak C	Area / Background (mm/s) Total
2-0-1-2	663438	0.107	438	305	0.0988	0.364	0.00525	0.0193	0.0531
5-0-2-2	663385	0.0970	503	305	0.102	0.363	0.00535	0.0192	0.0527
4-0-1-4	663430	0.0970	521	305	(0.075)*	0.363	(0.00399)	0.0192	0.0530
3-0-1-3†	663365	0.0916	287	305	0.0947	0.367	0.00498	0.0193	0.0526
3-0-3-4†	747414	0.0960	366	82	0.0948	0.371	0.00634	0.0248	0.0669
2-0-1-2	747054	0.0960	442	82	0.0942	0.369	0.00623	0.0244	0.0661
3-0-2-3	746649	0.0413	367	82	(0.155)	(0.347)	(0.00994)	(0.0222)	0.0640
3-0-2-4	746543	0.0413	413	82	0.108	0.368	0.00689	0.0234	0.0636

† Perfect fit used to generate thickness-corrected spectrum.

* Values in brackets are suspect because of overlap between peaks A and B (χ^2 = 521) or because of an unphysically wide line in peak B (χ^2 = 367).

The first piece of information to be extracted from Table 4.2 is the accuracy with which the background is determined: less than 0.1% fluctuations (this is relevant because equation 2.6 of the thickness-correction algorithm requires accurate values of BG). Next, an examination of the normalized and relative areas shows the numbers in brackets to differ significantly from the others. Verifying their fits shows, for χ^2 = 521, a line for peak A at 0.468 ± 0.349 mm/s which definitely overlaps with the line at 0.909 ± 0.269 mm/s of peak B, explaining the significantly smaller area for peak B in this fit. (No such overlap was obtained in the other fits which produced equally good values of χ^2.)

For the χ^2 = 367 fit, a σ of 0.982 mm/s was attributed to a line at 0.884 mm/s. Normally values of σ are about 0.1 mm/s in fits to mica spectra, and values greater than 0.30 to 0.35 mm/s should be considered unphysical. As a result, a significant amount of area normally attributed to peak C is being attributed to peak B in this fit, hence the large B areas and small C areas.

To avoid unphysical lines in subsequent mica fits and to help prevent the improper positioning of peaks (as occurred with the χ^2 = 521 fit), constraints were imposed upon the fitting parameters: values of σ were constrained to be less than 0.3 mm/s (or, on occasion, less than 0.35

mm/s). ω values (relative to α-Fe at 22 °C) for peak A were not allowed to be greater than about 0.10 - 0.11 mm/s; those for B were constrained to be from 0.75 to 1.0 mm/s; for C, not less than about 2 mm/s (except when fitting a peak to its low energy shoulder, at about 1.85 mm/s). And ω for peak D was constrained to be between 0.38 and 0.45 mm/s, with σ small (usually less than 0.1 mm/s). The constraints for peak D were determined based on information obtained from a previous study of $<Fe^{3+}>$ in mica [11].

Recalling Table 4.2, the remaining fits produce consistent areas. The total areas (normalized by BG) appear to vary by less than 1-2% (except for the fits with unphysically narrow Lorentzian half-widths: $\gamma_h < 0.097$ mm/s). The same applies to the normalized area of peak C. Peak B being smaller, its fluctuations are more important, about 7-8%. Relative uncertainties of ±1% and ±4% can then be estimated for area measurements of peaks C and B in other spectra.

4.2.3 Debye temperatures from uncorrected spectra

Ratios of the 82 K and 305 K peak areas (normalized by BG) given in Table 4.1 were used to calculate site-specific and effective Debye temperatures for each sample. These Debye temperatures (and f-factors at 300 K and 80 K) are

reported in Table 4.3. One must recall that the areas of Table 4.1 are from *perfect* fits, where care in avoiding peak overlap has been sacrificed for perfection of fit. In particular, MCC and IKO contain $Fe^{<3+>}$ and, with peak D present, the overlap of peaks A, D, and B implies large uncertainties in their areas (and in their site-specific Debye temperatures). The overlap between peaks D and B is in fact so important that only the sum of the areas of these peaks is reported here and used to obtain an effective Fe^{3+} Debye temperature.

Since the total area is well determined regardless of peak overlap, the values of $\overline{\theta_D}$ are precise, though not accurate. As explained in chapter 3, they are overestimates. Their inclusion here is for comparison with the Debye temperatures obtained from thickness-corrected spectra.

It is encouraging to note that, at least for the biotites (which should have the most dependable peak areas), $\theta_D^{[2+]} < \overline{\theta_D} < \theta_D^{[3+]}$. This concurs with the results of MOC2661. Thickness-corrected results should further confirm these observations.

4.3 Site-Specific Debye temperatures from uncorrected data

Sample	θ_D^{3+} (K)	f^{3+} 300 K	f^{3+} 80 K	$\theta_D^{[2+]}$ (K)	$f^{[2+]}$ 300 K	$f^{[2+]}$ 80 K	$\overline{\theta_D}$ (K)	$\overline{f}$ 300 K	$\overline{f}$ 80 K
BZ53	395	0.760	0.897	330	0.679	0.868	343	0.698	0.875
BL315	350	0.707	0.879	300	0.627	0.850	310	0.645	0.856
BL531	332	0.682	0.869	275	0.575	0.829	300	0.627	0.850
MCC	250	0.513	0.804	276	0.577	0.830	289	0.605	0.841
IKO	288	0.603	0.841	272	0.568	0.827	267	0.557	0.822

4.3 *Thickness-corrected spectra*

For accurate values of the effective and site-specific Debye temperatures, the spectra must be corrected for thickness effects. Armed with perfect fits, the values of n_a of section 2.2, spectral temperatures and (for the annite) the Debye temperature of the source, values of $\eta_R f_S$ for each spectrum can be calculated using algorithm 2.7. These in turn are used to generate the thickness-corrected spectra.

As described in section 4.2.2, fits to spectra which follow the fitting constraints outlined in that section should be able to determine the total and peak C areas to within ±1%, and peak B to within ±4% for the biotites. These uncertainties translate into values of ±0.005 and ±0.04 for the 300 K f-factors ($f^{[2+]}$ and $f^{[3+]}$) of BZ53, and ±0.002 and 0.015 for its 80 K f-factors. These can be used to estimate the minimum uncertainties in all f-factors presented in this section.

These $f^{[3+]}$ uncertainties are underestimates when applied to the IKO and MCC results. The presence of peak D reduces the accuracy of both peaks B and D. To handle the trade-offs between these peaks, it was decided to consider only the sum of their areas. The temperature dependence of

this sum reveals an effective θ_D^{3+} which can then be compared to the values of $\theta_D^{[3+]}$ obtained from the biotites to determine the $<Fe^{3+}>$ contribution to this Debye temperature.

In addition to the fitting uncertainty in peak area, these areas themselves are subject to uncertainty due to the thickness-correction process. The parameters (absorber temperature, n_a, source θ_D) used to generate the thickness-corrected spectra are subject to error. To gauge the effect of their uncertainties on thickness-corrected spectral areas (and on site-specific f-factors), each parameter was independently considered. When obtaining $\overline{\theta_D}$ (and generating thickness-corrected spectra) from pairs of uncorrected spectra and the best values of absorber temperature, n_a, and source θ_D, extra corrected pairs were also generated using a limiting value of one of these parameters.

Table 4.4 lists the various pairs of spectra generated and the values of the parameters used to do so, $\overline{\theta_D}$ and $\eta_H f_S$ being calculated from these values. Also in Table 4.4 are the names that label the various fits to the thickness-corrected spectra. These labels are used to identify the spectra and the fits of figure 4.2 (a - f) where selected fits are illustrated. The labels are used in Table 4.5, where the areas of each peak are given for each

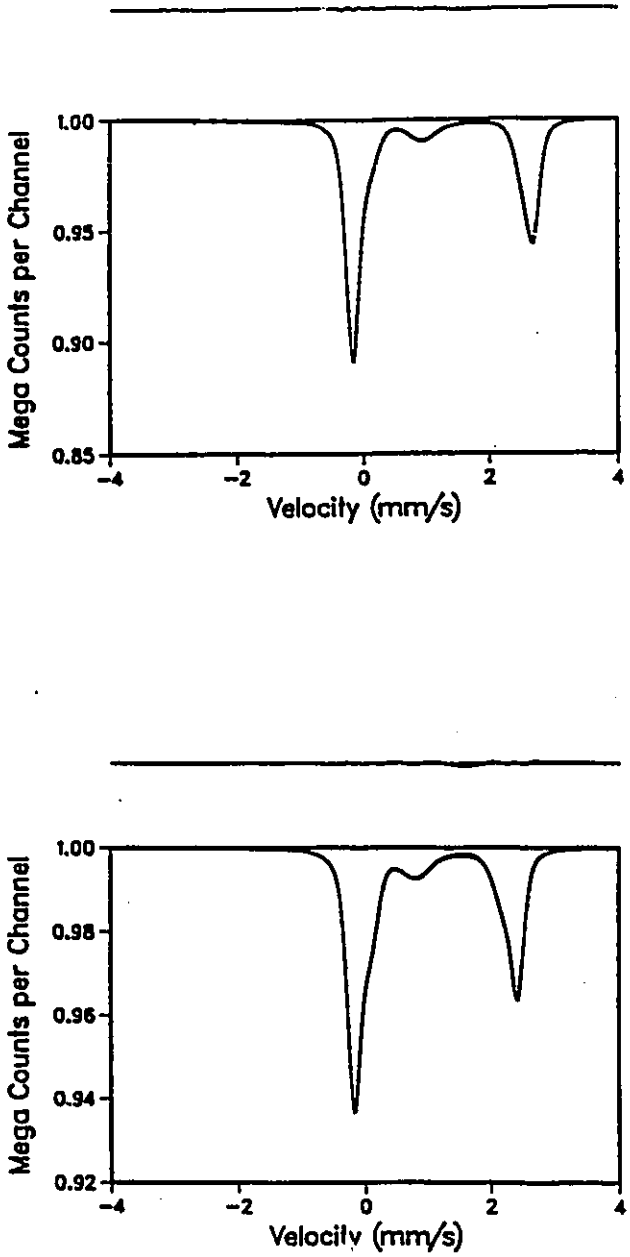

Figure 4.2 (a) L315LN1 (top) and L315RT1 (bottom) fits to 82 K and 305 K thickness-corrected L315 spectra.

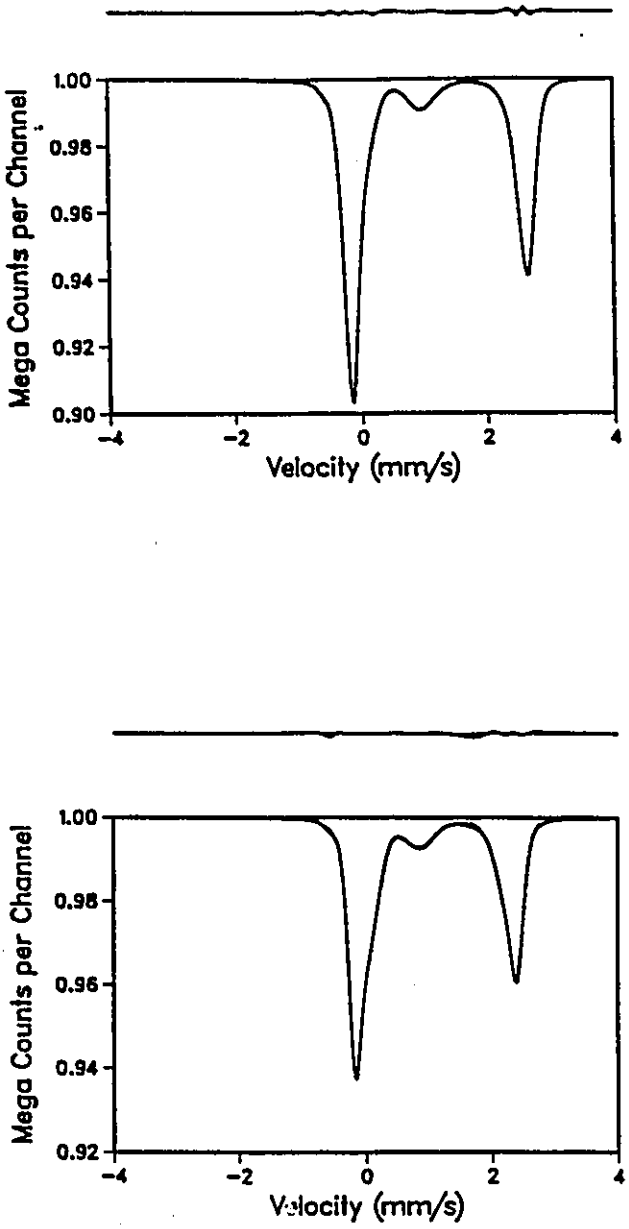

Figure 4.2 (b) Z53LN (top) and Z53RT (bottom) fits to the 82 K and 305 K thickness-corrected BZ53 spectra.

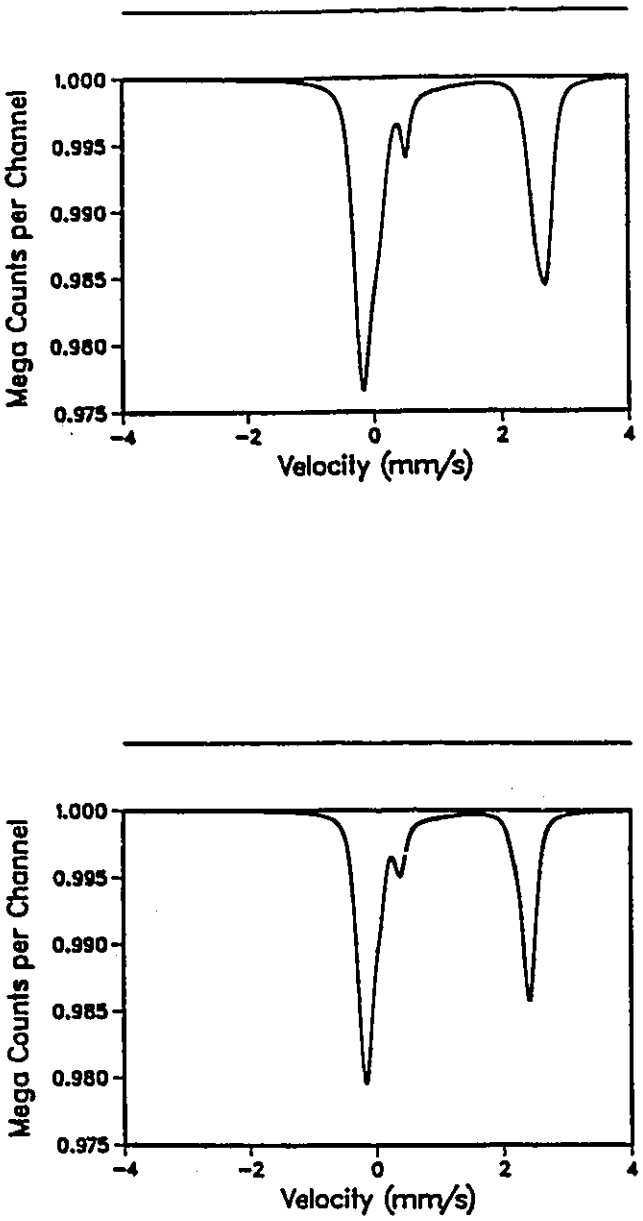

Figure 4.2 (c) MCCLN (top) and MCCRT (bottom) fits to the 82 K and 305 K thickness-corrected MCC spectra.

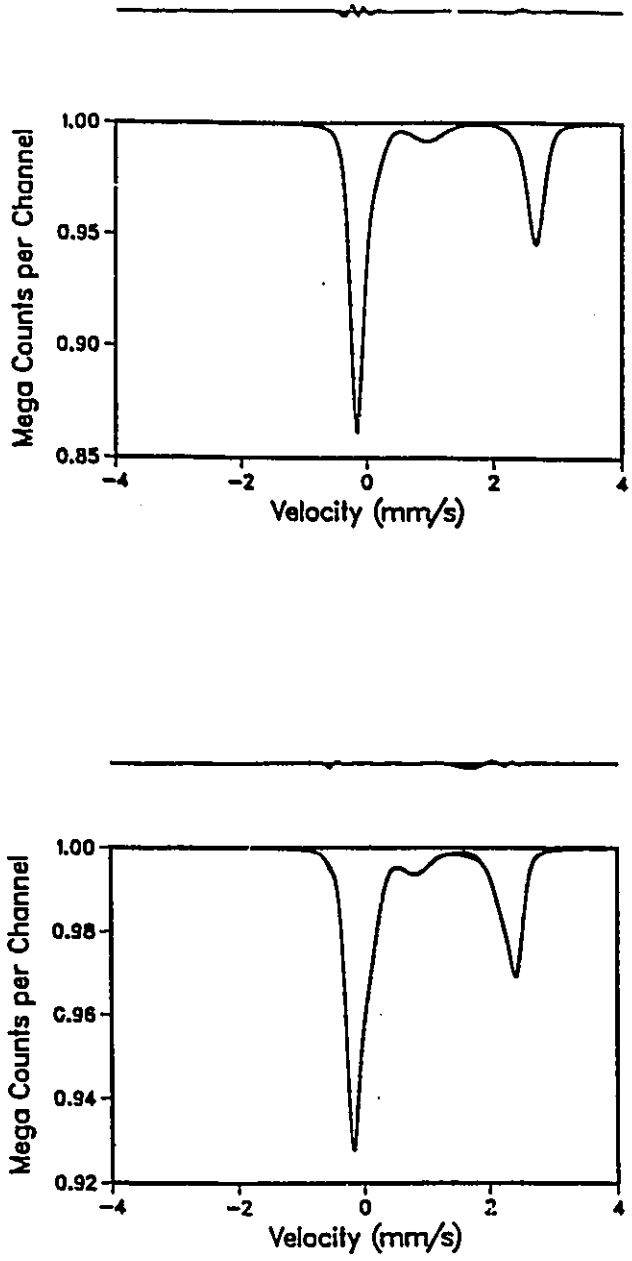

Figure 4.2 (d) MSCLNA (top) and MSCRTA (bottom) fits to the 82 K and 305 K thickness-corrected BL531 spectra generated using a limiting value of n_a.

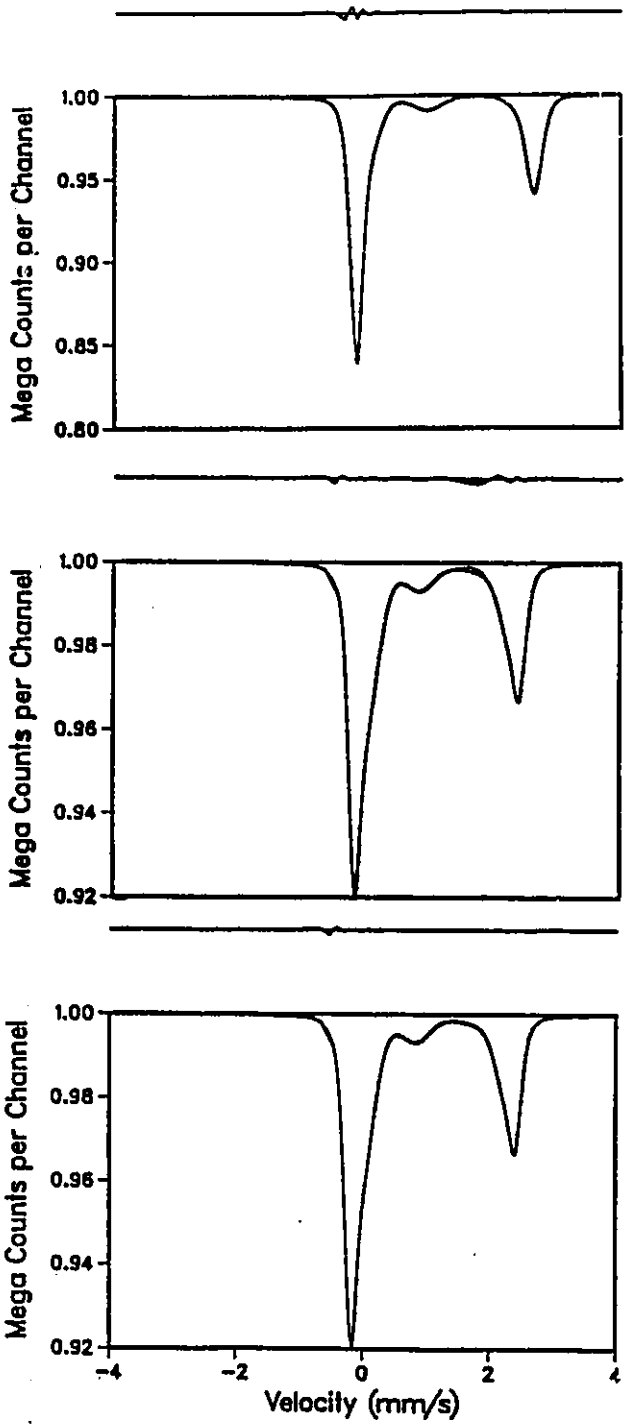

Figure 4.2 (e) MSCLN (top), MSCRT (middle), and MSCRT1 (bottom) fits to the 82 K and 305 K thickness-corrected BL531 spectra generated using the best value of n_a.

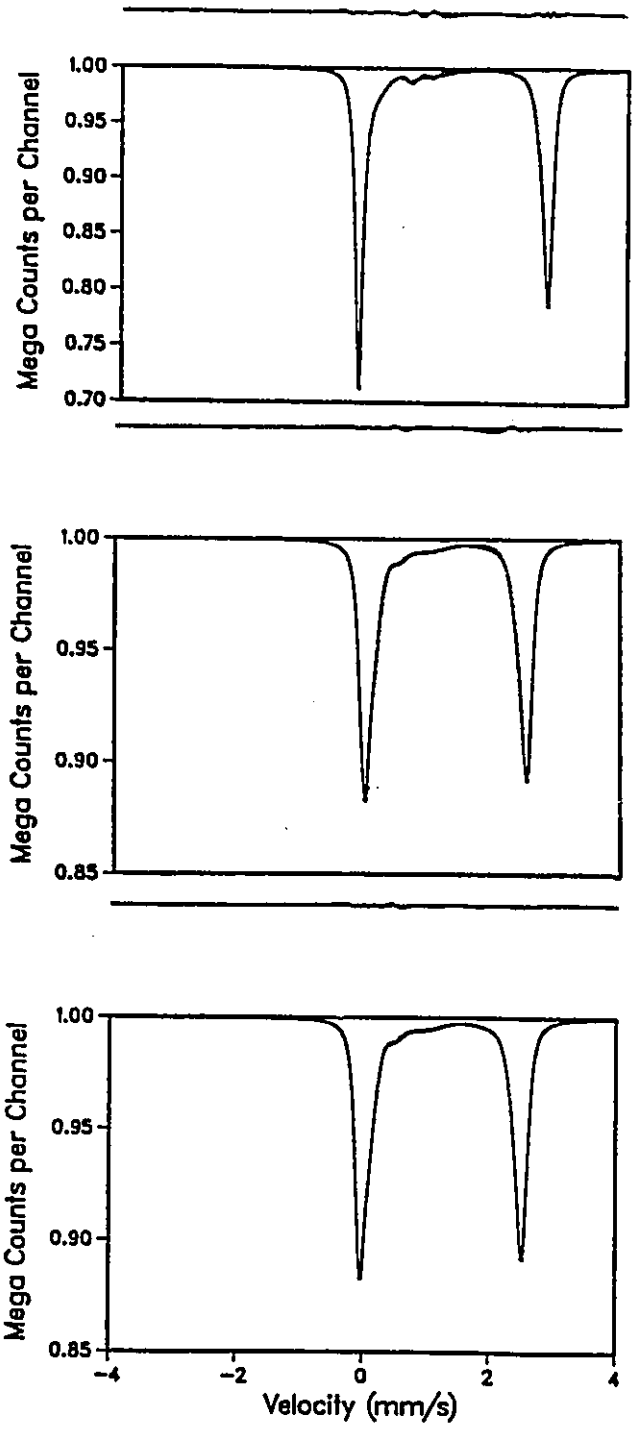

Figure 4.2 (f) IKOLNC (top), IKORTC (middle), and IKORTC1 (bottom) fits to the 83 K and 300 K thickness-corrected IKO spectra generated using a source Debye temperature of 420 K.

Table 4.4 $\eta_a f_s$ values used to thickness-correct spectra

Sample	Source θ_0 (K)	Source Temp. (K)	Abs. Temp. (K)	n_a (^{57}Fe/cm^2)	$\overline{\theta_0}$ (K)	$\eta_a f_s$ (counts)	Thickness-Corrected Fits
BL315	–	–	305	2.202×10^{18}	272.0	523054	L315RT1
			82			956403	L315LN1
BL315	–	–	305	–	–	509209†	L315RT2
			82	2.202×10^{18}	310.0‡	930927	L315LN2
BZ53	–	–	305	2.046×10^{18}	301.7	252349	*
			81			284322	*
BZ53	–	–	305	2.046×10^{18}	301.3	252667	Z53RT
			82			284460	Z53LN
BL531	–	–	305	2.664×10^{18}	251.9	406701	MSCRT, MSCRT1
			82			489036	MSCLN
BL531	–	–	305	2.400×10^{18}	257.0	434033	MSCRTA, MSCRTA1
			82			521901	MSCLNA
MCC	–	–	305	6.51×10^{17}	286.1	1466102	MCCRT
			82			1389852	MCCLN
IKO	400	300	300	4.102×10^{18}	253.5	197591	IKORTA, IKORTA1
		83	83			228689	IKOLNA
IKO	480	300	300	4.102×10^{18}	237.1	210882	IKORTB, IKORTB1
		83	83			231170	IKOLNB
IKO	420	300	300	4.102×10^{18}	248.0	201558	IKORTC, IKORTC1
		83	83			229431	IKOLNC

Notes: All values of $\overline{\theta_0}$ and $\eta_a f_s$ are calculated using the thickness-correction algorithm 2.6, with the following exceptions

‡ from the temperature dependance of uncorrected data and used to obtain $\eta_a f_s$ for that sample

† from equation 2.5, using backgrounds from the perfect fits (App. 4) and the value of $\eta_a f_s$ for the 82 K spectrum (930927).

* The corrected spectra were not fit in these cases.

Table 4.5 (a) Areas of thickness-corrected spectra.

Fit Name	Sample	χ^2	Temp. (K)	Areas (cts·mm/s) Peak A	Peak B*	Peak C	Total
MSCLN	BL531	178	82	17629	1587	7558	26774
MSCRT	BL531	41	305	11017	1239	4743	16999
MSCRT1	BL531	9	305	11034	1173	4885	17092
MSCLNA	BL531	123	82	15835	1528	6991	24354
MSCRTA1	BL531	8	305	10149	1096	4548	15793
MSCRTA	BL531	35	305	10134	1160	4414	15708
Z53LN	BZ53	53	82	12328	1615	7779	21722
Z53RT	BZ53	32	305	9055	1315	5677	16047
L315LN1	BL315	37	82	13495	1761	7415	22671
L315RT1	BL315	21	305	8995	1450	5051	15496
L315LN2	BL315	42	82	14045	1803	7667	23515
L315RT2	BL315	22	305	9296	1489	5204	15989
MCCLN	MCC	0.6	82	3876	555	2362	6793
MCCRT	MCC	0.1	305	2747	467	1606	4820
IKOLNC	IKO	678	83	21188	2062	18221	41471
IKORTC1	IKO	29	300	12626	1890	11598	26114
IKORTC	IKO	95	300	12631	1924	11390	25945
IKOLNA	IKO	716	83	21404	2071	18355	41835
IKORTA1	IKO	41	300	13009	1934	11890	26833
IKORTA	IKO	101	300	13023	1958	11724	26704
IKOLNB	IKO	596	83	20686	2059	17858	40603
IKORTB1	IKO	22	300	11719	1857	10805	24382
IKORTB	IKO	81	300	11795	1862	10673	24330

* Includes peak D when present (IKO, MCC).

Table 4.5 (b) Relative areas of thickness-corrected spectra.

Fit Name	Sample	χ^2	Temp. (K)	Relative Areas		
				Peak A	Peak B*	Peak C
MSCLN	BL531	178	82	0.658	0.0593	0.282
MSCRT	BL531	41	305	0.648	0.0729	0.279
MSCRT1	BL531	9	305	0.646	0.0686	0.286
MSCLNA	BL531	123	82	0.650	0.0627	0.287
MSCRTA1	BL531	8	305	0.643	0.0694	0.288
MSCRTA	BL531	35	305	0.645	0.0738	0.281
Z53LN	BZ53	53	82	0.568	0.0743	0.358
Z53RT	BZ53	32	305	0.564	0.0819	0.354
L315LN1	BL315	37	82	0.595	0.0777	0.327
L315RT1	BL315	21	305	0.580	0.0936	0.326
L315LN2	BL315	42	82	0.597	0.0767	0.326
L315RT2	BL315	22	305	0.581	0.0931	0.325
MCCLN	MCC	0.6	82	0.571	0.0817	0.347
MCCRT	MCC	0.1	305	0.570	0.0969	0.333
IKOLNC	IKO	678	83	0.511	0.0497	0.439
IKORTC1	IKO	29	300	0.483	0.0724	0.444
IKORTC	IKO	95	300	0.487	0.0742	0.439
IKOLNA	IKO	716	83	0.511	0.0495	0.439
IKORTA1	IKO	41	300	0.485	0.0721	0.443
IKORTA	IKO	101	300	0.488	0.0733	0.439
IKOLNB	IKO	596	83	0.509	0.0507	0.440
IKORTB1	IKO	22	300	0.481	0.0762	0.443
IKORTB	IKO	81	300	0.485	0.0765	0.439

* Includes peak D when present (IKO, MCC).

Table 4.5 (c) Number of lines fit to each peak.

Fit Name	Sample	χ^2	Temp. (K)	Number of lines (A-D-B-C)
MSCLN	BL531	178	82	2-0-1-2
MSCRT	BL531	41	305	2-0-1-2
MSCRT1	BL531	9	305	2-0-1-3
MSCLNA*	BL531	123	82	2-0-1-2
MSCRTA1	BL531	8	305	2-0-1-3
MSCRTA	BL531	35	305	2-0-1-2
Z53LN	BZ53	53	82	2-0-1-2
Z53RT	BZ53	32	305	2-0-1-2
L315LN1†	BL315	37	82	2-0-1-2
L315RT1	BL315	21	305	2-0-1-2
L315LN2	BL315	42	82	2-0-1-2
L315RT2	BL315	22	305	2-0-1-2
MCCLN	MCC	0.6	82	2-1-1-2
MCCRT	MCC	0.1	305	2-1-1-2
IKOLNC‡	IKO	678	83	2-1-1-2
IKORTC1	IKO	29	300	2-1-1-3
IKORTC	IKO	95	300	2-1-1-2
IKOLNA	IKO	716	83	2-1-1-2
IKORTA1	IKO	41	300	2-1-1-3
IKORTA	IKO	101	300	2-1-1-2
IKOLNB	IKO	596	83	2-1-1-2
IKORTB1	IKO	22	300	2-1-1-3
IKORTB	IKO	81	300	2-1-1-2

* The fit names for BL531 with "A" use an extreme value of n_a.

† The "1" and "2" fits of BL315 are fits to corrected spectra generated with different $\eta_M f_S$ values (see text and table 4.4).

‡ The "A", "B", and "C" label the IKO spectra generated with source Debye temperatures of 400 K, 480 K, and 420 K.

4.6 Site-Specific Debye temperatures from thickness-corrected data

Fit pair	θ_D^{3+} (K)	f^{3+} 300 K	f^{3+} 80 K	$\theta_D^{[2+]}$ (K)	$f^{[2+]}$ 300 K	$f^{[2+]}$ 80 K	$\overline{\theta_D}$ † (K)	$\overline{f}$ 300 K	$\overline{f}$ 80 K	$\overline{\theta_D}$ ‡ (K)
MSCLN MSCRT	332	0.682	0.869	247	0.505	0.801	250	0.513	0.804	252
MSCLN MSCRT1	303	0.633	0.852	255	0.527	0.810	252	0.519	0.807	252
MSCLNA MSCRTA1	290	0.607	0.842	257	0.532	0.812	256	0.529	0.811	257
MSCLNA MSCRTA	316	0.656	0.860	249	0.511	0.803	255	0.527	0.810	257
Z53LN Z53RT	361	0.722	0.884	297	0.621	0.847	301	0.631	0.851	301
L315LN1 L315RT1	370	0.733	0.887	271	0.566	0.826	272	0.568	0.827	272
L315LN2 L315RT2	373	0.736	0.889	269	0.561	0.824	270	0.564	0.825	–
MCCLN MCCRT	389	0.754	0.895	270	0.564	0.825	285	0.597	0.838	286
IKOLNC IKORTC1	520	0.849	0.927	248	0.508	0.802	245	0.500	0.798	248
IKOLNC IKORTC	645	0.896	0.943	243	0.494	0.796	244	0.497	0.797	248
IKOLNA IKORTA1	575	0.873	0.935	253	0.521	0.808	250	0.513	0.804	254
IKOLNB IKORTB1	483	0.829	0.920	236	0.474	0.787	234	0.468	0.784	237

† Obtained from temperature dependence of thickness-corrected total spectral area.

‡ From thickness-correction algorithm 2.6, used to correct spectra.

fit, in Table 4.6, where the areas of Table 4.5 have been used to obtain site-specific Debye temperatures and f-factors, and in Appendix 4 (A4.10 - A4.15), where the Voigt parameters for these fits are listed.

Now, finally, the effects of the uncertainties in absorber temperature (ΔT), in n_a, and in source Debye temperature can be discussed in detail.

To measure the effect of ΔT (which was 1 K at 82 K, 0.1 K at 305 K), the fits to sample BZ53 were used. Reducing the absorber temperature from 82 K to 81 K reduced the value of $\overline{\theta_D}$ obtained using algorithm 2.7 from 301.7 K to 301.3 K (see Table 4.4). The values of $\eta_M f_S$ are affected by less than 1%, and the total spectral area will be affected by a similar amount. Considering the limit in fitting accuracy of the total area is about 2%, the effects due to uncertainty in absorber temperature can be neglected.

The effects of Δn_a on the thickness-corrected spectral areas and site-specific f-factors are now examined. The greatest uncertainty is ±10%, for BL531. The effects of Δn_a will thus be considered for this sample as it is the limiting case for the samples studied. Spectra for BL531 labelled MSCLN, MSCRT, and MSCRT1 were generated using the nominal n_a value; those labelled MSCLNA, MSCRTA, MSCRTA1

used a limiting value (the "1" denotes a fit using an extra line to model the low energy shoulder of peak C). Comparing areas of MSCLN to MSCLNA (and RT to RTA, RT1 to RTA1) shows that decreasing n_a by 10% has decreased the areas by about 10% (Table 4.5 (a)). But since this decrease occurs in both the 82 K and 305 K spectra, the Debye temperatures and f-factors will be less sensitive to variations in n_a than the peak areas are.

A comparison (using Table 4.6) of f-factors obtained from the MSCLNA-MSCRTA pair to the MSCLN-MSCRT pair (and from the MSCLNA-MSCRTA1 pair to the MSCLN-MSCRT1 pair) shows the uncertainty in n_a to correspond to uncertainties of 0.025 and 0.005 in the 300 K $f^{[3+]}$ and $f^{[2+]}$ values of BL531, and to uncertainties of 0.010 and 0.002 in its 83 K f-factors. These are within the limits of fitting accuracy estimated at the start of this section.

The presence or absence of a line in the shoulder to peak C has a significant effect on the f-factors, however, as can be seen by comparing f-factors obtained from MSCLN-MSCRT to those of MSCLN-MSCRT1, and by comparing MSCLNA-MSCRTA results to MSCLNA-MSCRTA1 f-factors. This increases the uncertainties of the BL531 f-factors to 0.05 and 0.02 at 300 K (for $f^{[3+]}$ and $f^{[2+]}$), and to 0.018 and 0.01 for the f-factors at 80 K.

The uncertainty in source Debye temperature only affects the annite thickness-corrected spectra. All others were collected using the cold-finger cryostat where the source temperature is a constant, eliminating f_S from equation 2.6 (and thus from the thickness-correction procedure). But the source was at absorber temperature when the exchange-gas cryostat was used, so then the source Debye temperature must be considered.

Published room temperature values of f_S [20] correspond to a Debye temperature of 420 K. Pairs of spectra were generated using source Debye temperatures of 400 K, 420 K, and 480 K (these choices representing a reasonable range of possible source f-factors). The values of $\overline{\theta_D}$ obtained for each pair using algorithm 2.7 were 254 K, 248 K, and 237 K, respectively. The actual values of the site specific f-factors vary significantly with source Debye temperature, but the f^{3+}/f^{2+} ratios remain about the same, regardless of source Debye temperature used.

There remains a pair of spectra in tables 4.4 - 4.6 not yet explained: L315LN2 and L315RT2. For the liquid nitrogen temperature spectrum, $\eta_H f_S$ was calculated using the value of $\overline{\theta_D}$ obtained from the temperature dependence of the uncorrected L315 spectra, instead of from the $\overline{\theta_D}$ obtained from algorithm 2.7. $\eta_H f_S$ for the 305 K spectrum was

calculated using the 80 K spectrum value of $\eta_M f_S$, the backgrounds of the perfect fits, and equation 2.6. It can be seen from Table 4.6 that the f-factors obtained from this pair do not differ significantly from those obtained from the pair of L315 spectra generated from the value of $\overline{\theta_D}$ indicated by algorithm 2.7. This shows that for series of spectra collected under identical conditions, one need only obtain a reasonable guess of $\eta_M f_S$ for a single spectrum and the other values of $\eta_M f_S$ can hence be obtained using equation 2.6.

Sample to sample variations in Debye temperature and f-factor can be seen in Table 4.6. In particular, the $[Fe^{2+}]$ f-factors vary significantly between samples. A simple explanation might be that the fits to the different samples handle the low energy shoulder of peak C differently, i.e., the fitting uncertainty in $f^{[2+]}$ has been underestimated and the differences actually aren't significant. Or the f-factors may be correlated to the cell size within the mica lattices. Determining the significance and reasons for sample to sample variations in f-factor is a subject for further research.

But the goal of this chapter was to obtain site-specific f-factors. This has been achieved. All samples with spectra in corrected form, and most in

uncorrected form, showed f-factors to be site-specific, with $f^{[2+]} < f^{3+}$. This result is clear, but their values retain some uncertainty. From the f-factors in Table 4.6, Table 4.7 can be drawn showing site-specific f-factors for each sample, and the ratio of Fe^{3+} to $[Fe^{2+}]$ f-factors at room and liquid nitrogen temperatures, which are less sample dependent than the f-factors themselves are.

The $[Fe^{2+}]$ f-factors can be seen to differ significantly from the Fe^{3+} f-factors. The largest Fe^{3+} f-factors corresponded to samples containing $<Fe^{3+}>$, suggesting that $f^{<3+>}$ is greater than $f^{[3+]}$. Based on the apparent relative amounts of $<Fe^{3+}>$ and $[Fe^{3+}]$ in the spectra and the difference between f-factors for MCC and the biotites, f-factors were estimated for $<Fe^{3+}>$. The f^{3+} values from IKO were not used, however. Its peaks B and D were not clearly resolved by modelling the spectra with single Voigt lines, and the resulting values for f^{3+} are suspiciously large.

Chapter 5 models the annite spectra with Voigt doublets. The f-factors obtained for the annite by this method were smaller than the f-factors determined in this chapter for the other samples, but the ratios of f-factors in chapter 5 agreed within error with the ratios measured and estimated in this section.

Table 4.7 (a) f-factors at 300 K from Debye temperatures

Sample	f^{3+}	$f^{[2+]}$	$f^{3+} / f^{[2+]}$
BL531	0.63 ± 0.04	0.52 ± 0.01	1.20 ± 0.10
BL315	0.74 ± 0.04	0.563± 0.005	1.31 ± 0.08
BZ53	0.72 ± 0.04	0.621± 0.005	1.16 ± 0.07
AVG.†	0.69 ± 0.07	0.57 ± 0.05	1.22 ± 0.09
MCC	0.75 ± 0.04	0.564± 0.005	1.34 ± 0.08
IKO	(0.85)*	0.51 ± 0.01	(1.67)*
TOT. AVG.‡	0.70 ± 0.07	0.56 ± 0.06	1.25 ± 0.09

Table 4.7 (b) f-factors at 80 K from Debye temperatures

Sample	f^{3+}	$f^{[2+]}$	$f^{3+} / f^{[2+]}$
BL531	0.85 ± 0.015	0.810± 0.005	1.05 ± 0.02
BL315	0.888± 0.015	0.825± 0.002	1.08 ± 0.02
BZ53	0.884± 0.015	0.847± 0.002	1.04 ± 0.02
AVG.†	0.87 ± 0.02	0.83 ± 0.02	1.06 ± 0.02
MCC	0.895± 0.015	0.825± 0.005	1.08 ± 0.02
IKO	(0.93)*	0.80 ± 0.01	(1.16)*
TOT. AVG.‡	0.88 ± 0.02	0.82 ± 0.02	1.06 ± 0.02

† Average f-factors of samples without $<Fe^{3+}>$. The indicated uncertainty in the averages was chosen to include all data points and corresponds to about 1.5 x (std. dev. of data).

‡ Average f-factors of all samples (numbers in brackets excluded). Indicated uncertainties chosen to include all data points.

* Suspiciously large; not included in calculations of averages.

Table 4.7 (c) Average site-specific f-factors

	300 K	80 K	comments
$f^{[2+]}$	0.56 ± 0.06	0.82 ± 0.02	
$f^{[3+]}$	0.69 ± 0.07	0.87 ± 0.07	
$f^{<3+>}$	0.75 ± 0.10	0.90 ± 0.03	** estimate **
$f^{[3+]}/f^{[2+]}$	1.22 ± 0.09	1.06 ± 0.02	
$f^{<3+>}/f^{[2+]}$	1.3 ± 0.1	1.10 ± 0.05	** estimate **

** As explained in text (section 4.3)

Table 4.7 (c) states the final results: f-factors for each site, and ratios of f-factors. Here, the uncertainties quoted are large enough to include the f-factors for all samples, sample-specific f-factors with uncertainties being quoted in Table 4.7 (a) and (b).

5. Annite site populations

One of the main motivations for obtaining site-specific f-factors from sub-spectral areas is to use these f-factors to obtain accurate site populations. Among the samples used in this thesis, only the annite is powdered well enough to not exhibit texture effects. It is thus the only sample for which accurate sub-spectral areas (and hence, accurate site populations) can be readily determined because it is formed of symmetric doublets. This implies that the area of peak A must equal the sums of the areas of peaks B, C, and D, and that the total sub-spectral area for a given site is simply twice that of its high energy peak, B, C, or D (see figure 1.2). So the areas of peaks B, C, and D in thickness-corrected spectra, in combination with the site-specific f-factors obtained in chapter 4, are sufficient to reveal the iron site populations in annite.

These site populations are of particular importance in annite because, as mentioned in section 1.3, Fe^{3+} must, for structural reasons, exist in true annite. It had not yet been determined how much Fe^{3+} was required to obtain a stable structure, nor how much of it would be $[Fe^{3+}]$ as opposed to $<Fe^{3+}>$.

Modelling the annite spectra with Voigt singlets failed to resolve peaks B and D from each other or from peak A. The area of peak A should equal the sum of areas of peaks B, C, and D, but the difference was in fact comparable to the area of peak D. Not being able to determine how to distribute this area among the peaks contributed a large amount to the uncertainties of peaks B and D.

It was decided that Voigt doublets would be used to fit the spectra. This would impose A = B + C + D if our spectral interpretation (fig. 1.2) is correct. From previous work [11], some constraints were known as to the position and splittings of the doublets. The Voigt doublet minimization method was developed by D. Rancourt and J. Ping [10]; it makes use of MINUIT to obtain fits of Voigt doublets to spectral peaks. To model the annite, one doublet was needed for the $[Fe^{3+}]$ site, one for the $<Fe^{3+}>$ site, and two to three for the $[Fe^{2+}]$ site. The third $[Fe^{2+}]$ doublet corresponded to a low energy shoulder on peak C and to a high energy contribution to peak A. However, it is not possible to ascertain the exact position of the lower half of this doublet and as a result the accuracy is limited for both the $<Fe^{3+}>$ and $[Fe^{3+}]$ areas.

Fits were obtained for the 300 K and 83 K annite thickness-corrected spectra generated using a source Debye

temperature of 420 K, and for the 300 K spectrum generated using 400 K as a source Debye temperature. The 83 K spectrum is illustrated in figure 5.1 with the $<Fe^{3+}>$ and $[Fe^{3+}]$ sub-spectra obtained from fitting shown above the data. Table 5.1 summarizes the sub-spectral areas from each fit (the complete list of fitting parameters is given in Appendix 4: A4.16 - A4.18).

From the sub-spectral areas of Table 5.1, the f-factors were recalculated for each site. The results are quoted in Table 5.2. Included in this table for comparison are the f-factors given in Table 4.7 (c). The annite f-factors are significantly lower than those obtained in chapter 4. The f^{3+} / $f^{[2+]}$ ratios are also lower, though they do agree within error with the ratios given in Table 4.7 (c).

To obtain the annite site populations, one should first normalize the Fe^{3+} sub-spectral areas of Table 5.1 by dividing by the appropriate f^{3+} / f^{2+} ratio, then calculate the resulting relative sub-spectral areas. These relative normalized areas are the site populations within the annite. But one must decide whether to normalize the Fe^{3+} areas by the ratios given in Table 4.7 (c) or by those obtained from fitting doublets to the annite spectrum (as given in Table 5.2).

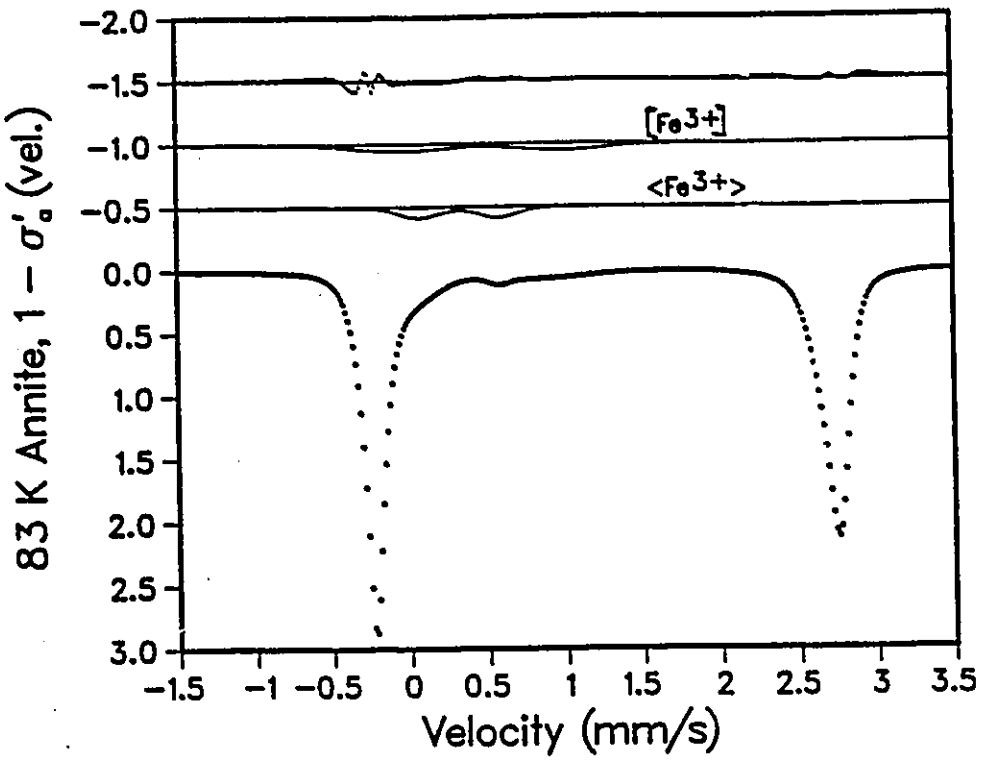

Figure 5.1 IKOLNCD1. Voigt doublet fit to 83 K thickness-corrected IKO spectrum generated using a source Debye temperature of 420 K. The fit itself is not shown, but the [Fe^{3+}] and <Fe^{3+}> sub-spectra are given, as well as the difference spectrum for the fit.

Table 5.1 (a) Annite thickness-corrected sub-spectral areas.

Fit Name	# dist.*	Areas (cts·mm/s)			
		$<Fe^{3+}>$	$[Fe^{3+}]$	$[Fe^{2+}]$	Total
IKORTCD1	1-1-2	1300	1842	22674	25816
IKORTCD2	1-1-3	1344	1358	23142	25844
IKORTAD1	1-1-2	1374	1854	23328	26556
IKORTAD2	1-1-3	1390	1396	23806	26592
IKOLNCD1	1-1-3	1966	2708	37096	41770
IKOLNC	Singlets	666	3457	36442	41471

Table 5.1 (b) Relative areas from annite thickness-corrected spectra

Fit Name	# dist.	Area / Total		
		$<Fe^{3+}>$	$[Fe^{3+}]$	$[Fe^{2+}]$
IKORTCD1	1-1-2	0.050	0.071	0.878
IKORTCD2	1-1-3	0.052	0.053	0.896
IKORTAD1	1-1-2	0.052	0.070	0.878
IKORTAD2	1-1-3	0.052	0.052	0.895
IKOLNCD1	1-1-3	0.047	0.065	0.894
IKOLNC	Singlets	0.016	0.083	0.879

* The number of Gaussian components in the distributions of quadrupole splittings [10] (i.e., the number of doublets) used to fit the $<Fe^{3+}>$ – $[Fe^{3+}]$ – $[Fe^{2+}]$ sub-spectra.

Table 5.2 Site-specific f-factors from doublet fits

	300 K	80 K	comments
$f^{[2+]}$	0.56 ± 0.06	0.82 ± 0.02	table 4.7 (c)
	0.50 ± 0.02	0.797± 0.007	doublet
$f^{[3+]}$	0.69 ± 0.07	0.87 ± 0.07	table 4.7 (c)
	0.46 ± 0.10	0.78 ± 0.05	doublet
$f^{<3+>}$	0.75 ± 0.10	0.90 ± 0.03	table 4.7 (c)
	0.56 + 0.03	0.825± 0.010	doublet
$f^{[3+]}/f^{[2+]}$	1.22 ± 0.09	1.06 ± 0.02	table 4.7 (c)
	0.9 + 0.2	0.98 ± 0.07	doublet
$f^{<3+>}/f^{[2+]}$	1.3 ± 0.1	1.10 ± 0.05	table 4.7 (c)
	1.13 ± 0.09	1.035± 0.020	doublet

It was decided that the ratios given in Table 4.7 (c) were more appropriate. The f-factors and f-factor ratios calculated in chapter 4 were obtained from several samples, most with relatively large amounts of $Fe^{[3+]}$. The $f^{[3+]} / f^{[2+]}$ ratio in Table 4.7 (c) should be more reliable than the $f^{<3+>} / f^{[2+]}$ ratio obtained in this section. So it is the ratios of Table 4.7 (c) which are used to normalize the sub-spectral areas of Table 5.1 to give the normalized areas and site populations quoted in Table 5.3.

Table 5.3 thus shows that in our synthetic annite, 90.5 ± 1.0 % of the iron sites are $[Fe^{2+}]$, 5.3 ± 1.0 % are $[Fe^{3+}]$, and 4.2 ± 0.3 % are $<Fe^{3+}>$. The $[Fe^{2+}]$ value is very reliable – even when calculated using single Voigts. The amounts of $<Fe^{3+}>$ and $[Fe^{3+}]$ are subject to the position of the third $<Fe^{2+}>$ doublet, but the consistency of the $<Fe^{3+}>$ and $[Fe^{3+}]$ amounts suggest these results are correct.

Table 5.3 (a) Annite spectral areas normalized by f-factors

Fit	Area (counts·mm/s) <Fe^{3+}>	[Fe^{3+}]	[Fe^{2+}]	Total
IKORTCD1	1000 ± 77	1510 ±111	22674	25184
IKORTCD2	1033	1113 ± 82	23142	25288
IKORTAD1	1056	1519	23328	25903
IKORTAD2	1069	1144	23806	26019
IKOLNCD1	1787 ± 81	2255 ± 48	37096	41138
IKOLNC	605 ± 28	3261 ± 62	36442	40308

Note: <Fe^{3+}> and [Fe^{3+}] areas normalized using appropriate f^{3+}/f^{2+} ratio from Table 4.7 (c).

Table 5.3 (b) Relative normalized areas (site populations)

Fit	<Fe^{3+}>/Total	[Fe^{3+}]/Total	[Fe^{2+}]/Total
IKORTCD1	0.040 ± 0.003	0.060 ± 0.004	0.900
IKORTCD2	0.041	0.044 ± 0.003	0.915
IKORTAD1	0.041	0.059	0.901
IKORTAD2	0.041	0.044	0.915
IKOLNCD1	0.043 ± 0.002	0.055 ± 0.001	0.902
IKOLNC	0.015 ± 0.001	0.081 ± 0.002	0.904
Average*	0.042 ± 0.003	0.053 ± 0.010	0.905 ± 0.010

* The average excludes IKOLNC for the f^{3+} values. The uncertainty in $f^{<3+>}$ is due to the $f^{<3+>}/f^{[2+]}$ uncertainty. Those indicated for $f^{[2+]}$ and $f^{[3+]}$ were chosen large enough to contain all data points (except $f^{[3+]}$ for IKOLNC).

6. Conclusions

This thesis reports the first conclusive measurements of the site-specific Mössbauer recoilless fractions (f-factors) for the tetrahedral ($f^{<3+>}$) and octahedral ($f^{[3+]}$, $f^{[2+]}$) iron sites in true trioctahedral mica.

The site-specific nature of the f-factors was determined in a preliminary study of a biotite single crystal. From the temperature dependence of the spectral areas of five spectra accumulated under identical conditions except for temperature, the effective Debye temperature ($\overline{\theta_D}$) for this biotite was calculated. This effective Debye temperature was used to generate thickness-corrected spectra with which the temperature dependence of peak C (see fig. 1.2) was used to obtain an [Fe^{2+}] Debye temperature ($\theta_D^{[2+]}$). The difference between $\overline{\theta_D}$ and $\theta_D^{[2+]}$ was found to be significant, implying that $f^{[3+]} > f^{[2+]}$.

A further series of experiments to quantify $f^{[2+]}$, $f^{[3+]}$, and $f^{<3+>}$ was undertaken. Pairs of spectra were accumulated at 82 K and 305 K for three biotites rich in [Fe^{3+}] and a phlogopite rich in <Fe^{3+}>; a synthetic annite powder was studied at 83 K and at 300 K. Algorithm 2.7 (developed in section 2.4) was used to obtain effective

Debye temperatures from the temperature dependence of the spectral areas. Thickness-corrected spectra were generated using this $\overline{\theta_D}$.

The temperature dependence of the thickness-corrected area of peak C (fig. 1.2) revealed the [Fe^{2+}] f-factor to be $f^{[2+]} = 0.56 \pm 0.06$ at 300 K and $f^{[2+]} = 0.82 \pm 0.02$ at 80 K. The temperature dependence of peak B in the biotites was used to obtain $f^{[3+]} = 0.69 \pm 0.07$ at 300 K, $f^{[3+]} = 0.87 \pm 0.07$ at 80 K. To handle the overlap between peaks B and D, the temperature dependence of their sum was used to obtain an effective f^{3+} for the phlogopite, from which $f^{<3+>}$ was estimated to be 0.75 ± 0.10 at 300 K, 0.90 ± 0.03 at 80 K.

The uncertainties indicated for the above f-factors are large enough to include the f-factors obtained for each sample (see Table 4.7). The uncertainties in f-factor for each sample are mainly due to the limits in accuracy of determining peak areas (the difficulties arising from the overlap of peaks were considered here). The sample-specific f-factor uncertainties are small enough that the sample-to-sample differences in f-factor are real. The cause of this sample dependence of the f-factors is the subject of future research. The <u>ratios</u> of f-factors have smaller sample-to-sample variations and eliminate much of the correlated

errors in the f-factors themselves. Our final values for $f^{[3+]} / f^{[2+]}$ are 1.22 ± 0.09 at 300 K, 1.06 ± 0.02 at 80 K, and for $f^{<3+>} / f^{[2+]}$, 1.3 ± 0.1 at 300 K and 1.10 ± 0.05 at 80 K, the quoted uncertainties corresponding to the ranges of sample-to-sample variations of the ratios.

Modelling the annite spectra with Voigt singlets did not manage to clearly resolve peaks B and D from each other or from peak A. The use of doublets to model its spectra provided more accurate areas. From the f-factors listed above and the sub-spectral thickness-corrected annite areas, the iron site populations within the annite were calculated to be 4.2 ± 0.3 % $<Fe^{3+}>$, 5.3 ± 1.0 % $[Fe^{3+}]$, and 90.5 ± 1.0 % $[Fe^{2+}]$.

The areas obtained from modelling the annite spectra with Voigt doublets were also used to recalculate the site-specific f-factors and their ratios. Values of the $f^{<3+>} / f^{[2+]}$ ratio were found to be 1.13 ± 0.09 and 1.035 ± 0.020 at 300 K and 80 K, respectively. These values agree within error with the ratios presented in the paragraphs above.

References

1. N. N. Greenwood and T. C. Gibb, Mössbauer Spectroscopy, Chapman and Hall, London, 1971.

2. L. May, An Introduction to Mössbauer Spectroscopy, Plenum Press, New York, 1971.

3. D. G. Rancourt, "Accurate site populations from Mössbauer spectroscopy." Nuclear Instruments and Methods in Physics Research, B44 (1989), 199-210.

4. E. R. Whipple, Quantitative Mössbauer Spectra and Chemistry of Iron, Ph.D. thesis, Massachusetts Institute of Technology, 1974.

5. D. R. Wones and H. P. Eugster, "Stability of biotite: experiment, theory, and application." American Mineralogist, 50 (1965), 1228-1272.

6. T. Zoltai and J. H. Stout, Mineralogy Concepts and Principles, Burgess Publishing Company, Minneapolis, 1984.

7. Micas, S. W. Bailey, Editor, Reviews in Mineralogy, volume 13, Mineralogical Society of America, 1984.

3. P. Hargraves, D. G. Rancourt, and A. E. Lalonde, "Single-crystal Mössbauer study of phlogopite mica." Canadian Journal of Physics, 68 (1990), 128-144.

9. F. James and M. Ross, "Minuit – a system for function minimization and analysis of the parameter errors and correlations." Computer Physics Communications, 10 (1975), 343-367.

10. D. G. Rancourt and J. Ping, "Voigt-based methods for arbitrary-shape static hyperfine parameter distributions in Mössbauer spectroscopy." Nuclear Instruments and Methods in Physics Research, B58 (1991), 85-97.

11. D. G. Rancourt, M.-Z. Dang, and A. E. Lalonde, "Mössbauer spectroscopy of tetrahedral Fe^{3+} in trioctahedral micas." American Mineralogist, in press.

12. A. E. Lalonde, "Hepburn intrusive suite: Peraluminous plutonism within a closing back-arc basin, Wopmay orogen, Canada." Geology, 17 (1989), 261-264.

13. D. D. Hogarth, F. F. Brown, and A. M. Prichard, "Biabsorption, Mössbauer spectra, and chemical investigation of five phlogopite samples from Québec." Canadian Mineralogist, 10 (1970), 710-722.

14. G. H. Faye and D. D. Hogarth, "On the origins of 'reverse pleochroism' of a phlogopite." Canadian Mineralogist, 10 (1969), 25-34.

15. I. A. D. Christie, D. G. Rancourt, G. Lamarche, M. Royer, H. Kodama, and J.-L. Robert, "Low temperature Mössbauer spectroscopy and magnetism of synthetic annite mica." Hyperfine Interactions (ICAME '91 Conference Proceedings), in press.

16. J. Puerta and P. Martin, "Three and four generalized Lorentzian approximations for the Voigt Line shape." Applied Optics, 20 (1981), 3923-3928.

17. O. Ballet and G, Amthauer, "Room temperature Mössbauer study of the electric field gradient tensor at the iron sites in sheet silicates." Journal of Physics C: Solid State Physics, 19 (1986), 7099-7112.

18. R. M. Housley, N. E. Erickson, and J. G. Dash, "Measurement of recoil-free fractions in studies of the Mössbauer effect." Nuclear Instruments and Methods in Physics Research, 27 (1964), 29-37.

19. D. G. Rancourt, M. Royer, and M.-Z. Dang, "Mössbauer recoiless fractions of octahedral Fe^{3+} and Fe^{2+} in mica." Poster presented at the 1990 Geological Association of Canada, Mineralogical Association of Canada (GAC-MAC) joint conference in Vancouver, 1990. Abstract published in Program with Abstracts, vol. 15 (GAC-MAC conference proceedings).

20. Z. M. Stadnik, "Mössbauer spectroscopy source materials and their properties." Mössbauer Effect Reference and Data Journal, 1 (1978), 217-224.

21. W. H. Press, B. P. Flannery, S. A. Teukolsky, and W. T. Vetterling, Numerical Recipes, the Art of Scientific Computing, Cambridge University Press, Cambridge, 1986.

Appendix 1. "Folding" spectra

The experimental setup used in this laboratory accumulates in 1024 channels of data two spectra which are mirror images of each other except that their backgrounds are parabolic with opposite curvatures. One of these "mirror images" is collected as the transducer accelerates towards the absorber, the other is collected as the transducer accelerates away from it. The process of folding generates a single spectrum with a flat background from the "mirror images".

The folding process is done in two steps. The first involves calibrating the energy (transducer velocity) scale of the spectrum, the second is the actual folding. Each requires a computer program.

CALFIT, the first program included in this appendix, is used to calibrate the energy scale. It analyzes the 1024 channel spectrum of an absorber with known peak energies (usually α-Fe) collected before (or after) the spectrum to be folded was collected.

The program fits the spectral peaks with Lorentzian

lines to determine the position of the center of the peak (in terms of "channels", treating the channels as a continuous variable rather than as a discrete one). The user enters the transducer velocity known to correspond to each peak (those for 22 °C α-Fe are encoded in the program for simplicity of use). Our setup uses a constant acceleration drive for the transducer, so the resulting plot of transducer velocity versus channel (each point corresponding to a peak in the calibration spectrum) consists of two straight lines, one of positive slope, the other negative, one for either "mirror image".

CALFIT performs a linear regression to obtain the slope and y-intercept of both lines. These parameters are sufficient to calculate the transducer velocity of a given channel, and are the output file of CALFIT.

The next program, FOLDER, "folds" one mirror image (corresponding to the 512 channels where the transducer velocity decreases with channel, call this half B) onto the other (half A). To do this, the transducer velocity is calculated for each channel in half A. The "channel" with the same transducer velocity in half B is then determined. The number of counts corresponding to this "channel" (which is normally between two actual channels) is calculated from a linear interpolation of the counts in both actual

surrounding channels. These counts are added to the counts in the channel of half A, and the total is divided by two (arbitrarily – so that folding doesn't double the background). Repeating these steps for all 512 channels of half A produces the folded spectrum.

The computer programs listed here were specifically developed for this laboratory. They make use of subroutines presented in Numerical Recipes [21].

Please note that certain lines in these programs were split into two because they were too long for the width restriction of this publication. A "_" indicates a line has been split.

```
$stack &h1000
10 REM Calfit by Michel Royer
20 REM program to study calibration spectra, fit their
30 REM peaks to Lorentzian lines on a linear background
40 REM and to obtain a relationship between transducer
50 REM velocity and channel number.
60 REM june, 1988
70 REM University of Ottawa
   rem program uses gradient technique to minimize chi-square,
   rem and is written in part for turbo basic.
   rem independant of # of channels
80 KEY OFF
105 OPTION BASE 1
110 DIM HT(1024),CHAN(1024),Z(5),HIGHCH(20),LOWCH(20),CTRCH(20)
111 DIM CH0(20),x(1024),sig(1024),covar(5,5),_
      alpha(5,5),lista%(5)
112 DIM VEL(15),CODE$(15),ENERGY(20),y(1024)
130 LARROW$ = CHR$(0) + CHR$(75)
131 RARROW$ = CHR$(0) + CHR$(77)
132 UARROW$ = CHR$(0) + CHR$(72)
133 DARROW$ = CHR$(0) + CHR$(80)
200 REM title page
210 CLS: SCREEN 2,0
214 DRAW "BM100,15;NE2;NH2;U4"
    GET (96,9)-(104,16),Z:PUT (96,9),Z
220 LOCATE 5,10
    PRINT "Calibration : CALFIT (CAL2) - by Michel Royer"
230 LOCATE 7,5
    PRINT"Program fits a calibration curve to Lorentzian"
240 PRINT"    lines to find energies for each channel,_
      and locates channels"
250 PRINT"    where local minima occur._
          Program used gradient technique."
260 PRINT:PRINT"   HIT ANY KEY TO BEGIN."
```

```
270 A$ = INKEY$: IF A$ = "" THEN 270
300 REM MAIN MENU
310 CLS: LOCATE 10,10:PRINT"Select one of the following."
320 LOCATE 12,20: PRINT"Quit"
330 LOCATE 14,20: PRINT"Directory"
340 LOCATE 16,20: PRINT"Load a file"
350 PRINT:PRINT"Use SPC or arrow keys to select,_
      <RET> to accept selection."
360 CHOICE = 0: OLD = 0
370 CHOICE = (CHOICE + 3) MOD 3: REM keep choice in range 0 - 2
380 LOCATE 12+2*OLD,18:PRINT" ":LOCATE 12+2*CHOICE, 18: PRINT">"
390 OLD = CHOICE
400 A$ = INKEY$: IF A$ = "" THEN 400
410 IF A$ = CHR$(13) THEN 450 :REM return accepts selection
420 IF A$ = " " OR A$=DARROW$ THEN CHOICE = CHOICE + 1:GOTO 370
430 IF A$ = UARROW$ THEN CHOICE = CHOICE - 1: GOTO 370
440 GOTO 400: REM a$ not valid for this menu
450 IF CHOICE = 0 THEN SCREEN 0,0: END
460 IF CHOICE = 2 THEN 600
470 REM show directory of files
480 DIR$ = "": LOCATE 20,1
490 PRINT:PRINT"Enter drive (default is current one)"
500 PRINT"e.g., c:*.cal"
510 LINE INPUT DIR$
515 IF DIR$ = "" THEN FILES : ELSE FILES DIR$
520 PRINT:PRINT"HIT ANY KEY TO CONTINUE"
530 A$ = INKEY$: IF A$ = "" THEN 530
540 GOTO 300
600 REM load file
610 LOCATE 20,1
    PRINT"Enter name of file to be loaded":LINE INPUT NMEIN$
615 PERD = INSTR(1,NMEIN$,".")
    IF PERD = 0 THEN PERD = LEN(NMEIN$) + 1
616 NMETMP$ = LEFT$(NMEIN$,PERD-1) + ".anl"
620 ?:?"And under what name do you want the analysis saved?"
625 PRINT"(default = ";NMETMP$;")"
```

```
630 LINE INPUT NMEOUT$
635 IF NMEOUT$ = "" THEN NMEOUT$ = NMETMP$
640 ON ERROR GOTO 700:FILES NMEOUT$ :REM goto line if new file
650 PRINT" **** WARNING **** This file already exists._
     Overwrite <Y/N>?"
655 ON ERROR GOTO 0
660 A$ = INKEY$
670 IF A$ = "N" OR A$ = "n" THEN 300
680 IF A$ <>"Y" AND A$ <>"y" THEN 660
685 GOTO  710
690 REM OK to write to file
700 RESUME 710
710 ON ERROR GOTO 0
715 ?:?"How many channels in the input file (max = 1024)"
716 input nchan%: if nchan% > 1024 then 715
720 PRINT:PRINT"Please wait a moment..."
725 MAX = 0:MIN = 9999999! : XMIN = 1
730 OPEN "i",#1,NMEIN$
740 FOR LIN = 0 TO nchan%\10 - 1
750   INPUT#1,A$: IF VAL(A$) < 1 THEN 750 :REM skip any blanks
751   if right$(a$,1) <> "." then a$ = a$ + "."
752   if val(a$)<1000000 then a$=right$("     "+a$,80)
760   FOR PSN = 1 TO 10
770     NBR = 10*LIN + PSN
780     CHAN(NBR) = VAL( MID$( A$,1+8*(PSN-1),7))
790     IF CHAN(NBR)>MAX THEN MAX = CHAN(NBR)
800     IF CHAN(NBR)<MIN THEN MIN = CHAN(NBR): XMIN = NBR
810   NEXT PSN
820 NEXT LIN
830 INPUT#1,A$:if val(a$) < 1 then 830
831 if right$(a$,1) <> "." then a$ = a$ + "."
832 if val(a$)<1000000 then_
     a$ = right$("     "+a$,8*(nchan% mod 10))
834 nbr1 = nbr + 1:for nbr = nbr1 to nchan%
840 CHAN(nbr) = VAL(MID$(A$,8*(nbr-nbr1)+1,7))
845 next nbr
```

```
850 CLOSE#1
860 ?:?"Do you wish to accept the computer's default values"
870 PRINT "during the fitting process?  (Y/N)"
880 A$ = INKEY$ : IF UCASE$(A$) <> "Y" AND UCASE$(A$) <>_
    "N" THEN 880
885 IF UCASE$(A$) = "Y" THEN AUTOM = 1: ELSE AUTOM = 0
890 NORMFLAG = 0
900 REM display graph
905 CLS
910 LOW= 1: HIGH= nchan%:GOSUB 5000 :REM plot all channels
920 LOCATE 5,1:PRINT"How many"
    PRINT"peaks are":PRINT"there?"
925 LOCATE 13,1:PRINT"Hit E to"
    PRINT"exit to":PRINT"main menu.":LOCATE 8,1
926 NPEAKS = 0: NPEAKS$ = "": I=0
930 A$ = INKEY$:IF A$ = CHR$(13) THEN 1000
940 IF A$ = "e" OR A$ = "E" THEN 300
950 IF A$<>CHR$(8) THEN 970
955 IF LEN (NPEAKS$) <1 THEN 970
960 NPEAKS$ = LEFT$(NPEAKS$,LEN(NPEAKS$)-1):PRINT A$;
970 IF A$ <"0" OR A$>"9" THEN 930
980 PRINT A$;: NPEAKS$ = NPEAKS$ + A$:GOTO 930
1000 NPEAKS =  VAL(NPEAKS$)
1010 IF NPEAKS = 0 THEN 900
1020 LOCATE 17,1:PRINT"Use arrows":PRINT"to select"
1050 REM define each peak
1060 TOL = 10 * SQR(CHAN(1))
1080 FOR PEAK = 1 TO NPEAKS
1090    I = I + 1
1100    IF I > nchan%-5 THEN I = nchan%-5:_
        ISTART = I:IFLAG = I: ICTR = I:GOTO
1200
1110    IF TOL > CHAN(I) - CHAN(I+5) THEN 1090
1120    ISTART = I + 5
1121 IFLAG = ISTART
1125 I = I + 7
```

```
1130    WHILE CHAN(I+2) < CHAN(I)
1140      I = I + 1
1150    WEND
1160    ICTR = I + 1
1165 I = I + 4
1170    WHILE TOL < CHAN(I+5) - CHAN(I)
1180      I = I + 1
1190    WEND
1200    IEND = I
1205 LOCATE 2,26:PRINT"low:";ISTART:LOCATE 2,45
       PRINT"high:";IEND
1210    LOCATE 19,1:PRINT"low channel "
1220    GOSUB 5500:LOCATE 2,30:PRINT ISTART
1230    A$ = INKEY$: IF A$ = CHR$(13) THEN 1300
1235    IF AUTOM = 1 THEN 1300
1240    IF A$ = "e" OR A$ = "E" THEN 300
1250    IF A$ <> LARROW$ AND A$ <> RARROW$ THEN 1230
1260    GOSUB 5500 : REM clear arrows
1270    IF A$ = LARROW$ THEN ISTART =1+_
          (ISTART+nchan%-2) MOD nchan%
1280    IF A$ = RARROW$ THEN ISTART =1+ ISTART MOD nchan%
1290    GOTO 1220
1300    LOCATE 19,1:PRINT"high channel"
1305    GOSUB 5500 : REM clear for next line
1310    GOSUB 5500:LOCATE 2,50:PRINT IEND
1320    A$ = INKEY$: IF A$ = CHR$(13) THEN 1400
1325    IF AUTOM = 1 THEN 1400
1330    IF A$ = "e" OR A$ = "E" THEN 300
1340    IF A$ <> LARROW$ AND A$ <> RARROW$ THEN 1320
1350    GOSUB 5500 : REM clear arrows
1360    IF A$ = RARROW$ THEN IEND =1+ IEND MOD nchan%
1370    IF A$ = LARROW$ THEN IEND =1+_
         (IEND+nchan%-2) MOD nchan%
1380    GOTO 1310
1400    GOSUB 5500: REM clear arrows
1410    LOWCH(PEAK) = ISTART: HIGHCH(PEAK) = IEND_
```

```
       : CTRCH(PEAK) = ICTR
1411   if istart > i or iend < iflag_
       then ctrch(peak) = istart/2 + iend/2
1412   i=iend
1420 NEXT
1450 REM start fitting to lorentzians
1460 FOR PEAK = 1 TO NPEAKS
1470 CLS:LOCATE 10,5
1480 PRINT"Please wait while the peaks are fit to_
          Lorentzian lineshapes."
1490 LOCATE 13,10:PRINT"Fitting peak #";PEAK
1500 LOCATE 17,12:PRINT"Iteration"
1510 GOSUB 6000 : REM fit to Lorentzian lineshape
1515 IF AUTOM = 1 THEN 1800 : ' DON'T PRINT RESULTS OF EACH FIT
1520 CLS:SCREEN 0,0:LOCATE 3,42:PRINT"Error"
1530 LOCATE 5,1:PRINT"Peak height"TAB(20);a(1);TAB(40);
1531 PRINT sqr(covar(1,1))
1540 LOCATE 7,1:PRINT"Half width gamma"TAB(20);a(2);TAB(40);
1541 PRINT sqr(covar(2,2))
1550 LOCATE 9,1:PRINT"Channel at center"TAB(20);a(3);TAB(40);
1551 PRINT sqr(covar(3,3))
1560 LOCATE 11,1:PRINT"Background: slope"TAB(20);a(4);TAB(40);
1561 PRINT sqr(covar(4,4))
1570 LOCATE 13,1:PRINT"Background: y-int"TAB(20);a(5);TAB(40);
1571 PRINT sqr(covar(5,5))
1572 LOCATE 15,1:PRINT"Chi-squared"TAB(20);chisq
1573 PRINT:PRINT" '' start"TAB(20);CHISTART
1574 PRINT:PRINT"No. of iter."TAB(20);ITER%
1580 PRINT:PRINT"Hit:    E to exit to main menu."
1590   PRINT"          D to display graph of fit."
1600   PRINT"          any other key to continue."
1610 A$ = INKEY$: IF A$ = "" THEN 1610
1620 IF A$ = "e" OR A$ = "E" THEN SCREEN 2,0:GOTO 300
1630 IF A$ <> "d" AND A$ <> "D" THEN 1800
1640 REM display fitted graph
1645 CLS : SCREEN 2,0
```

```
1650 LOCATE 5,1:PRINT"E = exit":PRINT" to main":PRINT" menu."
1660 LOCATE 10,1:PRINT"A = accept":PRINT" fit."
1670 LOCATE 15,1:PRINT"R = reject":PRINT" fit."
1672 LOCATE 20,1:PRINT"  = expt. data."
1673 PRINT"  = best fit."
1674 LINE(3,156)-(5,156):PSET(4,164)
1675 ISTART = LOWCH(PEAK):IEND = HIGHCH(PEAK)
1680 WHILE IEND - ISTART >100
1685   ISTART = ISTART + 1: IEND = IEND - 1
1690 WEND
1700 FOR I = ISTART TO IEND
1710 LINE (99+5*(I-ISTART),200-HT(I))_
     - (101+5*(I-ISTART),200-HT(I))
1720 BG = a(4)*I + a(5)
1725 LOR = a(1)*a(2)^2/((I-a(3))^2 + a(2)^2)
1730 HT = INT((BG-LOR - YMIN)*SLOPE + .5)
1740 PSET (100+5*(I-ISTART), 200-HT)
1770 NEXT
1780 A$ = INKEY$:IF A$ = "e" OR A$ = "E" THEN 300
1785 IF A$ = "R" OR A$ = "r" THEN CH0(PEAK)=0:GOTO 1810
1790 IF A$ <> "A" AND A$ <> "a" THEN 1780
1800 CH0(PEAK) = a(3)
1805 screen 2,0
1810 NEXT PEAK
1820 REM choose values for energies
1830 CLS: LOCATE 2,5
     PRINT"For each of the peaks, enter its corresponding"
1835 LOCATE 3,5
     PRINT"transducer velocity (in mm/s), or enter the"
1840 LOCATE 4,5:PRINT"appropriate code from the table."
1843 IF xmin < nchan%/2 + 1 THEN RM1$ = "first": RM2$ = "NEG."
1844 IF xmin > nchan%/2 THEN RM1$= "second": RM2$= "POS."
1845 PRINT "*** The ";RM1$;" half has a lower background, so"
1846 PRINT "    the first and last peaks have the most "_
          ;RM2$;" velocities."
1850 LOCATE 7,3:PRINT"peak    center"
```

```
1860 FOR PEAK = 1 TO NPEAKS:PRINT TAB(4);PEAK;TAB(11);
1870 IF CH0(PEAK) = 0 THEN ? "reject":ELSE PRINT CH0(PEAK)
1880 NEXT PEAK
1890 LOCATE 7,40:READ NCODE:PRINT"code";TAB(50);"velocity"
1900 FOR I = 1 TO NCODE
1910   READ CODE$(I),VEL(I)
1920   LOCATE 7+I,40: PRINT CODE$(I); TAB(50); VEL(I)
1930 NEXT : RESTORE
1940 IF NPEAKS > NCODE THEN VPOS = 7_
      + NPEAKS: ELSE VPOS = 7 + NCODE
1945 FOR PEAK = 1 TO NPEAKS: LOCATE 7+PEAK, 1: PRINT">"
1946 VEL = 0 : IF CH0(PEAK) = 0 THEN 2000
1950 LOCATE VPOS+1,5
     PRINT"Enter velocity or code:                    ";
1960 LOCATE VPOS+1,28: INPUT VEL$
1970 IF VAL(VEL$) <>0 THEN VEL = VAL(VEL$):GOTO 2000
1980 FOR I = 1 TO NCODE
     IF UCASE$(VEL$) = UCASE$(CODE$(I)) THEN VEL = VEL(I)
1990 NEXT: IF VEL = 0 THEN 1950
2000 ENERGY(PEAK) = VEL: LOCATE 7+PEAK, 1: PRINT" ": NEXT PEAK
2005 print: Print"Are these values correct (Y/N)?"
2006 a$ = inkey$
2007 if a$ = "n" or a$ = "N" then 1820
2008 if a$ <>"y" and a$ <>"Y" then 2006
2010 LOCATE 24,10:PRINT "Please wait..."
2020 REM regression
2025 R11 = 0: R12 = 0: R13 = 0: R14 = 0: N1 = 0
2026 R21 = 0: R22 = 0: R23 = 0: R24 = 0: N2 = 0
2030 FOR PEAK = 1 TO NPEAKS
2040   IF CH0(PEAK) < nchan%\2+1 THEN 2100
2050   R21 = R21 + CH0(PEAK) * ENERGY(PEAK)
2060   R22 = R22 + CH0(PEAK)
2070   R23 = R23 + ENERGY(PEAK)
2080   R24 = R24 + CH0(PEAK)^2
2090   N2 = N2 + 1: GOTO 2200
2100   R11 = R11 + CH0(PEAK) * ENERGY(PEAK)
```

```
2110  R12 = R12 + CH0(PEAK)
2120  R13 = R13 + ENERGY(PEAK)
2130  R14 = R14 + CH0(PEAK)^2
2140  IF CH0(PEAK) > 0 THEN N1 = N1 + 1
2200 NEXT PEAK
2210 SLPE1 = (N1*R11 - R12*R13) / (N1*R14 - R12*R12)
2220 SLPE2 = (N2*R21 - R22*R23) / (N2*R24 - R22*R22)
2230 ITCPT1 = R13/N1 - SLPE1 * R12/N1
2240 ITCPT2 = R23/N2 - SLPE2 * R22/N2
2250 REM plot of regression
2260 CLS:LOCATE 2,35:PRINT"Plot of regression."
2270 LINE (100,100)-(612,100)
2280 LOCATE 5,1:PRINT"E = exit":PRINT" to main":PRINT" menu."
2290 LOCATE 12,1:PRINT"Any other": PRINT" key to"
     PRINT" continue."
2292 YMAX = 0:FOR PEAK = 1 TO NPEAKS
2294 IF ABS(ENERGY(PEAK)) > YMAX THEN YMAX = ABS(ENERGY(PEAK))
2296 NEXT PEAK
2300 FOR PEAK = 1 TO NPEAKS
2310 X = 100 + CH0(PEAK)*512/nchan%: Y = 100_
     - INT(ENERGY(PEAK) * 50/YMAX + .5)
2320 PSET (X,Y) : NEXT PEAK
2330 FOR I = 1 TO nchan%\2
2340  X = 100 + I*512/nchan% : Y = 100_
    - INT((SLPE1*I + ITCPT1) * 50/YMAX + .5)
2350  PSET (X,Y): NEXT I
2360 FOR I = nchan%\2+1 to nchan%
2370  X = 100 + I*512/nchan% : Y = 100_
     - INT((SLPE2*I + ITCPT2) * 50/YMAX + .5)
2380  PSET (X,Y) : NEXT I
2390 A$ = INKEY$: IF A$ = "" THEN 2390
2391 IF A$ = "e" OR A$ = "E" THEN 300
2400 REM save results
2410 CLS:LOCATE 15,20
    PRINT"Do you want the results saved (Y/N)?"
2420 A$ = INKEY$
```

```
2430 IF A$ = "n" OR A$  = "N" THEN 300
2440 IF A$ <> "y" AND A$ <> "Y" THEN 2420
2450 OPEN "o",2, NMEOUT$
2460 PRINT#2, SLPE1, ITCPT1
2470 PRINT#2, SLPE2, ITCPT2
2480 CLOSE 2
2500 GOTO 300
4000 DATA 15
4001 REM all center shifts are wrt metallic iron at rm temp.
4005 REM metallic iron at room temperature
4010 DATA "Fe1",-5.3285
4020 DATA "Fe2", -3.0835
4030 DATA "Fe3", -0.8385
4040 DATA "Fe4", +0.8385
4050 DATA "Fe5", +3.0835
4060 DATA "Fe6", +5.3285
4065 REM alpha-Fe2O3 at room temperature
4070 DATA "aFO1", -8.09
4080 DATA "aFO2", -4.33
4090 DATA "aFO3", -0.81
4100 DATA "aFO4", +1.81
4110 DATA "aFO5", +5.33
4120 DATA "aFO6", +8.61
4125 REM Sodium NitroPrusside Na2[Fe(CN)5NO].2H2O
4130 DATA "SNP1", -1.113
4140 DATA "SNP2", +0.599
4145 REM Potassium FerroCyanide K4Fe(CN)6.3H2O
4150 DATA "PFC1", -0.045
5000 REM graph   subroutine to plot data on screen
5010 IF NORMFLAG =0 THEN GOSUB 5100
5015 CLS
5020 MIDDLE = INT(LOW!/2 + HIGH!/2)
5030 FACTOR = 512/(HIGH!-LOW!)
5040 FOR II = LOW! TO HIGH!
5050   LINE (356-FACTOR*(MIDDLE-II),180)_
      -(356-FACTOR*(MIDDLE-II),200-HT(II))
```

```
5060 NEXT
5070 LINE (99,16)-(99,180):LINE -(615,180)
5080 LOCATE 24,12:PRINT LOW!;:LOCATE 24,43:PRINT MIDDLE;
5085 LOCATE 24,75:PRINT HIGH!;
5090 RETURN
5100 REM normalize data
5110 ' normalizes data in chan(ii), places result in ht(ii)
5120 ' so that max ht - min ht = 3/4 of scrht,
5130 ' scrht being the height in pixels of the screen
5140 NORMFLAG = 1: SCRHT = 200
5150 RANGE = (MAX - MIN) * 2/3 : CENTER = MAX/2 + MIN/2
5160 YMIN = CENTER - RANGE : SLOPE = (SCRHT/2)/RANGE
5170 FOR II = 1 TO nchan%
       HT(II) = INT((CHAN(II)-YMIN)*SLOPE + .5)
5180 NEXT II: RETURN
5500 REM plot arrows
5510   PUT (100+ISTART*512/nchan%-4,200-HT(ISTART)-10),Z
5520   PUT (100+IEND*512/nchan%-4,200-HT(IEND)-10),Z
5550 RETURN
6000 REM Subroutine to fit lines to Lorentzians
6010 REM preparations...first guess
6015 REM parameters: h,gamma,i0,bgslope,bgintcpt
6030 a(1) = CHAN(LOWCH(PEAK))/2+CHAN(HIGHCH(PEAK))/2_
                        -CHAN(CTRCH(PEAK))
6031 a(1) = a(1) + SQR(a(1))
6040 ZZ = LOWCH(PEAK):HLF = CHAN(LOWCH(PEAK))/2_
                    + CHAN(CTRCH(PEAK))/2
6041 WHILE CHAN(ZZ) > HLF : ZZ = ZZ + 1 : WEND
6042 a(2) = CTRCH(PEAK) - ZZ
6050 a(3) = CTRCH(PEAK)
6060 a(4) = CHAN(HIGHCH(PEAK))-CHAN(LOWCH(PEAK))
6061 a(4) = a(4)/(HIGHCH(PEAK)-LOWCH(PEAK))
6070 a(5) = CHAN(LOWCH(PEAK)) - a(4) * LOWCH(PEAK)
6071 a(5) = a(5) + 10*SQR(abs(a(5)))
6080 iter% = 0: termflag% = 0: alambda = -1 'cause init.
6085 for i% = 1 to 5: lista%(i%) = i% : next i%
```

```
6086 for i% = lowch(peak) to highch(peak):j%=i%-lowch(peak)+1
6087  x(j%) = i%: y(j%) = chan(i%): sig(j%) = sqr(y(j%))
6088 next i%
6090 call mrqmin (x(),y(),sig(),j%,a(),5,lista%(),5,covar(),_
                 alpha(),5,chisq,alambda)
6100 chistart = chisq
6110 while termflag% < 2
6120   ochisq = chisq
6125   incr iter%
6126   locate 17,23 : ? iter%
6127   locate 20,25 : ? "Chi-squared:";chisq
6130   call mrqmin (x(),y(),sig(),j%,a(),5,lista%(),5,covar(),_
                 alpha(),5,chisq,alambda)
6140    if abs(ochisq - chisq) < 1 then
6150      termflag% = termflag% + 1
6160   else
6170      termflag% = 0
6180   end if
6190 wend
6200 alambda = 0      ' to get covariance matrix
6210 call mrqmin (x(),y(),sig(),j%,a(),5,lista%(),5,covar(),_
                 alpha(),5,chisq,alambda)
6220 return


rem ********************************************************

sub mrqmin (x(1),y(1),sig(1),ndata%,a(1),ma%,lista%(1),mfit%,_
           covar(2),alpha(2),nca%,chisq,alambda)
local mmax%,atry(),da(),kk%,j%
static ochisq,beta()
mmax% = 7
dim dynamic atry(mmax%),da(mmax%)

if alambda < 0 then       ' initialization
   kk% = mfit% + 1
```

```
   for j% = 1 to mfit%
      ihit% = 0
      for k% = 1 to mfit%
         if lista%(k%) = j% then incr ihit%
      next k%
      if ihit% = 0 then
         lista%(kk%) = j%
         incr kk%
      elseif ihit% > 1 then
         ? "improper permutation in lista"
         delay 5
      end if
   next j%
if kk% <> ma%+1 then ?"improper permutation in lista":delay 5
   alambda = 0.001
   call mrqcof (x(),y(),sig(),ndata%,a(),ma%,lista%(),mfit%,_
                alpha(),beta(),nca%,chisq)
   ochisq = chisq
   for j% = 1 to ma%: atry(j%) = a(j%): next j%
end if

for j% = 1 to mfit%
   for k% = 1 to mfit%
      covar(j%,k%) = alpha(j%,k%)
   next k%
   covar(j%,j%) = alpha(j%,j%) * (1! + alambda)
   da(j%) = beta(j%)
next j%
call gaussj (covar(), mfit%, nca%, da(), 1, 1)
if alambda = 0 then
   call covsrt (covar(), nca%, ma%, lista%(), mfit%)
   exit sub
end if
for j% = 1 to mfit%
   atry(lista%(j%)) = a(lista%(j%)) + da(j%)
next j%
```

```
call mrqcof (x(),y(),sig(),ndata%,atry(),ma%,lista%(),mfit%,_
             covar(),da(),nca%,chisq)
if chisq < ochisq then
   alambda = 0.1 * alambda
   ochisq = chisq
   for j% = 1 to mfit%
      for k% = 1 to mfit%
         alpha(j%,k%) = covar(j%,k%)
      next k%
      beta(j%) = da(j%)
      a(lista%(j%)) = atry(lista%(j%))
   next j%
else
   alambda = 10! * alambda
   chisq = ochisq
end if
end sub

rem ************************************************
sub mrqcof (x(1),y(1),sig(1),ndata%,a(1),ma%,lista%(1),mfit%,_
            alpha(2),beta(1),nalp%,chisq)
local mmax%,sig2i,j%,k%,i%,ymod,wt,dyda()
mmax% = 7
dim dynamic dyda(mmax%)

for j% = 1 to mfit%
   for k% = 1 to j%
      alpha(j%,k%) = 0
   next k%
   beta(j%) = 0
next j%
chisq = 0
for i% = 1 to ndata%
   call funcs(x(i%),a(),ymod,dyda(),ma%)
   sig2i = 1 / (sig(i%) * sig(i%))
   dy = y(i%) - ymod
```

```
   for j% = 1 to mfit%
      wt = dyda(lista%(j%)) * sig2i
      for k% = 1 to j%
         alpha(j%,k%) = alpha(j%,k%) + wt * dyda(lista%(k%))
      next k%
      beta(j%) = beta(j%) + dy * wt
   next j%
   chisq = chisq + dy * dy * sig2i
next i%
for j% = 2 to mfit%
   for k% = 1 to j% - 1
      alpha(k%,j%) = alpha(j%,k%)
   next k%
next j%
end sub


rem ***************************************************
sub gaussj (a(2),n%,np%,b(2),m%,mp%)
local nmax%,big%,irow%,icol%,i%,j%,k%,ipiv%(),indxr%(),indxc%(),_
      dum,pivinv,l%,ll%
nmax% = 7
dim dynamic ipiv%(nmax%),indxr%(nmax%),indxc%(nmax%)

for j% = 1 to n%
   ipiv%(j%) = 0
next j%
for i% = 1 to n%
   big = 0
   for j% = 1 to n%
      if ipiv%(j%) <> 1 then
         for k% = 1 to n%
            if ipiv%(k%) = 0 then
               if abs(a(j%,k%)) >= big then
                  big = abs(a(j%,k%))
                  irow% = j%
```

```
                icol% = k%
             end if
          elseif ipiv%(k%) > 1 then
             ? "singular matrix"
             delay 5
          end if
       next k%
    end if
next j%
incr ipiv%(icol%)
if irow% <> icol% then
    for l% = 1 to n%
       swap a(irow%,l%), a(icol%,l%)
    next l%
    for l% = 1 to m%
       swap b(irow%,l%), b(icol%,l%)
    next l%
end if
indxr(i%) = irow%
indxc(i%) = icol%
if a(icol%,icol%) = 0 then ? "singular matrix" : delay 5
pivinv = 1 / a(icol%,icol%)
a(icol%,icol%) = 1
for l% = 1 to n%
    a(icol%,l%) = a(icol%,l%) * pivinv
next l%
for l% = 1 to m%
    b(icol%,l%) = b(icol%,l%) * pivinv
next l%
for ll% = 1 to n%
    if ll% <> icol% then
       dum = a(ll%,icol%)
       a(ll%,icol%) = 0
       for l% = 1 to n%
          a(ll%,l%) = a(ll%,l%) - a(icol%,l%) * dum
       next l%
```

```
         for l% = 1 to m%
            b(ll%,l%) = b(ll%,l%) - b(icol%,l%) * dum
         next l%
      end if
   next ll%
next i%
for l% = n% to 1 step -1
   if indxr%(l%) <> indxc%(l%) then
      for k% = 1 to n%
         swap a(k%,indxr%(l%)), a(k%,indxc%(l%))
      next k%
   end if
next l%
end sub


rem ***************************************************
sub covsrt (covar(2),ncvm%,ma%,lista%(1),mfit%)
local i%,j%,temp

for j% = 1 to ma% - 1
   for i% = j% + 1 to ma%
      covar(i%,j%) = 0
   next i%
next j%
for i% = 1 to mfit% - 1
   for j% = i% + 1 to mfit%
      if lista%(j%) > lista%(i%) then
         covar(lista%(j%),lista%(i%)) = covar(i%,j%)
      else
         covar(lista%(i%),lista%(j%)) = covar(i%,j%)
      end if
   next j%
next i%
temp = covar(1,1)
for j% = 1 to ma%
```

```
   covar(1,j%) = covar(j%,j%)
   covar(j%,j%) = 0
next j%
covar(lista%(1),lista%(1)) = temp
for j% = 2 to mfit%
   covar(lista%(j%),lista%(j%)) = covar(1,j%)
next j%
for j% = 2 to ma%
   for i% = 1 to j% - 1
      covar(i%,j%) = covar(j%,i%)
   next i%
next j%
end sub

rem ***************************************************
sub funcs (x,a(1),y,dyda(1),ma%)
local bg,lor,den

'parameters are h, gamma, Io, slp, itcpt and are in A()
den = (x - a(3))^2 + a(2) * a(2)
bg = a(4) * x + a(5)
lor = a(1) * a(2) * a(2) / den
y = bg - lor
dyda(1) = -a(2) * a(2) / den
dyda(2) = -2 * a(1) * a(2) * ((x - a(3)) / den)^2
dyda(3) = -2 * a(1) * a(2) * a(2) * (x - a(3)) / (den * den)
dyda(4) = x
dyda(5) = 1
end sub
```

FOLDER.BAS

```
10 REM FOLDER (Moss2)  by Michel Royer
20 ' program will "fold" a data file,
21 ' display the resulting graph,
30 ' and allow comments to be included in the file.
40 ' June, 1988
50 ' University of Ottawa
60 ' doesn't assume 512 unfolded channels
100 REM initializations
110 KEY OFF: OPTION BASE 1
120 DIM C$(20), c(20), CHAN(1024), VEL(512),_
    HT(512), Z(5), TEM(512)
130 LARROW$ = CHR$(0) + CHR$(75)
140 RARROW$ = CHR$(0) + CHR$(77)
150 UARROW$ = CHR$(0) + CHR$(72)
160 DARROW$ = CHR$(0) + CHR$(80)
170 for c = 3 to 20:read c$:c(c)=len(c$):next:restore
200 REM title page
210 SCREEN 2,0: CLS
220 REM ready & clear arrow
230 DRAW "bm100,15; ne2; nh2; u4"
    GET (96,9)-(104,16),Z: PUT (96,9),Z
240 LOCATE 5,28: PRINT"FOLDER (MOSS2) - by Michel Royer"
250 LOCATE 8,5: PRINT"Program will_
    fold Mossbauer data files, display"
260 PRINT TAB(5);"the resulting graph,_
    and allow editing of comments."
270 LOCATE 20,5: PRINT"HIT ANY KEY TO BEGIN."
280 A$ = INKEY$: IF A$ = "" THEN 280
300 REM main menu
310 CLS
320 LOCATE 5,10: PRINT"Quit"
330 LOCATE 7,10: PRINT"Directory"
340 LOCATE 9,10: PRINT"Load unfolded data file"
350 LOCATE 11,10: PRINT"Load folded data file"
```

```
360 LOCATE 13,10: PRINT"Display graph of data"
370 LOCATE 15,10: PRINT"Edit comments"
380 LOCATE 17,10: PRINT"Save folded file"
390 LOCATE 19,5
     PRINT"Use arrow keys or spacebar to select option,"
400 PRINT TAB(5);"and <RETURN> to accept selection."
410 CHOICE = 0
420 LOCATE 5 + 2*CHOICE , 8 : PRINT ">"
430 A$ = INKEY$
440 IF A$ = CHR$(13) THEN 510
450 IF A$ = " " OR A$ = DARROW$ THEN INC = 1 : GOTO 480
460 IF A$ = UARROW$ THEN INC = -1: GOTO 480
470 GOTO 430
480 LOCATE 5 + 2*CHOICE , 8 : PRINT " "
490 CHOICE = (CHOICE + INC + 7) MOD 7
500 GOTO 420
510 REM choice accepted
520 IF CHOICE = 0 THEN SCREEN 0,0: END
530 ON CHOICE GOSUB 1000, 2000, 3000, 4000, 5000, 6000
540 GOTO 300
999 REM ******************************************************
1000 REM directory of files
1010 CLS
1020 LOCATE 5,10
      PRINT"Enter drive name (default is current one)."
1030 INPUT DRV$
1040 IF DRV$ = "" THEN FILES : ELSE FILES DRV$
1050 PRINT: PRINT"HIT ANY KEY TO CONTINUE."
1060 A$ = INKEY$: IF A$ = "" THEN 1060
1070 RETURN
1999 REM ************************************************************
2000 REM load unfolded file
2010 YMIN = 9999999!: XMIN = 1
2020 CLS: LOCATE 3,5
2030 PRINT"Enter the name of the data file_
      to be studied (eg, name.dat):"
```

```
2035 ? TAB(5); "(Simply hitting <RETURN> exits to main menu)
2040 INPUT NME$ : IF NME$ = "" THEN RETURN
2041 ?:?"How many channels should be_
       in this file (max=1024)?":input nchan%
2042 if nchan% > 1024 then 2041
2045 PRINT:PRINT"Loading ";NME$
2050 OPEN "i", 1, NME$
2060 FOR LIN = 0 TO nchan%\10-1
2070  INPUT#1, A$: IF VAL(A$) < 1 THEN 2070 : ' skip blanks
2071  if right$(a$,1) <> "." then a$ = a$ + "."
2075  if val(a$)<1000000 then a$ = right$("     "+a$,80)
2080  FOR PSN = 1 TO 10
2090   NBR = 10*LIN + PSN
2100   CHAN(NBR) = VAL( MID$(A$, 1+8*(PSN-1), 7))
2120   IF CHAN(NBR) < YMIN THEN_
      YMIN = CHAN(NBR) : XMIN = NBR
2130  NEXT PSN
2140 NEXT LIN
2150 INPUT#1, A$ : if val(a$) < 1 then 2150
2151 if right$(a$,1) <> "." then a$ = a$ + "."
2152 if val(a$) < 1000000 then a$ =_
    right$("     "+a$,8*(nchan% mod 10))
2153 nbr1 = nbr+1
2155 for nbr = nbr1 to nchan%
2160 CHAN(nbr) = VAL(MID$(A$,8*(nbr-nbr1) + 1,7))
2165 next nbr
2170 CLOSE 1
2180 PRINT:PRINT"Also enter the calibration file containing"
2190 PRINT"the folding parameters (eg, name.anl)"
2200 INPUT CALNME$
2210 PRINT:PRINT"Loading ";CALNME$
2220 OPEN "i", 1, CALNME$
2230 INPUT#1, SLP1, ITCPT1
2240 INPUT#1, SLP2, ITCPT2
2250 CLOSE 1
2260 C$(1) = "Slope 1:" + STR$(SLP1)+"  Itcpt 1:"+STR$(ITCPT1)
```

```
2270 C$(2) = "Slope 2:" + STR$(SLP2)+"  Itcpt 2:"+STR$(ITCPT2)
2285 REM fold data
2286 PRINT"Please wait while program folds data..."
2290 IF XMIN > nchan%\2 THEN 2400 : ' fold onto half 2
2300 REM fold onto half 1
2310 FOR I = 1 TO nchan%\2
2320  VEL(I) = I * SLP1 + ITCPT1
2330  I2 = (VEL(I) - ITCPT2) / SLP2
2340  I21 = INT(I2)
2350  IF I21 < nchan%\2 + 1 THEN CTS = CHAN(I): GOTO 2380
2360  IF I21 > nchan%-1 THEN CTS = CHAN(I): GOTO 2380
2370  CTS = CHAN(I21) + (I2 - I21) * (CHAN(I21+1) - CHAN(I21))
2380  CHAN(I) = INT( CHAN(I)/2 + CTS/2 + 0.5) ' force an integer
2390 NEXT I : nchan% = 2 * (nchan% \ 2) ' force an even number
2392 goto 2500
2400 REM fold onto half 2
2410 FOR I = nchan%\2 + 1 to nchan%
2420  VEL(I-nchan%\2) = I * SLP2 + ITCPT2
2430  I1 = (VEL(I-nchan%\2) - ITCPT1) / SLP1
2440  I11 = INT(I1)
2450  IF I11 < 1 THEN CTS = CHAN(I): GOTO 2480
2460  IF I11 > nchan%\2 - 1 THEN CTS = CHAN(I): GOTO 2480
2470  CTS = CHAN(I11) + (I1 - I11) * (CHAN(I11+1) - CHAN(I11))
2480  CHAN(I) = INT( CHAN(I)/2 + CTS/2 + 0.5)_
     ' force an integer
2490 NEXT I
2495 FOR I = 1 TO nchan%-nchan%\2: CHAN(I) =_
      CHAN(I+nchan%\2): NEXT
2500 REM reset comments
2510 FOR C = 3 TO 20: READ C$(C): NEXT: RESTORE
2520 REM find max and min counts
2530 XMAX = 1: XMIN = 1: YMAX = CHAN(1): YMIN = CHAN(1)
2535 nchan% = nchan% - nchan%\2  : ' nbr of folded channels
  IF VEL(1)>0. THEN
   CLS
   LOCATE 9,10: PRINT"There may be something wrong_
```

```
                    in the calibration file"
   LOCATE 24,5: PRINT"Press any key to continue"
2536 SCR$=INKEY$:IF SCR$="" THEN 2536
   FOR I=1 TO NCHAN%
   TEM(I)=VEL(I)
   NEXT I
   FOR I=1 TO NCHAN%
   VEL(I)=TEM(NCHAN%-I+1)
   NEXT I
   FOR I=1 TO NCHAN%
   TEM(I)=CHAN(I)
   NEXT I
   FOR I=1 TO NCHAN%
   CHAN(I)=TEM(NCHAN%-I+1)
   NEXT I
  END IF
2540 FOR I = 2 TO nchan%
2550 IF CHAN(I) > YMAX THEN YMAX = CHAN(I): XMAX = I
2560 IF CHAN(I) < YMIN THEN YMIN = CHAN(I): XMIN = I
2570 NEXT
2580 NORMFLAG = 0
2590 RETURN
2600 REM data
2610 DATA "filename:"
2620 DATA "substance:"
2630 DATA "absorber preparation:"
2640 DATA "sample treatment:"
2650 DATA "absorber temperature:"
2660 DATA "folded with:"
2670 DATA "running time:"
2680 DATA "date saved on disk:"
2690 DATA "remarks:"
2700 DATA " "," "," "," "," "," "," "," "," "," "
2999 REM ******************************************************
3000 REM load folded file
3010 CLS: LOCATE 5,5: PRINT"Enter name of file to be studied"
```

```
3020 ? TAB(5); "(Simply hitting <RETURN> exits to main menu)
3030 INPUT NME$: IF NME$ = "" THEN RETURN
3040 PRINT:PRINT"Loading "; NME$
3050 OPEN "i", 1, NME$
3055 input#1,nchan%
3060 FOR NUM = 1 TO nchan%
3070  INPUT#1, VEL(NUM), CHAN(NUM)
3080 NEXT
3081 ' REARRANGE IF OLDER FLD FILE!
3082 IF VEL(1) > 100 THEN
       FOR NUM = 1 TO NCHAN%
          SWAP VEL(NUM), CHAN(NUM)
       NEXT NUM
     END IF
3090 INPUT#1, XMIN, XMAX
3095 YMIN = CHAN(XMIN): YMAX = CHAN(XMAX)
3100 FOR C = 1 TO 20 : INPUT#1, C$(C) : NEXT
3110 CLOSE 1
3120 NORMFLAG = 0
3130 RETURN
3999 REM ******************************************************
4000 REM display graph
4005 gosub 4400 ' verify velocity scale
4010 IF NORMFLAG = 0 THEN GOSUB 4500
4020 CLS : X = 40 - INT(LEN(NME$) + .5) /2
4030 LOCATE 1,X: PRINT NME$
4040 LOCATE 3,15: PRINT"Channel:"
4050 LOCATE 3,35: PRINT"Velocity:"
4060 LOCATE 3,60: PRINT"# Counts:"
4070 LOCATE 10,1: PRINT"Hit E to":PRINT"escape to"
      PRINT"main menu"
4080 LOCATE 16,1: PRINT"Use arrow":PRINT"keys or"
      PRINT"'<', '>'"
4090 PRINT"to move":PRINT"the arrow"
4095 LOCATE 25,75: PRINT"mm/s";
4100 LINE (100,25) - (100,190) : LINE -(613,190)
```

```
4105 vnrm = 511/(m1-m)
4110 FOR I = 1 TO nchan%
4120     x = 101 + vnrm * (vel(I)-m)
4125     if x > 100 and x <= 612 then pset (x, 200-HT(I))
4130 NEXT
4131 REM X SCALE
4132 MAXTIC = INT(m + 0.5):MAXTIC1 = INT(m1 + 0.5)
4133 st=2
4134 IF (MAXTIC1-MAXTIC)<10 THEN st=1
4135 FOR I =MAXTIC TO MAXTIC1 STEP st
4136 COL = VNRM * (I - m)
4137 IF COL < 0 OR COL > 472 THEN 4140
4138 LINE (101+COL,188) - (101+COL,190)
4139 X = 12 + COL/8:LOCATE 25,X:PRINT I;
4140 NEXT
4145 I = 1 : inc = 1
4150 x = 96 + vnrm * (vel(i)-m)
4153 if x < 96 or x > 606 then 4270
4155 PUT(x, 200 - HT(I) - 6), Z
4160 LOCATE 3,23: PRINT I;"  "
4170 LOCATE 3,44: PRINT int(10000*VEL(I))/10000;"    "
4180 LOCATE 3,68: PRINT int(1000*CHAN(I))/1000;"    "
4190 A$ = INKEY$
4200 IF A$ = "e" OR A$ = "E" THEN RETURN
4210 IF A$ = RARROW$ THEN INC = 1: GOTO 4260
4220 IF A$ = LARROW$ THEN INC = -1: GOTO 4260
4230 IF A$ = ">" THEN INC = 10: GOTO 4260
4240 IF A$ = "<" THEN INC = -10: GOTO 4260
4250 GOTO 4190
4260 PUT(x, 200 - HT(I) - 6), Z
4270 I = 1 + ((I -1 + INC + nchan%) MOD nchan%)
4280 GOTO 4150
4400 rem ********************************
4410 rem verify velocity scale
4420 cls
4430 ?:?"What do you want for a minimum_
```

```
        velocity on the x axis (mm/s)?"
4440 ? "Just hitting <RETURN> selects the default."
4450 input a$
4460 m = val(a$)
4470 if m = 0 then
     m=-abs(vel(1)):m1=-m:GOTO 4490
     end if
4475 ?:?"What do you want for a maximum_
        velocity on the x axis (mm/s)?"
4480 input a$
4485 m1= val(a$)
4490 return
4499 REM ********************************
4500 REM normalize
4510 ' normalizes data in chan(i), places result in ht(i)
4520 ' so then max ht - min ht = 3/4 of scrht,
4530 ' scrht being the height of the screen in pixels
4540 NORMFLAG = 1: SCRHT = 200
4550 RANGE = (YMAX - YMIN) * 2/3 : CENTER = YMAX/2 + YMIN/2
4560 LOWEST = CENTER - RANGE : SLOPE = (SCRHT/2) / RANGE
4570 FOR I = 1 TO nchan%
4580  HT(I) = INT((CHAN(I) - LOWEST) * SLOPE + .5)
4590 NEXT
4600 RETURN
4999 REM ************************************************
5000 REM edit comments
5010 CLS
5020 FOR I = 1 TO 20 : PRINT I;")"; TAB(7); C$(I): NEXT
5030 LOCATE 22,1 : PRINT SPC(79):PRINT SPC(79): LOCATE 22,1
5040 ?"Enter the number of the comment you wish to edit, or"
5050 PRINT"'END' to return to main menu:";
5060 INPUT CHOICE$
5070 IF CHOICE$ = "end" OR CHOICE$ = "END" THEN RETURN
5080 CHOICE = VAL(CHOICE$)
5090 IF CHOICE < 3 OR CHOICE > 20 THEN 5030
5100 LOCATE 21,1: PRINT SPC(79)
```

```
      PRINT SPC(79): PRINT SPC(79): PRINT SPC(79);
5110 LOCATE 21,1: PRINT"Enter comment #";_
      CHOICE :?left$(c$(choice),c(choice))
5120 locate 22,1+c(choice):LINE INPUT
C$:c$(choice)=left$(c$(choice),c(choice))+c$
5130 IF LEN(C$(CHOICE)) > 72 THEN C$(CHOICE)_
       = LEFT$(C$(CHOICE),72)
5140 GOTO 5010
5999 REM ************************************************
6000 REM save file
6010 CLS: LOCATE 5,5
6020 PRINT"Under what name do you want the file saved?"
6025 PERD = INSTR(1,NME$,"."): IF PERD = 0 THEN PERD_
      = LEN(NME$) + 1
6026 NME$ = LEFT$(NME$, PERD-1) + ".fld"
6030 PRINT TAB(5); "(default = ";NME$; ")"
6040 PRINT TAB(5); "Enter E <RET> to escape to main menu."
6050 INPUT SNME$
6060 IF SNME$ = "e" OR SNME$ = "E" THEN RETURN
6070 IF SNME$ = "" THEN SNME$ = NME$
6080 ON ERROR GOTO 6150
6090 FILES SNME$
6100 REM no error => file exists
6110 PRINT:PRINT"WARNING!  This file already exists._
      Overwrite? (Y/N)"
6120 A$ = INKEY$
6130 IF A$ = "N" OR A$ = "n" THEN 6010
6140 IF A$ <> "y" AND A$ <> "Y" THEN 6120
6145 GOTO 6160 : REM skip resume statement
6150 RESUME 6160
6160 ON ERROR GOTO 0 : REM turn off error trapping
6165 PRINT"Please wait..."
6170 OPEN "o", 2, SNME$
  print#2, nchan%
  FOR I = 1 TO nchan%
  PRINT#2, USING "###.######"; VEL(I);
```

```
  PRINT#2, CHAN(I)
  NEXT
  PRINT#2, XMIN, XMAX
6220 FOR I = 1 TO 20: PRINT#2, C$(I) : NEXT
6230 CLOSE 2
6240 RETURN
```

Appendix 2. Minuit fitting subroutines

Included in this appendix are the two subroutines used with MINUIT to fit spectra. VOIGT was written by Peter Hargraves; it calculates the value of χ^2 (which MINUIT minimizes) from comparing Voigt singlets (calculated from the fitting parameters), subtracted from a background, to the peaks of a spectrum, attributing a common γ_h (underlying Lorentzian half-width at half maximum) to all Voigt lines.

The second minimization subroutine was used to fit Voigt doublets to the annite spectra. It is listed here for completeness; the reader is referred to the article by Rancourt and Ping [10] which discusses the physical model represented by this subroutine.

FILE: VOIGT FORTRAN * UNIV D'/OF OTTAWA CMS

```
C  THIS PROGRAM FITS TO INDEPENDENT VOIGT     LINES. IN EACH
C  CASE THE GAUSSIAN LW, HEIGHT,   POSITION ARE INDEPENDENT.
C  THIS VERSION FITS 4   LINES. OTHER NOS.  OF LINES CAN
C  BE HANDLED BY CHANGING THE VALUE OF MMM TO THE DESIRED NO.
C  OF LINES.  THIS VERSION ALLOWS A BLOCK OF POINTS TO BE OMMITED
C  FROM THE CHI SQUARED CALCULATIONS.
C
C  PARAMETERS X(I) AS GIVEN TO CONVERT ARE ASSIGNED AS FOLLOWS:
C
C  X(1) = BACKGROUND
C    2  = LINE WIDTH OF IST LINE    (HWHM IN MM/S)
C    3  = HEIGHT          "         ( IN NUMBER OF COUNTS)
C    4  = POSITION        "         (CENTRE VELOCITY IN MM/S)
C    5  =   LW          2ND
C    6  =   H            "
C    7  =   POSITION     "
C    8  =   LW          3RD
C    9  =   H            "
C   10  =   POSITION     "
C   11  =   LW          4TH
C   12  =   H            "
C   13      POSITION     "
C   14  =   LW OF THE LORENZIANS
C
C   SET LOG # FOR READ, WRITE AND PUNCH
      CALL MINTIO(10,6,7)
C CALL MINIUT
      CALL MINNEW
      STOP
      END
      SUBROUTINE FCN(NPAR,G,CHISQ,X,IFLAG)
C
      INTEGER STCHN,ENDCHN,IFLAG,NPAR,NDATA,MMM,CH1,CH2
      DOUBLE PRECISION G,X,CHISQ,THEO,U
      CHARACTER COM*78, NAM*8
      COMMON /PAREXT/U(150),NAM(30),WERR(150),MAXEXT,NU
      DIMENSION COM(20)
      DIMENSION G(71),VEL(512),CTS(512),X(71),THEO(512)
C
C  CHANGE VALUE OF MMM HERE ##########################################
      MMM= 6
C  ###################################################################
C
C  IFLAG=1: 1ST TIME THROUGH, READ IN DATA.
C
      IF (IFLAG .EQ. 1) THEN
      READ(10,11) NDATA, STCHN, ENDCHN,CH1,CH2
      WRITE(6,*) 'NDATA,STCHN,ENDCHN,CH1,CH2'
      WRITE(6,*) NDATA,STCHN,ENDCHN,CH1,CH2
11    FORMAT (1X,I5,4X,I5,4X,I5,4X,I5,4X,I5)
C  INPUT THE DATA
C
      DO 17 I = 1,NDATA
      READ (10,*) VEL(I),CTS(I)
C  15    FORMAT  (1X,F9.6,1X,I7)
```

```
17    CONTINUE
C
C
C  READ IN THE BLOCK OF COMMENTS
C
      READ (10,18) COM(1)
      DO 19 I= 1,20
      READ (10,18) COM(I)
18    FORMAT (A78)
19    CONTINUE
C
      ENDIF
C
C  NOW DO ACTUAL CHISQ CALCULATION  (IFLAG = 4)
C
      IF (IFLAG .EQ. 4) THEN
      CALL VOIGT(VEL,THEO,CTS,X,STCHN,ENDCHN,MMM,CHISQ,CH1,CH2)
      ENDIF
C
C
C  OUTPUT THE RESULTS  (IFLAG = 3)
C
      IF (IFLAG .EQ. 3) THEN
      WRITE (11,*) 1+ ENDCHN-STCHN
      DO 200 I=STCHN,ENDCHN

      WRITE (11,*)  VEL(I),THEO(I),CTS(I)
200   CONTINUE
C   CALCULATE CHI SQUARED ONE LAST TIME FOR OUTPUT
C
      CHISQ = 0
      DO 150 I=STCHN,ENDCHN
C     THEO(I)= 0.0
C     DO 160 J = 1,MMM
C     Z = X(3*J-1)**2
C     THEO(I) = X(3*J)*Z/((VEL(I)-X(3*J+1))**2 + Z) + THEO(I)
C 160 CONTINUE
C     THEO(I)= X(1)-THEO(I)
C TEST TO SEE IF I IS IN THE OMMITED RANGE.
      IF (I .GT. CH1 ) THEN
      GOTO 3000
      ENDIF
      GOTO 3020
3000  IF ( I .LT. CH2) THEN
      GOTO 150
      ENDIF
3020  CHISQ = CHISQ +((THEO(I) - CTS(I))**2)/CTS(I)
150   CONTINUE
      WRITE(11,*) 'CHI SQUARED IS'
      WRITE(11,*) CHISQ
C
      DO 130 I=1,20
      WRITE(11,*) COM(I)
130   CONTINUE
      DO 140 I=1,MMM*3+2
```

```
FILE: VOIGT    FORTRAN  *   UNIV D'/OF OTTAWA CMS


      WRITE (11,*) I,X(I),NAM(I)
140   CONTINUE
      WRITE (11,*) ';FIT USING MINUIT AND VOIGT'
      WRITE (11,*) 'STCHN,ENDCHN,CH1,CH2'
      WRITE (11,*) STCHN,ENDCHN,CH1,CH2
      ENDIF
      RETURN
      END
C
      SUBROUTINE VOIGT(VEL,THEO,CTS,X,STCHN,ENDCHN,MMM,CHISQ,CH1,CH2)
C
      REAL NUM, DEN,SUM
      INTEGER STCHN,ENDCHN,MMM,CH1,CH2,GAMMA,I,J
      DOUBLE PRECISION X,CHISQ,THEO,XX,YY
      DIMENSION VEL(512),CTS(512),X(71),THEO(512)
      GAMMA = 3*MMM+2
      CHISQ = 0.0
      DO 110 I=STCHN,ENDCHN
      THEO(I)=0.0
      DO 120 J=1,MMM
      XX=(VEL(I)-X(3*J+1))/(1.414214*X(3*J-1))
      YY = X(GAMMA)/(1.4142135*X(3*J-1))
      NUM =  -.3085*(YY+1.215) + .0210*(XX-1.2359)
      DEN = (YY + 1.2150)**2 + (XX - 1.2359)**2
      SUM = NUM/DEN
      NUM =      .5906*(YY+1.3509)   -1.1858*(XX - .3786)
      DEN = (YY+1.3509)**2 + (XX - .3786)**2
      SUM = SUM + NUM/DEN
      NUM =-.3085*(YY+1.215) -.0210*(XX +1.2359)
      DEN = (YY + 1.2150)**2 + (XX+1.2359)**2
      SUM = SUM + NUM/DEN
      NUM =  .5906*(YY + 1.3509) +1.1858*(XX + .3786)
      DEN = (YY + 1.3509)**2 + (XX + .3786)**2
      SUM = SUM +NUM/DEN
      THEO(I) = 1.253314*X(3*J)*X(GAMMA)*SUM/X(3*J-1) + THEO(I)
120   CONTINUE
      THEO(I) =-THEO(I) + X(1)
C  TEST TO SEE IF I IS IN THE OMMITED RANGE AND IF SO SKIP OVER
C  THE CHISQ CALCULATION.
      IF (I .GT. CH1) THEN
      GOTO 1500
      ENDIF
      GOTO 1510
1500  IF (I .LT. CH2) THEN
      GOTO 110
      ENDIF
1510  CHISQ = CHISQ +((THEO(I) - CTS(I))**2)/CTS(I)
110   CONTINUE
      RETURN
      END
```

```
FILE: MOSQ     FORTRAN  *   UNIV D'/OF OTTAWA CMS

C  A PROGRAM FOR FITTING DISTRIBUTION OF QUADRUPOLE SPLIT
C                          WRITTEN BY J. Y. PING.
C  THIS PROGRAM FITS THE DISTRIBUTION OF THE QUADRUPOLE SPLIT
C  FOR FE-57 MOSSBAUER SPECTRUM
C  THE SPECTRUM IS CONSIDERED AS A CONTRIBUTION OF SEVERAL
C  DIFFERENT FE SITES
C  FOR EACH SITE THE DISTRIBUTION OF QUADRUPOLE SPLIT
C  IS THE SUPERPOSITION OF SEVERAL GAUSSIAN DISTRIBUTIONS
C  THE MAXIMUM NUMBER OF PARAMETERS IS 150
C  THE MAXIMUM NUMBER OF ADJUSTABLE PARAMETERS IS 80
C  PARAMETERS A(I) ARE ASSIGNED AS FOLLOWS:
C  A(1) = Height of the high energy line of distribution No.1
C  A(2) = Gaussian half width of Q.S. of distribution No.1
C  A(3) = Center position of Q.S. of distribution No.1
C  A(.) = Height of the high energy line of distribution No.2
C  A(.) = Gaussian half width of Q.S. of distribution No.2
C  A(.) = Center position of Q.S. of distribution No.2
C  ......
C  A(.) = Background
C  A(.) = Lorentzian HWHM
C  A(.) = Center shift at Q=0 at site No.1
C  A(.) = C.S.-Q.S. coupling parameter at site No.1
C  A(2) = Ratio (h-/h+) at site No.1
C  A(.) = Center shift at Q=0 at site No.2
C  A(.) = C.S.-Q.S. coupling parameter at site No.2
C  A(.) = Ratio (h-/h+) at site No.2
C  ......
C
C  SET LOG # FOR READ, WRITE AND PUNCH
      CALL MINTIO(10,6,7)
C  CALL MINIUT
      CALL MINNEW
      STOP
      END
C  SUBROUTINE OF FCN
      SUBROUTINE FCN(NPAR,G,CHISQ,A,IFLAG)
      IMPLICIT DOUBLE PRECISION (A-H,O-Z)
      CHARACTER NAM*8
      COMMON /PAREXT/U(150),NAM(30),WERR(150),MAXEXT,NU
      DIMENSION A(150),G(150),X(512),Y(512),NDIST(14)
      DIMENSION TIT1(10),TIT2(10),TIT3(10),QAVER(14),DAVER(14)
      GOTO(10,20,30,40,50,60),IFLAG
C  INPUT DATA (IFLAG=1)
10    READ(10,'(10A8)')TIT1
      READ(10,'(10A8)')TIT2
      READ(10,'(10A8)')TIT3
      READ(10,*)NSITE
      N=0
      DO 110 I=1,NSITE
      READ(10,*)NDIST(I)
      N=N+NDIST(I)
110   CONTINUE
      NTPAR = NSITE*3+N*3+2
      READ(10,*)NDATA
      DO 120 I=1,NDATA
```

```
FILE: MOSQ     FORTRAN  *   UNIV D'/OF OTTAWA CMS

      READ(10,*)X(I),Y(I)
120   CONTINUE
20    CONTINUE
C  COMPUTE CHI-SQUARE (IFLAG=4)
40    CHISQ=0.
      DO 130 I=1,NDATA
        CALL VOIGT(X(I),A,YTHEO,NSITE,NDIST,N)
        YEXP=Y(I)
        DY=YEXP-YTHEO
        CHISQ=CHISQ+DY*DY/YEXP
130   CONTINUE
      RETURN
C  OUTPUT THE RESULTS (IFLAG=3)
30    CHISQ=0.
      WRITE(12,'(I4)')NDATA
      DO 140 I=1,NDATA
        CALL VOIGT(X(I),A,YTHEO,NSITE,NDIST,N)
        YEXP=Y(I)
        WRITE(12,'(F12.6,F12.1,F12.1)')X(I),YTHEO,YEXP
        DY=YEXP-YTHEO
        CHISQ=CHISQ+DY*DY/YEXP
140   CONTINUE
      WRITE(11,150)
150   FORMAT(///21X,'Distribution of Quadrupole Split')
      WRITE(11,160)TIT1,TIT2,TIT3
160   FORMAT(/1X,'Experiment sample:'/1X,10A8/
     *       1X,'Experiment condition:'/1X,10A8/
     *       1X,'Experiment date:'/1X,10A8)
      WRITE(11,170)CHISQ
170   FORMAT(/1X,'Chi-square:',F20.3)
      WRITE(12,*) 'CHI-SQUARED IS'
      WRITE(12,*) CHISQ
      WRITE(11,180)
180   FORMAT(/1X,'Site No. Dist. No.    Height          Half Width
     *  Position'/22X,'(Counts)           (mm/s)           (mm/s)')
      NC=1
      DO 210 I1=1,NSITE
      ND=N*3+I1*3
      DEL0=A(ND)
      DEL1=A(ND+1)
      SUMP=0.
      AVERQ=0.
      DO 200 I2=1,NDIST(I1)
      SUMP=SUMP+A(NC)
      AVERQ=AVERQ+A(NC+2)*A(NC)
      WRITE(11,190)I1,I2,A(NC),A(NC+1),A(NC+2)
190   FORMAT(1X,I3,6X,I3,F17.1,2F17.5)
      NC=NC+3
200   CONTINUE
      QAVER(I1)=AVERQ/SUMP
      DAVER(I1)=DEL0+DEL1*QAVER(I1)
210   CONTINUE
      FWHM=2.*A(NC+1)
      WRITE(11,220)A(NC),A(NC+1),FWHM
220   FORMAT(/1X,'Background     (Counts):',F11.1/1X,'Lorentzian HWHM
```

```
FILE: MOSQ     FORTRAN  *   UNIV D'/OF OTTAWA CMS

     */s):',F11.5/12X,'FWHM (mm/s):',F11.5)
      WRITE(11,230)
230   FORMAT(/1X,'Site No. Center shift at Q.S.=0  C.S.-Q.S. coupling
     *rameter   Ratio (h-/h+)'/18X,'(mm/s)')
      NC=NC+2
      DO 250 I=1,NSITE
      WRITE(11,240)I,A(NC),A(NC+1),A(NC+2)
240   FORMAT(1X,I3,F20.5,F27.5,F24.5)
      NC=NC+3
250   CONTINUE
      WRITE(11,260)
260   FORMAT(/24X,'Distribution of C.S.'
     */1X,'Site No. Dist. No.    Half Width    Position'
     */25X,'(mm/s)        (mm/s)')
      NC=1
      DO 280 I1=1,NSITE
      ND=N*3+I1*3
      DEL0=A(ND)
      DEL1=A(ND+1)
      DO 280 I2=1,NDIST(I1)
      SIGMAD=ABS(DEL1)*A(NC+1)
      D0=DEL0+DEL1*A(NC+2)
      WRITE(11,270)I1,I2,SIGMAD,D0
270   FORMAT(1X,I3,6X,I3,5X,F13.5,F13.5)
      NC=NC+3
280   CONTINUE
      WRITE(11,290)
290   FORMAT(/16X,'Average Q.S.',6X,'Average C.S.'
     */1X,'Site No.',10X,'(mm/s)',12X,'(mm/s)')
      DO 310 I=1,NSITE
      WRITE(11,300)I,QAVER(I),DAVER(I)
300   FORMAT(1X,I3,F21.5,F18.5)
310   CONTINUE
      CHIR=CHISQ/(NDATA-NPAR)
      WRITE(11,320)CHIR
320   FORMAT(/1X,'Reduced chi-square :',F8.3)
50    CONTINUE
60    CONTINUE
      DO 61 I=1,20
61    WRITE (12,*) I
      DO 62 I = 1,NTPAR
62    WRITE (12,*) I, A(I), NAM(I)
      SAIT = 0.
      DO 64 I = 1, NSITE
         SAI = 0.
         DO 63 J = 1, NDIST(I)
63          SAI = SAI + A(3*J + 3*I - 5) * A(3*N + 2)
            SAIT = SAIT + SAI
         WRITE (12,330) 'SPECTRAL AREA, SITE ',I,SAI
330   FORMAT (A20, I2, ':', F9.1)
64    CONTINUE
      WRITE (12,*) 'TOTAL AREA:',SAIT
      RETURN
      END
C  SUBROUTINE OF VOIGT
```

FILE: MOSQ FORTRAN * UNIV D'/OF OTTAWA CMS

```
      SUBROUTINE VOIGT(X,A,Y,NSITE,NDIST,N)
      IMPLICIT DOUBLE PRECISION (A-H,O-Z)
      DIMENSION A(150),AK(4),BK(4),GK(4),DK(4),BB(2),NDIST(14)
      DATA AK/-1.215,-1.3509,-1.215,-1.3509/
      DATA BK/1.2359,0.3786,-1.2359,-0.3786/
      DATA GK/-0.3085,0.5906,-0.3085,0.5906/
      DATA DK/0.0210,-1.1858,-0.0210,1.1858/
      DATA BB/0.5,-0.5/
      GAMMA=A(N*3+2)
      Y=0.
      NC=1
      DO 30 NS=1,NSITE
      ND=N*3+NS*3
      DEL0=A(ND)
      DEL1=A(ND+1)
      RATIO=A(ND+2)
      DO 20 J=1,NDIST(NS)
      H=A(NC)
      SIGMAQ=A(NC+1)
      QS=A(NC+2)
      DO 10 NL=1,2
      SIGM=DEL1+BB(NL)
      SIGMA=SIGMAQ*ABS(SIGM)
      OMEGA=DEL0+SIGM*QS
      IF(NL.EQ.2)H=H*RATIO
      XX=(X-OMEGA)/SIGMA/1.4142136
      YY=GAMMA/SIGMA/1.4142136
      SUM=0.
      DO 5 K=1,4
      TM1=YY-AK(K)
      TM2=XX-BK(K)
      SUM=SUM+(GK(K)*TM1+DK(K)*TM2)/(TM1*TM1+TM2*TM2)
5     CONTINUE
      Y=Y+YY*SUM*H
10    CONTINUE
      NC=NC+3
20    CONTINUE
30    CONTINUE
      Y=A(NC)-1.7724539*Y
      RETURN
      END
```

Appendix 3. Thickness-correction programs

Here are the programs used by algorithm 2.7 to obtain the effective Debye temperature and values of $\eta_H f_S$ from pairs of spectra. THIKCOR is the main program, the others (except SSFFAC) are subroutines called by THIKCOR. SSFFAC is a short but useful program that uses these THIKCOR subroutines to determine a Debye temperature from sub-spectral areas at two known temperatures.

SSFFAC.BAS

```
$INCLUDE "F2TD.BAS"
$INCLUDE "TD2F.BAS"
 DEF FNE1(x) = x/(exp(x)-1)
 input "what is area 1 " ,A1
 input "what is temp. 1 ",T1
 input "what is area 2 ",A2
 input "what is temp.2 ",T2
 call f2td (t1,a1,t2,a2, td)
 ? "the Debye temperature  is ",TD
 end
```

```
' Thikcor.bas
' Michel Royer, Nov. 1989.
' Univ. of Ottawa

cls: ?"            Thikcor"
?:?"        by Michel Royer"

?:?
?"a)  Given the voigt parameters and the temperatures of two"
?" spectra of a sample, this program calculates the effective"
?" Debye temp. of the sample and 'etam fs' for each spectrum."

?:?"b)  It can be used to get 'etam fs' from the Debye temp."
?"for a single sample"

?:?"c)  or it can also just calculate_
        an f-factor given a Debye temp."

' Program requires the subroutines
' F2TB, TB2F, SOLV4ETA, EQNA (found
'  in fneqna.bas)

' Functions required:  E1, A, V

' For calculations of source f-factors,
' the Debye temp. of rhodium is used

DEF FNE1(X) = X / (EXP(X) - 1)
DEF FNA(X,Y) = LOG(1 - X/Y)

def fnv(ht,gam,sig,cs,eng)
' function calculates height of voigt at energy ENG

local kk, xx, yy
```

```
xx = (eng-cs)/(sig*sqr(2))
yy = gam / (sig*(sqr(8)))
kk = 0

for ii% = 1 to 4
  num = gg(ii%) * (yy - aa(ii%)) + dd(ii%) * (xx - bb(ii%))
  den = (yy - aa(ii%))^2 + (xx - bb(ii%))^2
  kk = kk + num/den
next ii%

fnv = kk * pi * ht * gam / (sig * sqr( 8*pi ) )
end def


' Include code for subroutines

$include "fneqna.bas"
$include "solv4eta.bas"
$include "f2td.bas"
$include "td2f.bas"

'define parameters
tdsource = 420          ' debye temp of rhodium matrix +/- 16
pi = 4 * atn(1)
kmax% = 100                    '  * max # of voigt patterns
gamma0 = .09702                 '  natural linewidth
sig0 = 2.563e-18 ' square cm's     ' intrinsic cross section

dim par1(kmax%,4),par2(kmax%,4)
dim gg(4),aa(4),bb(4),cc(4)

gg(1) = -0.3085 : gg(2) =  0.5906 : gg(3) = -0.3085
gg(4) =  0.5906 : aa(1) = -1.2150 : aa(2) = -1.3509
aa(3) = -1.2150 : aa(4) = -1.3509 : bb(1) =  1.2359
bb(2) =  0.3786 : bb(3) = -1.2359 : bb(4) = -0.3786
```

```
xx = (eng-cs)/(sig*sqr(2))
yy = gam / (sig*(sqr(8)))
kk = 0

for ii% = 1 to 4
  num = gg(ii%) * (yy - aa(ii%)) + dd(ii%) * (xx - bb(ii%))
  den = (yy - aa(ii%))^2 + (xx - bb(ii%))^2
  kk = kk + num/den
next ii%

fnv = kk * pi * ht * gam / (sig * sqr( 8*pi ) )
end def


' Include code for subroutines

$include "fneqna.bas"
$include "solv4eta.bas"
$include "f2td.bas"
$include "td2f.bas"

'define parameters
tdsource = 420          ' debye temp of rhodium matrix +/- 16
pi = 4 * atn(1)
kmax% = 100                    '  * max # of voigt patterns
gamma0 = .09702                 '  natural linewidth
sig0 = 2.563e-18 ' square cm's    ' intrinsic cross section

dim par1(kmax%,4),par2(kmax%,4)
dim gg(4),aa(4),bb(4),cc(4)

gg(1) = -0.3085 : gg(2) =  0.5906 : gg(3) = -0.3085
gg(4) =  0.5906 : aa(1) = -1.2150 : aa(2) = -1.3509
aa(3) = -1.2150 : aa(4) = -1.3509 : bb(1) =  1.2359
bb(2) =  0.3786 : bb(3) = -1.2359 : bb(4) = -0.3786
```

```
dd(1) =  0.0210 : dd(2) = -1.1858 : dd(3) = -0.0210
dd(4) =  1.1858

' parameter file must follow this format:
' # of peaks
' height 1
' underlying FWHM 1
' standard dev 1
' center shift 1
' repeat with ht2, fwhm2, stdev2, cs2, 3, 4, etc...
' background
' temperature

?:?"So, which option do you want (a,b,c)?"
10 a$ = inkey$
if a$ = "a" or a$ = "A" then
 flag = 0
 elseif a$ = "b" or a$ = "B" then
 flag = 1
 elseif a$ = "c" or a$ = "C" then
 flag = 2
 else
 flag = 999
end if

if flag = 999 then goto 10


if flag <> 2 then

?"Assume the source(s) at (constant) room temperature? (Y/N)"
11 a$ = inkey$ : flag1 = 0
if a$ = "y" or a$ = "Y" then flag1 = 1
if a$ = "n" or a$ = "N" then flag1 = 2
if flag1 = 0 then goto 11
```

```
' must get name of voigt parameter file
?:?:? "What is the name of the file_
     that contains the (fit) voigt parameters"
dummy$="": if flag = 0 then dummy$ = "lower temperature "
? " of the ";dummy$;"spectrum?"
input name1$

if flag1 = 2 then
  ?"What is the source temp.?"
  input tsource1
  call td2f (tsource1, tdsource, fs1)
else
  fs1 = 1
end if

if flag = 0 then
?:? "And what is the name of the_
      file for the higher T spectrum?"
input name2$
if flag1 = 2 then
  ?"And what is the source temp.?"
  input tsource2
  call td2f (tsource2, tdsource, fs2)
else
  fs2 = 1
end if
end if

?:?"What is NA, the number of atoms per square centimeter?"
input na

else            ' do the iflag=2 bit (part c)
?:?"What is the temperature of the spectrum?"
input tmp1
end if
```

```
if flag < 2 then
?:? "Loading parameters..."

open name1$ for input as #1
input #1, nk1%
for k% = 1 to nk1%
  for i% = 1 to 4
    input #1, par1(k%,i%)
next i%,k%
input #1, bg1
input #1, tmp1

if flag = 0 then
open name2$ for input as #2
input #2,nk2%
for k% = 1 to nk2%
  for i% = 1 to 4
    input #2, par2(k%,i%)
next i%,k%
input #2, bg2
input #2, tmp2
close 2
end if

close 1
end if



itr = 0
otd = 0   ' old Debye temp.
fl$="" : if flag = 0 then fl$ = "starting guess of the "
print "What is the ";fl$;"Debye temp.? ": input td

' start main loop
```

```
while abs(td - otd) > 0.1
   otd = td

   incr itr
   if flag = 0 then ?:?"Iteration:";itr

   ?" get f-factor f1"
   call td2f (tmp1,td,f1)
   ?f1
   if flag = 2 then 999


   ?" calculate etam fs (1)"
   int1 = pi * sig0 * gamma0 * na * f1/2
   ?"Integral must equal ";int1
   call solv4eta (par1(),nk1%,4,bg1,int1,eta1)
   ? "etam fs (1) =";eta1
   if flag = 1 then 999


   ?" calculate etam fs (2)  "
   eta2 = eta1 * (bg2 / bg1) * fs2/fs1

   ? eta2

   ?" calculate f2"
   call eqna (par2(), nk2%, 4, eta2, int2)
   f2 = 2*int2 / (pi * sig0 * gamma0 * na)
   ?"f2 =";f2

   if eta2 > 1.01 * (eta1*bg2*fs2/(fs1*bg1)) then
   eta1 = eta2 * (bg1/bg2) * fs1/fs2
   call eqna (par1(), nk1%, 4, eta1, int1)
   f1 = 2*int1 / (pi * sig0 * gamma0 * na)
   end if
```

```
   ?" calculate Debye temp (TD)"
   call f2td (tmp1, f1, tmp2, f2, td)

   ?:?"Debye temp: ";td, "diff from last: ";abs(td-otd)
wend

?:?
?"  The Debye temperature is: ";td
?:?"  Etam Fs for the spectrum at ";tmp1;" K is: ";eta1
?:?"  Etam Fs for the spectrum at ";tmp2;" K is: ";eta2

999 ?"I'm done!" :end
```

SOLV4ETA.BAS

```
' solv4eta.bas
' Michel Royer, Nov. 1989.
' Univ of Ottawa

' Written for use with THIKCOR.BAS

sub solv4eta (v(2),nk%,np%,bg,thri,etamfs)

'equates integral of eqn 15 to thri to calculate etam * fs.
'uses subroutine EQNA which uses functions A and V

LOCAL L1, IL2, TOL, DIFF, L1, L2
STATIC SAV1, SAV2

'calculate limits for etamfs
l1 = bg*.75 : l2 = 0
for k% = 1 to nk%
l2 = l2 + v(k%,1)
next k%
l2 = l2 * .75
tol = thri * .0001

' use linear relaticn between log's to find etamfs

IF sav1 = 0 THEN
   call eqna (v(),nk%,np%,l1,sav1)
   call eqna (v(),nk%,np%,l2,sav2)
end if
il1 = SAV1 : il2 = SAV2
diff = abs(thri - il1)

while diff > tol
   swap l1,l2
   swap il1,il2
```

```
    slp = log(l2/l1) / log(il2/il1)
    l1 = l2 * ((thri/il2) ^ slp)
    call eqna (v(),nk%,np%,l1,il1)
    diff = abs(thri - il1)
wend

etamfs = l1

end sub
```

FNEQNA.BAS

```
sub eqna (par(2),nk%,np%,eta,intgrl)

' FNEQNA.BAS
' CALCULATES INTEGRAL OF EQN 15 (THICKNESS EFFECTS PAPER)
' Michel Royer, Nov. 1989.

' For use with THIKCOR.BAS
' routine is given etam fs (in eta) and
' returns the integral in intgrl
' uses functions A and V

'define parameters
local prod(), h, nchan%, ll, ul, sum, sum1, sum2,_
                sum3, sum4, x1, x2
local x3, gamma0

' I'm really tired of getting etamfs's out of range, so
' I'm gonna make this subroutine increase eta when this
' happens till this routine works!

on error goto bug

dim dynamic prod(nk%)

2   'this had better work...

pi = 4 * atn(1)
nchan% = 1500 : ll = -15 : ul = 15 :' THESE MAY BE CHANGED
h = (ul-ll)/nchan%
gamma0 = .09702

sum1=0: sum2=0: sum3=0
x1 = 0: x2 = 0: x3 = 0
```

```
?"integrating"
for k% = 1 to nk%
  prod(k%) = par(k%,1)*par(k%,2) / (par(k%,2)-gamma0)
  x1 = x1 + prod(k%) * fnv(1,par(k%,2)-gamma0,_
                      par(k%,3),par(k%,4),ll)
  x2 = x2 + prod(k%) * fnv(1,par(k%,2)-gamma0,_
                      par(k%,3),par(k%,4),ul)
  x3 = x3 + prod(k%) * fnv(1,par(k%,2)-gamma0,_
                      par(k%,3),par(k%,4),ll+h)
next k%
sum1 = (fna(x1,eta) + fna(x2,eta))/3 + fna(x3,eta) * 4/3

for j% = 1 to (nchan%-2)/2
  i%=2*j%
  x1 = 0: x2 = 0
  for k% = 1 to nk%
    x1 = x1 + prod(k%) * fnv(1,par(k%,2)-gamma0,_
                par(k%,3),par(k%,4),ll+h*i%)
    x2 = x2 + prod(k%) *
fnv(1,par(k%,2)-gamma0,par(k%,3),par(k%,4),ll+h*(i%+1))
  next k%
  sum2 = sum2 + fna(x1,eta)
  sum3 = sum3 + fna(x2,eta)
next j%
sum = -(sum1 + (4*sum2 + 2*sum3)/3)*h

sum4 = 0
for k% = 1 to nk%
    sum4 = sum4 + par(k%,2)*(par(k%,2)-gamma0)_
                  *par(k%,1)/(4*ul*eta)
    sum4 = sum4 - par(k%,2)*(par(k%,2)-gamma0)_
                  *par(k%,1)/(4*ll*eta)
next k%

intgrl = sum + sum4
```

```
?"int: ";intgrl
if intgrl = 0 then end
goto 5

bug:
?eta
eta = eta*1.1
?err, eta
resume 2

5 on error goto 0
end sub
```

TD2F.BAS

```
SUB TD2F (TK,TD,FF)

' Michel Royer
' U of Ottawa, November 1989
' for use with THIKCOR.BAS

' GIVEN TK (TEMP IN KELVIN) AND TD (DEBYE TEMP),
' ROUTINE RETURNS FF, THE F-FACTOR.

' routine uses function fne1(x)

LOCAL A, NSTP, DELTA, PSUM, SUM

A = TD / TK
NSTP = 500     ' # of intervals in numerical integration
DELTA = A / NSTP   ' size of intervals
PSUM = 0

' INTEGRATE
FOR J = 1 TO nstp-1
   PSUM = PSUM + FNE1 (J * DELTA)
NEXT J
SUM = (PSUM + FNE1(A)/2) * DELTA

ER = 34.098     ' = (6 * Recoil E) / (4k)
FF = EXP((-ER/TD)*(1+4*SUM/(A*A)))

end sub
```

F2TD.BAS

```
SUB F2TD (TK1,F1, TK2,F2, TD)

' F2TD.BAS
' Written by Michel Royer
' Univ. of Ottawa,
' November 1989

' for use with THIKCOR.BAS
' Given TK1, TK2 (temp. in deg. K)
' and f-factors of spectra (F1, F2)
' routine returns the Debye temp. in TD

' Uses the subroutine TD2F, function E1,
' and straigt line curve of ln(TD) vs F

local tol,diff,fthry,ftd1,ftd2,td1,td2,f11,f12,f21,f22
static savf11, savf12, savf21, savf22

' set "limits" for TD
td1 = 300  :  td2 = 400
if savf1 = 0 then
   call td2f (tk1,td1,savf11)
   call td2f (tk1,td2,savf12)
   call td2f (tk2,td1,savf21)
   call td2f (tk2,td2,savf22)
end if

f11 = savf11 : f12 = savf12 : f21 = savf21 : f22 = savf22
ftd1 = (f11 - f21) / (abs(tk1-tk2) * f11)
ftd2 = (f12 - f22) / (abs(tk1-tk2) * f12)
fthry = (f1 - f2) / (abs(tk1 - tk2) * f1)
?"fthry",fthry
?ftd1
?ftd2
```

```
diff = abs(fthry - ftd1)
tol = abs(.00001 * fthry)

' loop until ftd1 is with tol of fthry

while diff > tol
   swap td1, td2
   swap ftd1, ftd2
   slp = log(td2/td1) / (ftd2-ftd1)
   td1 = td2 * exp(-slp * (ftd2-fthry))
   call td2f (tk1, td1, f11)
   call td2f (tk2, td1, f21)
   ftd1 = (f11 - f21) / (abs(tk1-tk2) * f11)
   diff = abs (fthry-ftd1): ? ftd1
wend

td = td1

end sub
```

Appendix 4. Values of fitting parameters

Sample	MOC2661	MOC2661	MOC2661	MOC2661
Temp. (K)	296.5	244	187	158
χ^2	241	222	221	298
BG	824604	114913	579451	327369
γ_h (mm/s)	0.1181	0.07772	0.1197	0.1179
σ_1 (mm/s)	0.0939	0.315	0.159	0.115
h_1 (counts)	87041	40497	120621	41946
ω_1 (mm/s)	-0.171	-0.078	-0.152	-0.183
σ_2 (mm/s)	0.183	0.828	0.147	0.195
h_2 (counts)	116953	7801	35817	51423
ω_2 (mm/s)	0.033	0.479	0.152	0.004
Area/BG, A	0.0292	0.0327	0.0323	0.0336
σ_3 (mm/s)	0.192	0.273	0.233	0.178
h_3 (counts)	14300	1413	12771	6808
ω_3 (mm/s)	0.830	0.740	0.823	0.891
Area/BG, B	0.00205	0.00096	0.00264	0.00245
σ_4 (mm/s)	0.237	0.306	0.280	0.334
h_4 (counts)	36330	22381	5584	2635
ω_4 (mm/s)	2.253	2.400	2.040	2.052
σ_5 (mm/s)	0.130	–	0.133	0.157
h_5 (counts)	66724	–	24545	28884
ω_5 (mm/s)	2.411	–	2.342	2.464
σ_6 (mm/s)	–	–	0.149	0.119
h_6 (counts)	–	–	54405	18784
ω_6 (mm/s)	–	–	2.561	2.597
Area/BG, C	0.0148	0.0151	0.0175	0.0181
Total Area/BG	0.0461	0.0488	0.0524	0.0542

Sample	MOC2661
Temp. (K)	106
χ^2	250
BG	729405
γ_h (mm/s)	0.09996
σ_1 (mm/s)	0.102
h_1 (counts)	98790
ω_1 (mm/s)	-0.184
σ_2 (mm/s)	0.232
h_2 (counts)	108530
ω_2 (mm/s)	-0.060
σ_3 (mm/s)	0.133
h_3 (counts)	52344
ω_3 (mm/s)	0.016
σ_4 (mm/s)	0.100
h_4 (counts)	3222
ω_4 (mm/s)	0.352
Area/BG, A	0.0360
σ_5 (mm/s)	0.182
h_5 (counts)	18781
ω_5 (mm/s)	0.909
σ_6 (mm/s)	0.400
h_6 (counts)	3423
ω_6 (mm/s)	0.950
Area/BG, B	0.00304
Total Area/BG	0.0591

σ_7 (mm/s)	0.251
h_7 (counts)	45670
ω_7 (mm/s)	2.493
σ_8 (mm/s)	0.141
h_8 (counts)	100432
ω_8 (mm/s)	2.600
Area/BG, C	0.0200

Fit Name	MOC106	MOC158	MOC187	MOC244	MOC297
Sample	MOC2661	MOC2661	MOC2661	MOC2661	MOC2661
Temp.(K)	106	158	187	244	296.5
χ^2	21	13	7	3	2
γ_h (mm/s)	0.04907	0.05680	0.05244	0.04989	0.05438
σ_1 (mm/s)	0.0818	0.0953	0.116	0.328	0.0823
h_1 (counts)	136922	128206	96662	200060	100188
ω_1 (mm/s)	-0.160	-0.160	-0.156	-0.064	-0.155
σ_2 (mm/s)	0.186	0.196	0.222	0.220	0.187
h_2 (counts)	204253	152603	188823	79162	143080
ω_2 (mm/s)	-0.0532	-0.028	-0.046	-0.084	0.002
Area, A	16741	15949	15971	13930	13229
σ_3 (mm/s)	0.216	0.189	0.231	0.350	0.216
h_3 (counts)	21335	15841	17985	20712	14687
σ_3 (mm/s)	0.894	0.887	0.843	0.838	0.818
Area, B	1047	900	943	1033	799
σ_4 (mm/s)	0.238	0.126	0.300	0.300	0.124
h_4 (counts)	53990	45195	11229	7854	64396
ω_4 (mm/s)	2.516	2.467	2.090	2.000	2.406
σ_5 (mm/s)	0.124	0.300	0.179	0.277	0.252
h_5 (counts)	106304	79176	123680	123977	42757
ω_5 (mm/s)	2.598	2.493	2.497	2.409	2.284
Area, C	7866	7064	7075	6577	5827
Total Area	25654	23913	22989	21541	19855

Sample	BL531	BL531	BL315	BL315
Temp. (K)	82	305	82	305
χ^2	591	410	1067	545
BG	2086803	1735633	2960084	1619141
γ_h (mm/s)	0.1001	0.1100	0.1261	0.1294
σ_1 (mm/s)	0.113	0.0884	0.0907	0.0701
h_1 (counts)	469535	189896	612581	182394
ω_1 (mm/s)	-0.165	-0.182	-0.173	-0.192
σ_2 (mm/s)	0.124	0.143	0.106	0.125
h_2 (counts)	105444	138072	155445	123823
ω_2 (mm/s)	0.122	0.067	0.105	0.048
Area/BG, A	0.0276	0.0208	0.0327	0.0245
σ_3 (mm/s)	0.219	0.239	0.219	0.236
h_3 (counts)	79333	46905	135741	57936
ω_3 (mm/s)	0.955	0.843	0.954	0.832
Area/BG, B	0.00380	0.00297	0.00578	0.00463
σ_4 (mm/s)	0.189	0.179	0.112	0.159
h_4 (counts)	45066	70640	286746	82399
ω_4 (mm/s)	2.430	2.196	2.569	2.218
σ_5 (mm/s)	0.119	0.0884	0.0564	0.0591
h_5 (counts)	265093	92411	190559	103976
ω_5 (mm/s)	2.653	2.410	2.712	2.419
Area/BG, C	0.0149	0.0103	0.0203	0.0149
Total Area/BG	0.0463	0.0341	0.0588	0.0440

Sample	MCC	MCC	IKO	IKO
Temp. (K)	82	305	83	300
χ^2	397	500	435	306
BG	3222035	3398791	392785	397962
γ_h (mm/s)	0.1218	0.1164	0.1147	0.1222
σ_1 (mm/s)	0.0919	0.0947	0.0720	0.0486
h_1 (counts)	263971	276369	182534	73406
ω_1 (mm/s)	-0.185	-0.164	-0.231	-0.048
σ_2 (mm/s)	0.0925	0.0479	0.156	0.101
h_2 (counts)	125306	45577	59710	79681
ω_2 (mm/s)	0.072	0.071	0.0211	0.102
Area/BG, A	0.0147	0.0110	0.0707	0.0470
σ_3 (mm/s)	0.671	0.0534	0.0409	0.0903
h_3 (counts)	50093	42573	9063	10918
ω_3 (mm/s)	0.500	0.380	0.576	0.526
σ_4 (mm/s)	0.020	0.403	0.303	0.271
h_4 (counts)	37107	18340	33012	17950
ω_4 (mm/s)	0.514	0.653	0.849	0.979
Area/BG, B+D	0.00330	0.00209	0.0123	0.00886
σ_5 (mm/s)	0.111	0.0607	0.244	0.273
h_5 (counts)	174198	24830	14624	9833
ω_5 (mm/s)	2.575	2.182	2.517	2.045
σ_6 (mm/s)	0.0542	0.0688	0.0926	0.0970
h_6 (counts)	78771	169077	131195	60685
ω_6 (mm/s)	2.732	2.403	2.680	2.424
σ_7 (mm/s)	–	–	0.0482	0.0576
h_7 (counts)	–	–	76872	75642
ω_7 (mm/s)	–	–	2.784	2.547
Area/BG, C	0.00956	0.00664	0.0650	0.0449
Total Area/BG	0.0276	0.0198	0.1480	0.1008

Sample	BZ53	BZ53
Temp. (K)	82	305
χ^2	366	287
BG	747414	663365
γ_h (mm/s)	0.09602	0.09161
σ_1 (mm/s)	0.0531	0.0762
h_1 (counts)	4432	4407
ω_1 (mm/s)	-0.556	-0.552
σ_2 (mm/s)	0.115	0.0890
h_2 (counts)	215992	96407
ω_2 (mm/s)	-0.157	-0.186
σ_3 (mm/s)	0.130	0.164
h_3 (counts)	57545	104254
ω_3 (mm/s)	0.128	0.046
Area/BG, A	0.0357	0.0283
σ_7 (mm/s)	0.298	0.299
h_7 (counts)	9954	11542
ω_7 (mm/s)	2.274	1.846
σ_8 (mm/s)	0.160	0.164
h_8 (counts)	43733	75972
ω_8 (mm/s)	2.491	2.259
σ_9 (mm/s)	0.0535	0.0869
h_9 (counts)	17606	52406
ω_9 (mm/s)	2.502	2.416
σ_{10}(mm/s)	0.102	–
h_{10}(counts)	121808	–
ω_{10}(mm/s)	2.670	–
Area/BG, C	0.0248	0.0193
Total Area/BG	0.0668	0.0526

	82 K	305 K
σ_4	0.182	0.220
h_4	20618	36080
ω_4	0.928	0.841
σ_5	0.171	–
h_5	10914	–
ω_5	0.957	–
σ_6	0.281	–
h_6	17801	–
ω_6	1.060	–
Area/BG, B	0.0063	0.0050

Sample	BZ53	BZ53
Temp. (K)	82	305
χ^2	413	521
BG	746543	663430
γ_h (mm/s)	0.04102	0.09703
σ_1 (mm/s)	0.239	0.273
h_1 (counts)	61591	4354
ω_1 (mm/s)	-0.427	-0.386
σ_2 (mm/s)	0.137	0.115
h_2 (counts)	414511	143310
ω_2 (mm/s)	-0.152	-0.146
σ_3 (mm/s)	0.146	0.0830
h_3 (counts)	129818	39123
ω_3 (mm/s)	0.148	0.151
σ_4 (mm/s)	–	0.300
h_4 (counts)	–	16616
ω_4 (mm/s)	–	0.468
Area/BG, A	0.0333	0.0297
σ_4 (mm/s)	0.294	–
h_4 (counts)	20578	–
ω_4 (mm/s)	0.837	–
σ_5 (mm/s)	0.283	0.220
h_5 (counts)	104888	27287
ω_5 (mm/s)	0.970	0.909
Area/BG, B	0.00689	0.00399
Total Area/BG	0.0636	0.0530

	82 K	305 K
σ_6	0.299	0.293
h_6	41724	749
ω_6	2.206	2.001
σ_7	0.149	0.166
h_7	76740	28290
ω_7	2.459	2.066
σ_8	0.145	0.112
h_8	299259	88089
ω_8	2.658	2.346
σ_9	0.0886	0.048
h_9	7532	14356
ω_9	3.104	2.500
Area/BG, C	0.0234	0.0192

Sample	BZ53	BZ53
Temp. (K)	82	305
χ^2	367	503
BG	746649	663385
γ_h (mm/s)	0.04130	0.09702
σ_1 (mm/s)	0.209	0.108
h_1 (counts)	48418	115259
ω_1 (mm/s)	-0.432	-0.156
σ_2 (mm/s)	0.136	0.187
h_2 (counts)	411222	26037
ω_2 (mm/s)	-0.151	-0.066
σ_3 (mm/s)	0.142	0.202
h_3 (counts)	116138	19105
ω_3 (mm/s)	0.148	0.012
σ_4 (mm/s)	–	0.0125
h_4 (counts)	–	2673
ω_4 (mm/s)	–	0.092
σ_5 (mm/s)	–	0.0937
h_5 (counts)	–	29861
ω_5 (mm/s)	–	0.167
Area/BG, A	0.0318	0.0282
σ_6 (mm/s)	0.982	0.110
h_6 (counts)	104576	6178
ω_6 (mm/s)	0.884	0.770
σ_7 (mm/s)	0.214	0.271
h_7 (counts)	75082	30428
ω_7 (mm/s)	0.947	0.881
Area/BG, B	0.00994	0.00535
Total Area/BG	0.0640	0.0527

	82 K	305 K
σ_8	0.171	0.194
h_8	10914	49335
ω_8	0.957	2.165
σ_9	0.281	0.108
h_9	17801	81636
ω_9	1.060	2.386
σ_{10}	–	–
h_{10}	–	–
ω_{10}	–	–
Area/BG, C	0.0222	0.0192

Sample	BZ53	BZ53
Temp. (K)	82	305
χ^2	442	438
BG	747054	663438
γ_h (mm/s)	0.09602	0.1074
σ_1 (mm/s)	0.0851	0.0937
h_1 (counts)	103896	111765
ω_1 (mm/s)	-0.174	-0.171
σ_2 (mm/s)	0.196	0.124
h_2 (counts)	171928	64483
ω_2 (mm/s)	-0.059	0.096
Area/BG, A	0.0355	0.0285
σ_3 (mm/s)	0.222	0.235
h_3 (counts)	48452	32426
ω_3 (mm/s)	0.977	0.848
Area/BG, B	0.00623	0.00525
σ_4 (mm/s)	0.146	0.175
h_4 (counts)	50002	51599
ω_4 (mm/s)	2.462	2.190
σ_5 (mm/s)	0.113	0.0924
h_5 (counts)	139877	67768
ω_5 (mm/s)	2.655	2.395
Area/BG, C	0.0244	0.0193
Total Area/BG	0.0661	0.0531

Fit Name	MSCLN	MSCRT	MSCRT1	MSCRTA
Sample	BL531	BL531	BL531	BL531
Temp.(K)	82	305	305	305
χ^2	178	41	9	36
γ_h (mm/s)	0.04916	0.04907	0.04907	0.04907
σ_1 (mm/s)	0.0794	0.0682	0.0683	0.0690
h_1 (counts)	300185	96732	96976	87283
ω_1 (mm/s)	-0.162	-0.179	-0.179	-0.180
σ_2 (mm/s)	0.120	0.176	0.177	0.178
h_2 (counts)	58382	127794	127885	119230
ω_2 (mm/s)	0.083	-0.009	-0.008	-0.010
Area, A	17629	11017	11034	10134
σ_3 (mm/s)	0.210	0.227	0.208	0.227
h_3 (counts)	32289	25241	23895	23640
σ_3 (mm/s)	0.957	0.845	0.838	0.846
Area, B	1587	1239	1173	1160
σ_4 (mm/s)	0.197	0.173	0.287	0.174
h_4 (counts)	38121	55125	8600	51473
ω_4 (mm/s)	2.550	2.255	1.859	2.254
σ_5 (mm/s)	0.100	0.0747	0.151	0.0751
h_5 (counts)	115609	41534	53667	38478
ω_5 (mm/s)	2.652	2.423	2.279	2.423
σ_6 (mm/s)	–	–	0.0697	–
h_6 (counts)	–	–	37276	–
ω_6 (mm/s)	–	–	2.431	–
Area, C	7558	4743	4885	4414
Total Area	26774	16999	17092	15708

Fit Name	MSCLNA	MSCRTA1	Z53LN	Z53RT
Sample	BL531	BL531	BZ53	BZ53
Temp. (K)	82	305	82	305
χ^2	123	8	53	32
γ_h (mm/s)	0.04907	0.04907	0.04907	0.05787
σ_1 (mm/s)	0.0853	0.0691	0.0803	0.0720
h_1 (counts)	275558	87538	142145	82429
ω_1 (mm/s)	-0.160	-0.180	-0.158	-0.177
σ_2 (mm/s)	0.113	0.178	0.192	0.149
h_2 (counts)	47416	119298	109097	74039
ω_2 (mm/s)	0.108	-0.009	-0.042	0.037
Area, A	15835	10149	12328	9055
σ_3 (mm/s)	0.217	0.207	0.197	0.212
h_3 (counts)	31147	22331	32915	22719
ω_3 (mm/s)	0.963	0.838	0.972	0.853
Area, B	1528	1096	1615	1315
σ_4 (mm/s)	0.0867	0.298	0.157	0.156
h_4 (counts)	65488	8455	35897	46106
ω_4 (mm/s)	2.659	1.871	2.484	2.220
σ_5 (mm/s)	0.158	0.151	0.104	0.0794
h_5 (counts)	76979	49452	122640	51999
ω_5 (mm/s)	2.608	2.278	2.646	2.401
σ_6 (mm/s)	–	0.0703	–	–
h_6 (counts)	–	34775	–	–
ω_6 (mm/s)	–	2.432	–	–
Area, C	6991	4548	7779	5677
Total Area	24354	15793	21722	16047

Fit Name	L315LN1	L315RT1	L315LN2	L315RT2
Sample	BL315	BL315	BL315	BL315
Temp. (K)	82	305	82	305
χ^2	37	21	42	22
γ_h (mm/s)	0.06975	0.07171	0.07003	0.07150
σ_1 (mm/s)	0.0731	0.0715	0.0716	0.0711
h_1 (counts)	163755	88822	169899	92059
ω_1 (mm/s)	-0.166	-0.176	-0.166	-0.175
σ_2 (mm/s)	0.0981	0.101	0.0983	0.102
h_2 (counts)	29715	36615	30670	37969
ω_2 (mm/s)	0.108	0.0828	0.107	0.082
Area, A	13495	8995	14045	9296
σ_3 (mm/s)	0.204	0.233	0.203	0.233
h_3 (counts)	25242	20219	25754	20825
ω_3 (mm/s)	0.949	0.824	0.949	0.824
Area, B	1761	1450	1803	1489
σ_4 (mm/s)	0.104	0.151	0.103	0.151
h_4 (counts)	52869	30169	54492	31142
ω_4 (mm/s)	2.560	2.226	2.561	2.226
σ_5 (mm/s)	0.0610	0.0599	0.0603	0.0598
h_5 (counts)	53433	40269	54996	41650
ω_5 (mm/s)	2.698	2.421	2.698	2.421
Area, C	7415	5051	7667	5204
Total Area	22671	15496	23515	15989

Fit Name	MCCLN	MCCRT	IKOLNC	IKORTC1
Sample	MCC	MCC	IKO	IKO
Temp. (K)	82	305	83	300
χ^2	0.6	0.1	678	29
γ_h (mm/s)	0.07765	0.06655	0.05747	0.06289
σ_1 (mm/s)	0.0846	0.0908	0.0222	0.0390
h_1 (counts)	33061	35375	300093	110947
ω_1 (mm/s)	-0.185	-0.163	-0.225	-0.036
σ_2 (mm/s)	0.0959	0.0486	0.163	0.0912
h_2 (counts)	16850	5901	68581	89815
ω_2 (mm/s)	0.067	0.070	-0.065	0.094
Area, A	3876	2747	21188	12626
σ_3 (mm/s)	0.0237	0.0585	0.295	0.0700
h_3 (counts)	5007	5588	5801	7572
ω_3 (mm/s)	0.514	0.381	0.574	0.480
σ_4 (mm/s)	0.300	0.283	0.300	0.349
h_4 (counts)	2133	1420	30078	22485
ω_4 (mm/s)	0.960	0.850	0.788	0.909
Area, B+D	555	467	2062	1890
σ_5 (mm/s)	0.101	0.0610	0.0767	0.243
h_5 (counts)	19962	3034	121100	7684
ω_5 (mm/s)	2.571	2.184	2.669	2.080
σ_6 (mm/s)	0.0492	0.0666	0.0312	0.0954
h_6 (counts)	10452	21092	195951	62945
ω_6 (mm/s)	2.727	2.403	2.755	2.426
σ_7 (mm/s)	–	–	–	0.0486
h_7 (counts)	–	–	–	113783
ω_7 (mm/s)	–	–	–	2.534
Area, C	2362	1606	19221	11598
Total Area	6793	4820	41471	26114

Fit Name	IKOLNA	IKORTA1	IKOLNB	IKORTB1
Sample	IKO	IKO	IKO	IKO
Temp. (K)	83	300	83	300
χ^2	716	41	596	22
γ_h (mm/s)	0.05749	0.06286	0.05590	0.06043
σ_1 (mm/s)	0.0213	0.0382	0.0260	0.0420
h_1 (counts)	303758	115317	296294	103097
ω_1 (mm/s)	-0.225	-0.035	-0.226	-0.037
σ_2 (mm/s)	0.161	0.0901	0.167	0.0947
h_2 (counts)	68169	91631	73726	90836
ω_2 (mm/s)	-0.065	0.094	-0.070	0.092
Area, A	21404	13009	20686	11719
σ_3 (mm/s)	0.0285	0.070	0.0328	0.0800
h_3 (counts)	5737	7198	5927	7724
ω_3 (mm/s)	0.574	0.480	0.574	0.480
σ_4 (mm/s)	0.300	0.350	0.300	0.350
h_4 (counts)	30288	23574	30910	23002
ω_4 (mm/s)	0.785	0.891	0.791	0.902
Area, B+D	2071	1934	2059	1857
σ_5 (mm/s)	0.0763	0.0700	0.0814	0.080
h_5 (counts)	121249	3835	133483	4149
ω_5 (mm/s)	2.669	1.964	2.675	1.961
σ_6 (mm/s)	0.0308	0.102	0.0323	0.109
h_6 (counts)	198032	71369	185960	76360
ω_6 (mm/s)	2.755	2.429	2.756	2.438
σ_7 (mm/s)	–	0.0469	–	0.0490
h_7 (counts)	–	113942	–	98288
ω_7 (mm/s)	–	2.533	–	2.534
Area, C	18355	11890	17858	10805
Total Area	41835	26833	40603	24382

Fit Name	IKORTA	IKORTC	IKORTB
Sample	IKO	IKO	IKO
Temp. (K)	300	300	300
χ^2	101	95	81
γ_h (mm/s)	0.06287	0.06289	0.06307
σ_1 (mm/s)	0.0383	0.0390	0.0408
h_1 (counts)	115505	111292	105106
ω_1 (mm/s)	-0.035	-0.036	-0.036
σ_2 (mm/s)	0.0901	0.0906	0.0891
h_2 (counts)	91633	89546	81924
ω_2 (mm/s)	0.095	0.095	0.098
Area, A	13023	12631	11795
σ_3 (mm/s)	0.0700	0.0700	0.0800
h_3 (counts)	7647	7520	7860
ω_3 (mm/s)	0.480	0.480	0.480
σ_4 (mm/s)	0.350	0.350	0.350
h_4 (counts)	23489	23073	21663
ω_4 (mm/s)	0.920	0.920	0.934
Area, B+D	1958	1924	1862
σ_5 (mm/s)	0.107	0.107	0.108
h_5 (counts)	69752	67317	63128
ω_5 (mm/s)	2.424	2.422	2.421
σ_6 (mm/s)	0.0477	0.0488	0.0504
h_6 (counts)	116723	113800	106190
ω_6 (mm/s)	2.532	2.532	2.532
Area, C	11724	11390	10673
Total Area	26704	25945	24330

Material: IKO Fit label: IKORTCD1
Temperature: 300 K
Chi-square: 192 Lor. HWHM (γ_h) (mm/s): 0.06194

Site no.	Dist. no.	Height (counts)	Half Width (mm/s)	Position (mm/s)
1	1	10490	0.1662	0.4197
2	1	14869	0.3928	0.8405
3	1	74900	0.1951	2.3479
3	2	108138	0.0863	2.5699

Site no.	Center shift at Q.S.=0 (mm/s)	C.S.-Q.S. coupling parameter	Ratio (h-/h+)
1	0.3300	0.000	1.000
2	0.6000	0.000	1.000
3	1.2236	0.01088	1.000

Material: IKO Fit label: IKORTCD2
Temperature: 300 K
Chi-square: 89 Lor. HWHM (γ_h) (mm/s): 0.05323

Site no.	Dist. no.	Height (counts)	Half Width (mm/s)	Position (mm/s)
1	1	12614	0.2030	0.4000
2	1	12761	0.2949	0.9173
3	1	112995	0.2203	2.4076
3	2	94988	0.0863	2.5717
3	3	9511	0.5255	1.2600

Site no.	Center shift at Q.S.=0 (mm/s)	C.S.-Q.S. coupling parameter	Ratio (h-/h+)
1	0.3300	0.000	1.000
2	0.6000	0.000	1.000
3	1.2270	0.00950	1.000

Material: IKO Fit label: IKORTAD1

Temperature: 300 K

Chi-square: 204 Lor. HWHM (γ_h) (mm/s): 0.06148

Site no.	Dist. no.	Height (counts)	Half Width (mm/s)	Position (mm/s)
1	1	11174	0.1708	0.4214
2	1	15077	0.3834	0.8460
3	1	77651	0.1955	2.350
3	2	112057	0.0854	2.569

Site no.	Center shift at Q.S.=0 (mm/s)	C.S.-Q.S. coupling parameter	Ratio (h-/h+)
1	0.3300	0.000	1.000
2	0.6000	0.000	1.000
3	1.2213	0.01175	1.000

Material: IKO Fit label: IKORTAD2

Temperature: 300 K

Chi-square: 98 Lor. HWHM (γ_h) (mm/s): 0.05245

Site no.	Dist. no.	Height (counts)	Half Width (mm/s)	Position (mm/s)
1	1	13242	0.2050	0.4000
2	1	13315	0.2933	0.9182
3	1	118283	0.2210	2.4095
3	2	98887	0.0857	2.5708
3	3	9778	0.5223	1.2615

Site no.	Center shift at Q.S.=0 (mm/s)	C.S.-Q.S. coupling parameter	Ratio (h-/h+)
1	0.3300	0.000	1.000
2	0.6000	0.000	1.000
3	1.2244	0.01053	1.000

Material: IKO Fit label: IKOLNCD1

Temperature: 82 K

Chi-square: 1096 Lor. HWHM (γ_h) (mm/s): 0.05220

Site no.	Dist. no.	Height (counts)	Half Width (mm/s)	Position (mm/s)
1	1	18830	0.207	0.508
2	1	25940	0.550	1.041
3	1	144134	0.038	2.988
3	2	189276	0.124	2.921
3	3	21878	0.362	2.627

Site no.	Center shift at Q.S.=0 (mm/s)	C.S.-Q.S. coupling parameter	Ratio (h-/h+)
1	0.3225	0.000	1.000
2	0.4674	0.000	1.000
3	0.7274	0.178	1.000

Appendix 5. Calculating the Voigt Function

The Voigt lineshape is the convolution of a Lorentzian lineshape with a Gaussian distribution of Lorentzian line positions. This is expressed in equation A5.1.

$$V(h, \gamma, \sigma, \omega; \psi) = \int_{-\infty}^{+\infty} G(z)\, L(\psi - z)\, dz \qquad (A5.1)$$

where

$$G(z) = \frac{1}{\sigma\sqrt{2\pi}} \exp\left[- (z - \omega)^2 / 2\sigma^2 \right] \qquad (A5.2)$$

and

$$L(\psi - z) = \frac{h\gamma^2/4}{(\psi - z)^2 + \gamma^2/4} \qquad (A5.3)$$

The Voigt, as a function of energy, ψ, is described by four parameters: full width at half maximum of the Lorentzian (γ), Lorentzian height (h), center position (ω), and Gaussian standard deviation (σ).

In this thesis, the actual calculation of the Voigt function is done with the following formula [16]:

$$V(h,\gamma,\sigma,\omega;\psi) = \frac{\pi\ h\ \gamma}{\sqrt{8\pi}\ \sigma}\ K(x,\ y) \qquad (A5.4)$$

where $x = (\psi - \omega)/(\sigma\sqrt{2})$, $y = \gamma/(\sigma\sqrt{8})$, and $K(x, y)$ is approximated by

$$K(x,\ y) = \sum_{k=1}^{4} \frac{g_k(y-a_k) + d_k(x-b_k)}{(y-a_k)^2 + (x-b_k)^2} \qquad (A5.5)$$

the coefficients being

k	a_k	b_k	g_k	d_k
1	-1.2150	1.2359	-0.3085	0.0210
2	-1.3509	0.3786	0.5906	-1.1858
3	-1.2150	-1.2359	-0.3085	-0.0210
4	-1.3509	-0.3786	0.5906	1.1858